



**HAL**  
open science

# Metabolite detection using organic electronic devices for point-of-care diagnostics

Anna Maria Pappa

► **To cite this version:**

Anna Maria Pappa. Metabolite detection using organic electronic devices for point-of-care diagnostics. Other. Université de Lyon, 2017. English. NNT : 2017LYSEM020 . tel-02003606

**HAL Id: tel-02003606**

**<https://theses.hal.science/tel-02003606v1>**

Submitted on 1 Feb 2019

**HAL** is a multi-disciplinary open access archive for the deposit and dissemination of scientific research documents, whether they are published or not. The documents may come from teaching and research institutions in France or abroad, or from public or private research centers.

L'archive ouverte pluridisciplinaire **HAL**, est destinée au dépôt et à la diffusion de documents scientifiques de niveau recherche, publiés ou non, émanant des établissements d'enseignement et de recherche français ou étrangers, des laboratoires publics ou privés.



N°d'ordre NNT : 2017LYSEM020

**THESE de DOCTORAT DE L'UNIVERSITE DE LYON**  
opérée au sein de  
**l'Ecole des Mines de Saint-Etienne**

**Ecole Doctorale N° 488**  
**Sciences, Ingénierie, Santé**

**Spécialité de doctorat : Microélectronique**  
**Discipline : Bioélectronique**

Soutenue publiquement le 12/09/2017, par:  
**Anna-Maria Pappa**

---

**Metabolite detection using organic  
electronic devices for point-of-care  
diagnostics**

---

Devant le jury composé de :

Mailley, Pascal  
Rodney O'Connor  
Salleo, Alberto  
Offenhauser, Andreas  
Inal, Sahika

PhD  
Ass. Professeur  
Professeur  
Professeur  
Ass. Professeur

CEA, LETI  
Mines-Saint Etienne  
Stanford University  
Forschungszentrum Julich  
KAUST

Présidente  
Examineur  
Rapporteur  
Rapporteur  
Examinatrice

Owens, Roisin

Professeur

Mines-Saint Etienne

Directeur de thèse

**EMSE : Enseignants-chercheurs et chercheurs autorisés à diriger des thèses de doctorat (titulaires d'un doctorat d'État ou d'une HDR)**

ABSI	Nabil	CR	Génie industriel	CMP
AVRIL	Stéphane	PR2	Mécanique et ingénierie	CIS
BALBO	Flavien	PR2	Informatique	FAYOL
BASSEREAU	Jean-François	PR	Sciences et génie des matériaux	SMS
BATTAIA				
GUSCHINSKAYA	Olga	CR	Génie industriel	FAYOL
BATTON-HUBERT	Mireille	PR2	Sciences et génie de l'environnement	FAYOL
BERGER DOUCE	Sandrine	PR2	Sciences de gestion	FAYOL
BIGOT	Jean Pierre	MR(DR2)	Génie des Procédés	SPIN
BILAL	Essaid	DR	Sciences de la Terre	SPIN
BLAYAC	Sylvain	MA(MDC)	Microélectronique	CMP
BOISSIER	Olivier	PR1	Informatique	FAYOL
BONNEFOY	Olivier	MA(MDC)	Génie des Procédés	SPIN
BORBELY	Andras	MR(DR2)	Sciences et génie des matériaux	SMS
BOUCHER	Xavier	PR2	Génie Industriel	FAYOL
BRODHAG	Christian	DR	Sciences et génie de l'environnement	FAYOL
BRUCHON	Julien	MA(MDC)	Mécanique et ingénierie	SMS
BURLAT	Patrick	PR1	Génie Industriel	FAYOL
COURNIL	Michel	PR0	Génie des Procédés	DIR
DAUZERE-PERES	Stéphane	PR1	Génie Industriel	CMP
DEBAYLE	Johan	CR	Image Vision Signal	CIS
DELAFOSSÉ	David	PR0	Sciences et génie des matériaux	SMS
DELORME	Xavier	MA(MDC)	Génie industriel	FAYOL
DESRAYAUD	Christophe	PR1	Mécanique et ingénierie	SMS
DOLGUI	Alexandre	PR0	Génie Industriel	FAYOL
DRAPIER	Sylvain	PR1	Mécanique et ingénierie	SMS
FAVERGEON	Loïc	CR	Génie des Procédés	SPIN
FEILLET	Dominique	PR1	Génie Industriel	CMP
FRACZKIEWICZ	Anna	DR	Sciences et génie des matériaux	SMS
GARCIA	Daniel	MR(DR2)	Génie des Procédés	SPIN
GAVET	Yann	MA(MDC)	Image Vision Signal	CIS
GERINGER	Jean	MA(MDC)	Sciences et génie des matériaux	CIS
GOEURIOT	Dominique	DR	Sciences et génie des matériaux	SMS
GONDRAN	Natacha	MA(MDC)	Sciences et génie de l'environnement	FAYOL
GRAILLOT	Didier	DR	Sciences et génie de l'environnement	SPIN
GROSSEAU	Philippe	DR	Génie des Procédés	SPIN
GRUY	Frédéric	PR1	Génie des Procédés	SPIN
GUY	Bernard	DR	Sciences de la Terre	SPIN
HAN	Woo-Suck	MR	Mécanique et ingénierie	SMS
HERRI	Jean Michel	PR1	Génie des Procédés	SPIN
KERMOUCHE	Guillaume	PR2	Mécanique et Ingénierie	SMS
KLOCKER	Helmut	DR	Sciences et génie des matériaux	SMS
LAFORÉST	Valérie	MR(DR2)	Sciences et génie de l'environnement	FAYOL
LERICHE	Rodolphe	CR	Mécanique et ingénierie	FAYOL
LI	Jean-Michel		Microélectronique	CMP
MALLIARAS	Georges	PR1	Microélectronique	CMP
MAURINE	Philippe	Ingénieur de recherche	Microélectronique	CMP
MOLIMARD	Jérôme	PR2	Mécanique et ingénierie	CIS
MONTHEILLET	Frank	DR	Sciences et génie des matériaux	SMS
MOUTTE	Jacques	CR	Génie des Procédés	SPIN
NEUBERT	Gilles	PR	Génie industriel	FAYOL
NIKOLOVSKI	Jean-Pierre	Ingénieur de recherche		CMP
NORTIER	Patrice	PR1		SPIN
OWENS	Rosin	MA(MDC)	Microélectronique	CMP
PICARD	Gauthier	MA(MDC)	Informatique	FAYOL
PJOLAT	Christophe	PR0	Génie des Procédés	SPIN
PJOLAT	Michèle	PR1	Génie des Procédés	SPIN
PINOLI	Jean Charles	PR0	Image Vision Signal	CIS
POURCHEZ	Jérémy	MR	Génie des Procédés	CIS
ROBISSON	Bruno	Ingénieur de recherche	Microélectronique	CMP
ROUSSY	Agnès	MA(MDC)	Génie industriel	CMP
ROUSTANT	Olivier	MA(MDC)	Mathématiques appliquées	FAYOL
ROUX	Christian	PR	Image Vision Signal	CIS
STOLARZ	Jacques	CR	Sciences et génie des matériaux	SMS
TRIA	Assia	Ingénieur de recherche	Microélectronique	CMP
VALDIVIESO	François	PR2	Sciences et génie des matériaux	SMS
VIRICELLE	Jean Paul	DR	Génie des Procédés	SPIN
WOLSKI	Krzystof	DR	Sciences et génie des matériaux	SMS
XIE	Xiaolan	PR1	Génie industriel	CIS
YUGMA	Gallian	CR	Génie industriel	CMP
BERGHEAU	Jean-Michel	PU	Mécanique et Ingénierie	ENISE
BERTRAND	Philippe	MCF	Génie des procédés	ENISE
DUBUJET	Philippe	PU	Mécanique et Ingénierie	ENISE
FEULVARCH	Eric	MCF	Mécanique et Ingénierie	ENISE
FORTUNIER	Roland	PR	Sciences et Génie des matériaux	ENISE
GUSSAROV	Andrey	Enseignant contractuel	Génie des procédés	ENISE
HAMDI	Hédi	MCF	Mécanique et Ingénierie	ENISE
LYONNET	Patrick	PU	Mécanique et Ingénierie	ENISE
RECH	Joël	PU	Mécanique et Ingénierie	ENISE
SMUROV	Igor	PU	Mécanique et Ingénierie	ENISE
TOSCANO	Rosario	PU	Mécanique et Ingénierie	ENISE
AHOUANI	Hassan	PU	Mécanique et Ingénierie	ENISE

Στους γονείς μου,  
Μαρία & Δημήτρη

# Résumé

---

De nos jours, efficacité et précision des diagnostics médicaux sont des éléments essentiels pour la prévention en termes de santé et permettre une prise en charge rapide des maladies des patients. Les récentes innovations technologiques, particulièrement dans les domaines de la microélectronique et des sciences des matériaux ont permis le développement de nouvelles plateformes personnalisées de diagnostics portatifs. Les matériaux électroniques organiques qui ont déjà par le passé démontré leur potentiel en étant intégrés dans des produits de grande consommation tels que les écrans de smartphones ou encore les cellules solaires montrent un fort potentiel pour une intégration dans des dispositifs biomédicaux. En effet, de par leurs natures et leurs propriétés physiques et chimiques, ils peuvent être à la fois en contact avec les milieux biologiques et constituer l'interface entre les éléments biologiques à l'étude, et les dispositifs électroniques. L'objectif de mes travaux de thèse est d'étudier et évaluer les performances des matériaux organiques électroniques intégrés dans des dispositifs biomédicaux en étudiant leurs interactions avec des milieux biologiques et par l'utilisation et l'optimisation de ces dispositifs permettre la détection de métabolites tel que le glucose ou lactate par exemple. Pendant ma thèse, j'ai notamment créé une plateforme de diagnostics combinant à la fois microfluidique et électronique organique permettant la multi détection de métabolites présents dans des fluides corporels humains, j'ai également conçu des capteurs intégrant des transistors organiques au sein des circuits électroniques classiques afin de détecter la présence des cellules tumorales. D'autres applications biologiques ont également été envisagées telles que la détection d'acides nucléiques par l'utilisation d'une approche simple de biofonctionnalisation. Bien que l'objectif ma thèse était de de créer des capteurs biomédicaux en utilisant une approche in vitro, il pourrait être également possible d'intégrer ces dispositifs « in vivo » ou encore dans des e-textiles.

# Abstract

---

Rapid and early diagnosis of disease plays a major role in preventative healthcare. Undoubtedly, technological evolutions, particularly in microelectronics and materials science, have made the hitherto utopian scenario of portable, personalized diagnostics a reality. Organic electronic materials, having already demonstrated a significant technological maturity with the development of high tech products such as displays for smartphones or portable solar cells, have emerged as especially promising candidates for biomedical applications. Their soft and fuzzy nature allows for an almost seamless interface with the biological milieu rendering these materials ideally capable of bridging the gap between electronics and biology. The aim of this thesis is to explore and validate the capabilities of organic electronic materials and devices in real-world biological sensing applications focusing on enzyme-based metabolite sensing, by combining both the right materials and device engineering. We show proof-of-concept studies including for example microfluidic integrated organic electronic platforms for multiple metabolite detection in bodily fluids, as well as more complex organic transistor circuits for metabolite detection in tumor cell cultures. Taking advantage of the structural versatility of organic electronics, we extend our repertoire and explore a new class of materials bringing new insights on enzyme-based metabolite sensing. Finally, we attempt to get a more fundamental understanding of the effect of the critical interface between the biological milieu and the device, getting useful insights for novel biosensing applications such as nucleic acid sensing. Although the focus is on *in vitro* metabolite monitoring, the findings generated throughout this work can be extended to a variety of other sensing strategies as well as to applications including on body (wearable) or even *in vivo* sensing.

# Table of contents

---

<b>Résumé.....</b>	<b>1</b>
<b>Abstract .....</b>	<b>2</b>
<b>Introduction .....</b>	<b>6</b>
<b>Chapter 1: State-of-the-art in Organic Electronics for Point-of-Care Metabolite Monitoring.....</b>	<b>9</b>
1. Biosensors as Analytical Tools in Point-of-care Diagnostics .....	13
2. Organic Electronics at the Interface with Biology: state of the art in metabolite sensing	14
2.1 <i>Conducting polymers as efficient electron relays</i> .....	15
2.2 <i>Conducting polymers as permselective membranes for improved selectivity</i> .....	17
2.3 <i>Nanostructured organic electronic materials for improved sensitivity</i> .....	17
2.4 <i>Conducting Polymer- based devices</i> .....	18
3. Highly integrated Organic Electronic Devices for Point of Care Metabolite Sensing...	19
3.1 <i>In vitro metabolite biosensors</i> .....	19
3.2 <i>Wearable Metabolite Biosensors</i> .....	22
3.3 <i>Implantable Biosensors</i> .....	27
4. Conclusions .....	27
Acknowledgements.....	28
References.....	29
<b>Chapter 2: Organic Transistor Arrays Integrated with Finger-Powered Microfluidics for Multianalyte Saliva Testing.....</b>	<b>38</b>
1. Introduction.....	40
2. Results and discussion .....	42
2.1 <i>OEET biofunctionalization and use for enzymatic sensing</i> .....	42
2.2 <i>Characterization of biofunctionalised OEETs</i> .....	44

2.3 Selective multianalyte detection in complex media using the OEET array .....	46
2.4 On-chip multianalyte detection in saliva using the OEET.....	47
3. Conclusions .....	<b>50</b>
4. Experimental Section.....	<b>50</b>
Acknowledgements.....	<b>53</b>
References.....	<b>53</b>
Supporting Information .....	<b>56</b>
<b>Chapter 3: Lactate Detection in Tumor Cell Cultures Using Organic Transistor Circuits .....</b>	<b>58</b>
1. Introduction.....	<b>60</b>
2. Results and Discussion.....	<b>61</b>
3. Conclusions .....	<b>67</b>
4. Experimental Section.....	<b>67</b>
Acknowledgements .....	<b>69</b>
References.....	<b>70</b>
Supporting Information .....	<b>73</b>
<b>Chapter 4: Metabolite detection with an N-type accumulation mode organic electrochemical transistor.....</b>	<b>76</b>
1. Introduction.....	<b>78</b>
2. Results and Discussion.....	<b>80</b>
2.1 Characterization of the N-type organic semiconductor and proposed sensing mechanism.....	80
2.2 Accumulation mode N-type OEETs.....	82
2.3 Highly sensitive mediator-free lactate detection with the N-type OEETs .....	83
2.4 Device operation parameters tune sensor analytical characteristics.....	85
3. Conclusions .....	<b>86</b>
References.....	<b>86</b>
<b>Chapter 5: Polyelectrolyte Layer by Layer Assembly on Organic Electrochemical Transistors.....</b>	<b>89</b>



1. Introduction.....	<b>91</b>
2. Experimental Section.....	<b>93</b>
3. Results and Discussion.....	<b>95</b>
3.1 LbL on top of PEDOT:PSS : Optimizing the immobilization of the supporting layer by QCM-D.....	95
3.2 Characterization of LbL on top of an OECT.....	97
3.3 LbL for the controlled immobilization and monitoring of nucleic acid .....	101
4. Conclusions .....	<b>103</b>
Acknowledgments .....	103
References.....	<b>104</b>
Supporting information.....	<b>109</b>
<b>Conclusions and Outlook.....</b>	<b>114</b>
<b>Scientific Contributions.....</b>	<b>120</b>
<b>Acknowledgements.....</b>	<b>122</b>

# Introduction

---

Rapid and early diagnosis of disease plays a major role in preventative healthcare. Biosensor technology, has significantly advanced, from the first reported “enzyme electrode” by Clark and Lyons, able to measure accurately glucose concentrations in whole blood samples, to recent research prototypes of miniaturized sensor chips able to measure real-time multiple metabolites. Undoubtedly, the technological evolution particularly in microelectronics and in materials science has made the previously utopian scenario of portable, point-of-care personalized diagnostic tests a reality, paving the way to a more decentralized preventative healthcare system.

Organic electronics, including carbon-based semiconducting materials, have demonstrated a significant technological maturity with the development of high tech products such as displays for smartphones or portable solar cells, due to the chemical tunability of their electronic properties as well as their low-temperature and thus low-cost processing. Moreover, their organic soft and fuzzy nature allows for an almost seamless and direct interface with the biological milieu rendering those materials ideal for bridging the gap between electronics and biology. Indeed, “organic bioelectronic” devices are attractive for a wide range of biomedical applications including neurophysiology, in vitro toxicology, metabolite sensing etc.

**This thesis focuses on** the use of organic electronic devices, namely organic electrochemical transistors (OECTs), as compact miniaturized metabolite sensing platforms aiming to address unmet clinical needs. The biosensing scheme developed herein relies on the electrochemical detection of critical metabolites (i.e., glucose, lactate and cholesterol) using enzymes as biorecognition elements due to their high selectivity and their excellent catalytic activity. As such, focus is given to the surface functionalization of the semiconductor in order to achieve a good communication with the enzyme’s active site for optimized analytical sensor performance. Alongside the workhorse conducting polymer poly(3,4-ethylenedioxythiophene) polystyrene sulfonate (PEDOT:PSS), we explore a new class of materials, specially customized to meet the device and sensor requirements. We show proof-of-concept studies including microfluidic integrated OECT-based platforms for multiple metabolite detection in bodily fluids as well as metabolite detection in tumor cell cultures using complex transistor circuits.

We also explore different sensing strategies and demonstrate nucleic acid sensing using a simple biofunctionalization approach. Overall, the aim of this thesis is to explore and validate the capabilities of organic electronic materials and devices for biological sensing applications. Although the focus is on *in vitro* metabolite detection, we believe that the input provided throughout this work can be extended to a variety of other sensing strategies as well as to applications including *on body* or even *in vivo* sensing.

**In more details, Chapter 1** gives an overview of the state of the art in enzyme-based electrochemical detection of metabolites using organic electronic materials and devices. Focus is given to the especially promising class of polymer-based electronics, the conducting polymers (CPs), however in the cases where the examples of CP based biosensors are still scarce, examples with carbon-based nanomaterials are highlighted in order to show the potential of organic electronic materials. Particularly, the key properties that render those materials ideal transducers for metabolite monitoring including better electrochemical communication at the bio-electronic interface, faster electron transfer, lower signal-to-noise ratio etc, as well as for the system's integration in real – world applications are thoroughly discussed. We approach this by taking into account both the advantages offered by the devices enabled by those materials, as well as by their bulk properties, all contributing to an ideal interface with the biorecognition elements as well as with the complex biological milieu. We also highlight early breakthroughs, and key developments offered by this class of biosensors. Finally, we discuss in this respect the niche for organic electronic metabolite sensors for state-of-the art future point-of-care diagnostics.

**Chapter 2** reports on a compact multianalyte biosensing platform that is composed of an organic electrochemical transistor (OECT) microarray integrated with a pumpless “finger-powered” microfluidic, for the quantitative screening of glucose, lactate, and cholesterol levels. A biofunctionalization method is designed, which provides selectivity towards specific metabolites as well as minimization of any background interference. In addition, a simple method is developed to facilitate multi-analyte sensing and avoid electrical crosstalk between the different transistors by electrically isolating the individual devices. The resulting biosensing platform, verified using human samples, offers the possibility to be used in easy-to-obtain biofluids with low abundance metabolites, such as saliva.

**Chapter 3** reports on a biosensing platform based on an organic transistor circuit for metabolite detection in highly complex biological media such as cell culture media. Due to the complexity and high biological interference in the media a sensor circuit is developed that

provides inherent background subtraction allowing thus for highly specific and sensitive lactate detection in tumor cell cultures. The proposed sensing platform can be used for the detection of lactate produced from circulating tumor cells in blood, thus paving the way to an in vitro prognostic model of the degree of malignancy in primary tumors as well as of the probability of metastasis.

**Chapter 4** reports, for the first time, an accumulation mode electrochemical transistor comprising an N-type organic semiconductor in the channel, for enzymatic detection of lactate. Without the need for an electron-transfer mediator, the channel is doped when lactate is oxidised by the enzyme lactate oxidase present in the electrolyte, leading to a sensor with superior sensitivity and detection range compared to PEDOT:PSS analogues. This is due to the operation principle of this transistor type which allows for the bioelectrocatalytic reactions to occur at the channel. By fine tuning the semiconductor to improve its interactions with the enzyme, we can detect lactate with high sensitivity and in a wide concentration range within the physiologically relevant concentrations in blood and sweat.

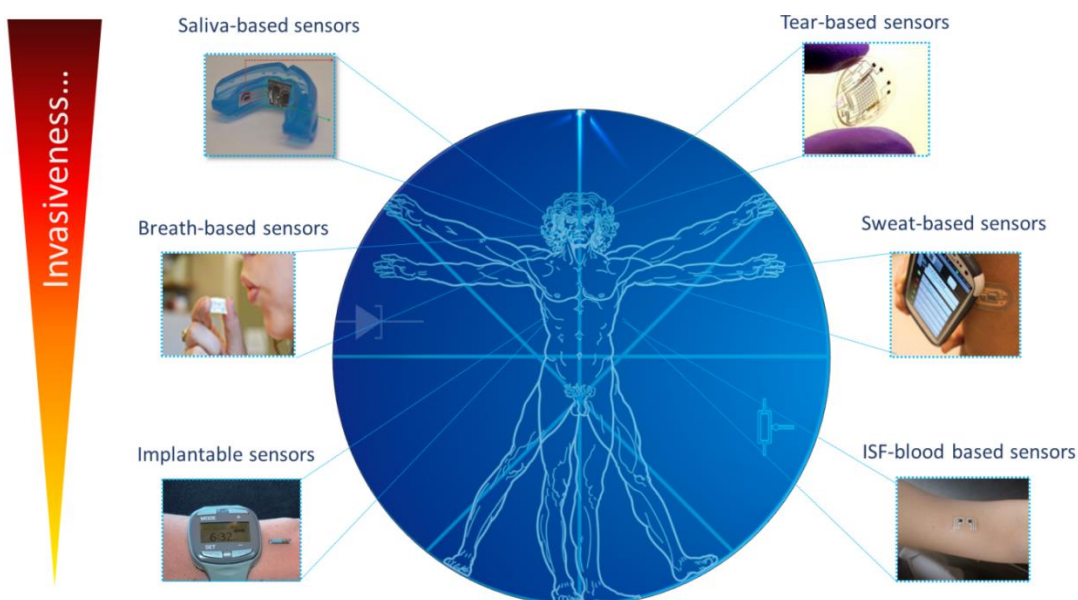
**Chapter 5** describes a biofunctionalization method comprised of oppositely charged polyelectrolyte multilayers (PEMs) built up in a layer-by-layer (LbL) assembly on top of the conducting polymer channel of an OECT. This aims to combine the advantages of well-established PEMs with a high performance electronic transducer. The multilayered film is a model system to investigate the impact of biofunctionalization on the operation of OECTs comprising a PEDOT:PSS film as the electrically active layer. Understanding the mechanism of ion injection into the channel that is in direct contact with charged polymer films provides useful insights for novel biosensing applications such as nucleic acid sensing. Moreover, LbL is demonstrated to be a versatile electrode modification tool enabling tailored surface features in terms of thickness, softness, roughness, and charge. LbL assemblies built up on top of conducting polymers will aid the design of new bioelectronic platforms for drug delivery, tissue engineering, and medical diagnostics.

**This thesis concludes with** an overview of the overall findings followed by a discussion and outlook.

# Chapter 1

---

## State-of-the-art in Organic Electronics for Point-of-Care Metabolite Monitoring



The present Chapter is based on the following publication:

**“Organic Electronics for Point-of-Care Metabolite Monitoring”**

*A.M. Pappa, O. Parlak, G. Sheiblein, P. Mailley, A. Salleo and R.M. Owens*

*Invited Review in Trends in Biotechnology, submitted*

## **Abstract**

In this review we focus on demonstrating how organic electronic materials can provide solutions to key problems in biosensing thanks to their unique materials properties and implementation in innovative device configurations. We highlight specific examples from literature where these materials solve multiple issues related to complex sensing environments. We benchmark these examples by comparing to state of the art, often commercially available sensing using alternative technologies. We have categorized our examples by sample type, focusing on sensing from bodily fluids *in vitro*, also on wearable sensors which have attracted significant interest due to their integration with everyday life activities. We finish by describing a future trend for *in vivo*, implantable sensors which hopes to build on current progress from sensing in biological fluids *ex vivo*.

### Author's contribution:

For the present publication, used as chapter 1 in this thesis my contribution was the bibliographic review of the state of the art in organic electronic materials for use in metabolite sensing, their role in solving current issues related to sensing performance and especially in real world applications, focusing on the *in vitro* applications.

## **Glossary**

A **Biosensor** is an analytical device that consists of a biorecognition element which can specifically interact with an analyte and produce physical, chemical or electrical signals [1]. An **Analyte** is a compound (e.g. glucose, lactate, drug, pesticide) whose concentration is to be measured.

**Biorecognition elements include** biological components or derivatives that specifically interact with the analyte of interest (e.g. enzymes, organelles, cells, tissues, antibodies and nucleic acids)

A **Transducer** is a device that converts the biological signal that is generated to a readable signal: electrical, optical or mechanical.

**Metabolites** are the intermediates and products of metabolism.

**Multiplexing involves the** incorporation of multiple sensing capabilities in terms of analyte diversity

**Electrochemical enzyme-based sensing** relies on coupling a redox reaction catalyzed by an enzyme with an electrochemical transducer using techniques such as amperometry, potentiometry, and voltammetry [7, 12].

**Amperometry** measures the current of the working electrode set out of equilibrium at a fixed potential. Thus, when the substrate reaches the active site of the immobilised enzyme, electrons are rapidly exchanged [12].

**Direct Electron transfer (DET)** involves direct electron transfer between the redox active center of the catalytic biorecognition element (e.g. enzyme) and the electrode in the absence of an electron transfer mediator.

**Mediated electron transfer (MET)** occurs with the help of small molecules that shuttle electrons between the biorecognition element and the electrode [13, 14].

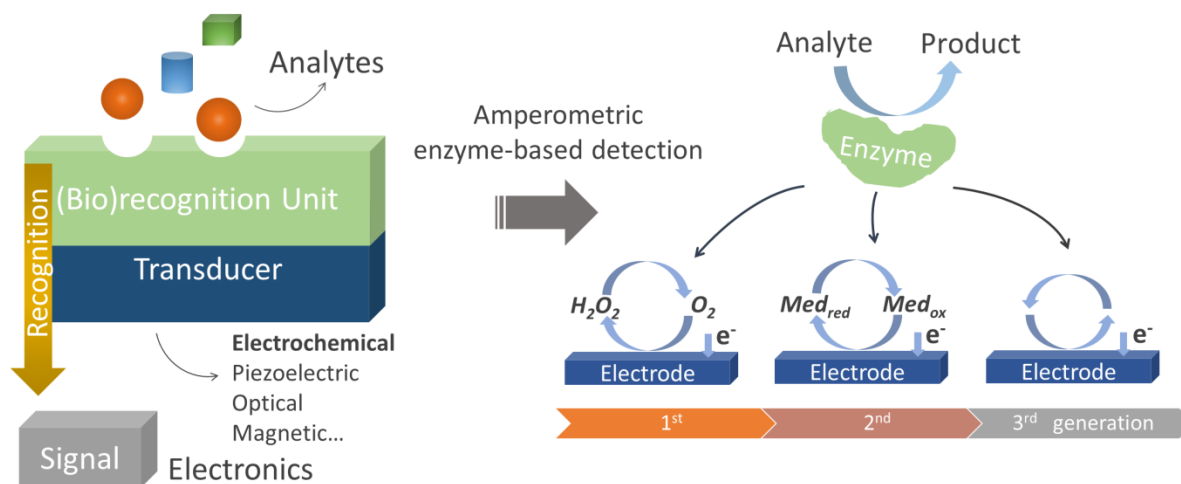
**Conjugated Polymers** contain alternating single and double bonds on the polymer backbone allowing stabilization of the structure of the molecule upon addition or subtraction of a charge, through redox activation, conferring on it electronically conducting behavior. These polymers when subjected to redox activation generate polyionic structures in which charge compensation takes place, in a similar manner to the doping in inorganic semiconductors.

**Conducting Polymers or (CPs)** or, more precisely, intrinsically conducting polymers are organic polymers that conduct electricity, having either metallic conductivity or semiconductor properties. CPs can exhibit **mixed conduction** which is the ability to conduct both ionic and electronic current.

**Organic electrochemical transistors (OECTs)** are electrolyte-gated organic thin film transistors (EGTs) where, unlike the conventional EGTs [15, 16], the doping level modulation occurs in the bulk of the CP film resulting in especially high currents for very small gate fluctuations (sub Volts), a property also known as **transconductance** [17, 18]. When coupled with biorecognition elements, this inherent amplification results in highly sensitive transduction of a biological event i.e., the enzymatic detection of metabolites.

**Poly(3,4-ethylenedioxythiophene)-poly(styrenesulfonate) (PEDOT:PSS)** is an intrinsically doped p-type semiconductor and is the champion material used to date in OECTs. Such transistors have been shown to exhibit the highest transconductance values among their electrolyte-gated counterparts [17].

### Box 1. Biosensors and enzymatic electrochemical detection



**What is a biosensor?** The biosensor, first introduced by Leland C. Clark Jr. and co-workers in 1962,[1] is defined as an analytical device incorporating a biorecognition element within or associated with physiochemical transducers (classified as optical, electrochemical or mechanical[2-4])

**What does a biosensor do?** It generates a digital electronic signal based on the concentration of specific chemicals or end products of a given biochemical reaction in an analytical standard.[5]

**What is a biosensor used for?** Applications ranging from medical diagnostics to drug discovery, food safety, process control and environmental monitoring, to defence and security applications.[6]

**Electrochemical techniques** possess many advantages that allow fabrication of portable, miniaturized, low-cost, often label-free and simple-to-operate analytical devices that interface with biological components.[7-9] The working mechanism relies on selective recognition of a target analyte by a biomolecule or biomacromolecular complex, which in turn produces a measurable electrochemical signal. Although a variety of biorecognition elements can be employed, electrochemical detection techniques rely predominantly on enzymes.

**Enzyme-based electrochemical sensors** are typically preferred for metabolite monitoring due to high selectivity, catalytic activity and fast acting properties of enzymes at the electrode interface.[10, 11]



## 1. Biosensors as Analytical Tools in Point-of-care Diagnostics

Today's **biosensor** (see Glossary) market represents a US\$ 13 billion annual turnover, and has rapidly become an invaluable tool to reduce healthcare costs and enhance the patient's quality of life [6, 19]. Thus, the development of novel concepts and methodologies in biosensor technology for more effective diagnostic solutions is anticipated to have a significant economical and societal impact beyond the single patient outcome.

Continuous and **multiplexed** monitoring, non-invasiveness, portability, long-term stability, ease in device integration and compatibility with flexible substrates and low cost technologies are only some of the numerous challenges for a biosensor to enter the market. Many prototypes have been developed, however only a very limited number of such systems have made it to commercialization.[20, 21] Failures have been attributed to (bio)incompatibility, environmental factors and technological limitations [6, 13] Undoubtedly, a key step towards advanced biosensors for continuous monitoring of **analytes** in complex and sometimes harsh biological environments is the development/integration of materials with more favorable mechanical properties, long life-times, anti-biofouling capabilities as well as ease of integration with miniaturized sensor technologies, all at low cost and with minimum power consumption needs.

**Electrochemical enzyme- based sensing** is a viable approach for a wide repertoire of metabolic targets , due to the high selectivity and excellent catalytic activity of the enzymes as biorecognition elements coupled with their label-free, fast and simple detection principle (see **Box**). Indeed, since its inception by Leland C. Clark Jr [1] academic research in this field has continued unabated in parallel with commercial developments predominantly in glucose sensing. In such approaches, the selectivity and sensitivity of the biosensors can be sought by establishing an exclusive and intimate interface between the transducer and the enzyme thus reducing interference as well as improving the efficiency of the **electron transfer** (ET) involved in the redox reactions, [22]. Hence, the concept of “functional” electronic materials that can simultaneously provide an ideal immobilization matrix and an efficient signal transducer has fundamentally changed the understanding of how to develop efficient biosensors.[23]

In this review, recent advances in enzyme-based electrochemical detection of human metabolites in real samples using **organic electronic** materials are described. We place a

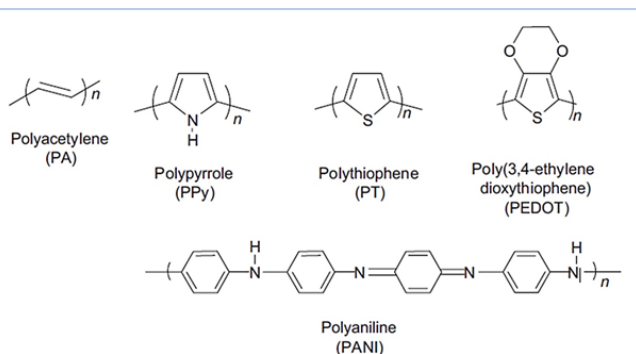
particular focus on the promising class of polymer-based electronics and more specifically electrically **conducting polymers** (CPs), however in the cases where such examples are still scarce, we showcase alternatives with carbon-based nanostructures, particularly in cases where their operation in real world applications pushes the state of the art thanks to their materials properties. We highlight the key properties that render organic electronic materials ideal transducers for metabolite monitoring, including better electrochemical communication at the bio-electronic interface, faster electron transfer, lower signal-to-noise ratio etc, as well as for the system's integration in real-world applications Finally, we discuss the niche for organic electronic metabolite sensors for state-of-the art point-of-care diagnostics (POC), as categorised into three groups; *in vitro*, wearable and implantable biosensors.

## 2. Organic Electronics at the Interface with Biology: state of the art in metabolite sensing

### Box 2. Organic Electronic Materials

**Organic electronic materials**, including **conjugated polymers**, **small molecules** and **carbon based nanomaterials** exhibit multiple advantages over their inorganic equivalents, such as ease in processability, compatibility with flexible substrates, as well as low-cost and environmentally-friendly manufacturing [24-27]. **Organic electronics** is a field of research that has rapidly come to the fore for biological applications including biosensing, owing to their literal flexibility and tunability to adapt to challenging performance requirements in biological milieu [28, 29]. Additionally, their intrinsic unique properties including high surface-to-volume ratio (owing to their nanometer scale molecular structures), high electrical conductivity, chemical stability, and excellent mechanical properties render them not only ideal substrates for chemical modification and bioreceptor immobilization but also excellent electronic signal transducers [30, 31].

#### Conducting Polymers



**Conducting Polymers** is an especially promising class of electronic materials. The doping or de-doping of such conjugated polymers can be reversible and triggered by chemical, electrical or biological events [32-34] showing great potential for applications such as biosensing [35, 36]. Polypyrrole (PPy), Polyaniline (PANI), and

Poly(3,4-ethylenedioxythiophene) (PEDOT), are the predominantly studied ones in biological applications due to their biocompatibility & ease of processability.

Ability to operate in harsh biological environments, enhanced sensitivity and selectivity, and demonstrated potential for low cost production, are just some of the reasons that poise organic electronic materials to revolutionize the biosensing arena (see **Box 2**). Some of the earliest demonstrations of organic bioelectronics were in sensing of metabolites from biological samples, and so this technology has reached a level of maturity where performance must be compared to state of the art devices or methods using other technologies.

## 2.1 Conducting polymers as efficient electron relays

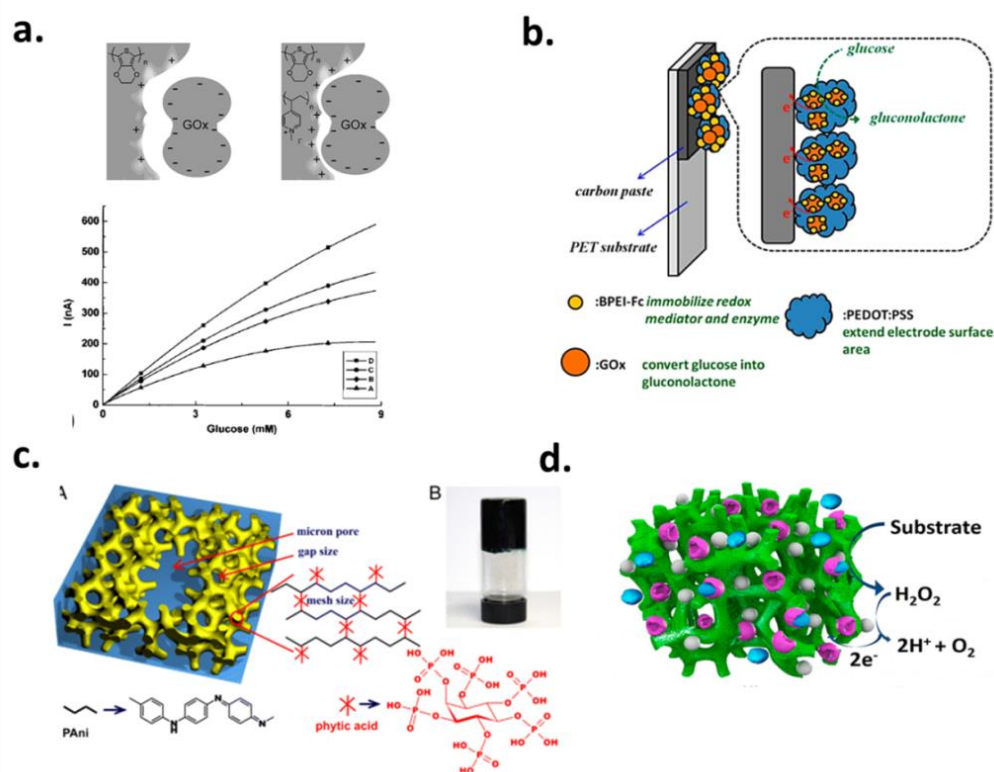


**Figure 1: Organic electronic materials as efficient enzyme immobilization matrices and transducers for metabolite detection.** (a) Weak and strong electrostatic binding of glucose oxidase onto PEDOT matrix due to the positive charged PMVP inside the matrix and current response of the corresponding biosensor at 0.3 V vs Ag/AgCl reference electrode as a function of glucose concentration for PEDOT only (A), as well as different PEDOT/PMVP molar ratio: 6(B), 3(C) and 2(D). Copyright © 2001 WILEY-VCH Verlag GmbH & Co. KGaA, Weinheim (b) Schematic diagram of the working electrode coated with ferrocene-branched polyethylenimine, PEDOT:PSS and glucose oxidase for glucose detection with increased sensitivity. Copyright © 2013 American Chemical Society. (c) Chemical structure of phytic acid gelled and doped PANI hydrogel. Copyright © 2007 American Chemical Society. (d) Schematic of the PANI hydrogel matrix integrating platinum nanoparticles and

the corresponding enzymes for the detection of uric acid, cholesterol and triglyceride. Copyright © 2007 American Chemical Society

Efficient electrical communication between the biorecognition element (enzyme) and the electrode is rather challenging when it comes to the design of metabolite biosensors. In most cases, the distance between the active site of the enzyme and the electrode surface is too long for DET, due to shielding by the protein shell. Since ET via a tunneling mechanism is rarely encountered in traditional electrodes, the establishment of electron relays that allow for fast ET, avoiding free-diffusing redox species between the electrode and the enzyme is crucial. In this context, organic electronic materials represent very promising candidates for molecular wiring owing to their polymeric nature and conducting behavior. Nevertheless, their ability to be electrochemically polymerized in the presence of biologically active molecules allows for an intimate and spatially controlled enzyme localization inside their matrix, resulting in a conducting ramified network. [37]

PPy was the first CP that was shown to provide an electron relay between the surface of the electrode and the active site of the enzyme, significantly enhancing the biosensors analytical characteristics [38, 39]. However, due to poor electrochemical stability (potentially affecting long-term functionality) [40], efforts shifted to other CPs such as PEDOT, a polythiophene derivative which due to its low bandgap and high electrochemical stability in the oxidized state, emerged as a more stable candidate [41]. The first example of a PEDOT- based glucose sensors with potential for long-term measurements was presented by Kros et al. [42]. They physically incorporated a positively charged polymer in the conducting matrix of the biosensor, allowing for more efficient ET due to the increased electrostatic interaction of the positively charged entrapped polymer with the negatively charged enzyme (**Figure 1a**). In a more direct approach, Thompson et al compared chemical vs electrochemical incorporation of GOx directly into PEDOT during polymerization, concluding that the chemical polymerization resulted in more efficient enzyme entrapment and thus DET [43].

An alternative strategy to improve the electron relay in the CPs post-synthesis involves intermixing with redox hydrogels, shown to exhibit fast substrate and counter ion diffusion properties, with high flexibility and fast electron transfer rates. The non-conducting nature of such hydrogels impedes their efficient and spatially localized immobilization on the active electrode surface, therefore their combination with CPs can overcome this issue and result in an ideal electron-transfer pathway. PEDOT:PSS was used to enhance the poor performance of a mediator based biosensor by its incorporation in nanocomposite enzyme electrodes, resulting in improved electron hopping in terms of the electron diffusion coefficient as well as the charge

transfer resistance (**Figure 1b**).[44] Going one step further, the Bao group developed intrinsically conducting nanostructured PANI- redox hydrogels. The high surface area and interconnected CP hydrogels not only resulted in excellent electronic conductivity and electrochemical properties but also served as an efficient catalytic substrate for the enzymatic determination of glucose, yielding excellent analytical biosensor properties.[45] In another approach, a CP -based glucose-permeable redox hydrogel was formed by cross-linking polymer acid-templated PANI along with GOx, leading to the electrical wiring of the enzyme, allowing the electrocatalytic oxidation of glucose at low oxidation potentials (**Figure 1c**). [46] More recently, CP hydrogels with high permeability to enzymes were used to fabricate metabolite biosensors with excellent sensing performance without the need for a mediator (**Figure 1d**). [47]

## 2.2 Conducting polymers as permselective membranes for improved selectivity

Another striking feature of CPs is their potential to be used as permselective membranes for the elimination of interference induced by electroactive compounds, particularly important when it comes to real-world applications, due to the increased complexity of the biological milieu. As such, overoxidized polypyrrole (OPPy) has been employed for the development of interference-free biosensors, as a cation exchange film that can repel common interferents found in complex media, and also limit protein binding, due to the oxygen-containing groups introduced onto its surface. Additionally, its controlled deposition via electropolymerisation renders it a versatile approach for permselective membranes. [48] PANI–polyisoprene films have been also used as an immobilization matrix for GOx and the resulting composite film was found to exhibit high permselectivity allowing selective H<sub>2</sub>O<sub>2</sub> detection over common electroactive interferents. [49]

## 2.3 Nanostructured organic electronic materials for improved sensitivity

Arguably, nanostructured sensing elements provide higher sensitivity due to increased surface to volume ratio. Due to the versatility in processing organic electronic materials, nanoscale structures can be easily achieved to improve both the enzyme immobilization efficiency and the sensitivity and stability of the sensor. Yang et al recently developed PEDOT nanofibers carrying GOx on top of a Pt electrode resulting in increased entrapment of the enzyme owing to its nanoscale matrix but also to a reduction in the electrode impedance, achieving glucose detection at relatively low polarization potentials [50].

## 2.4 Conducting Polymer– based devices

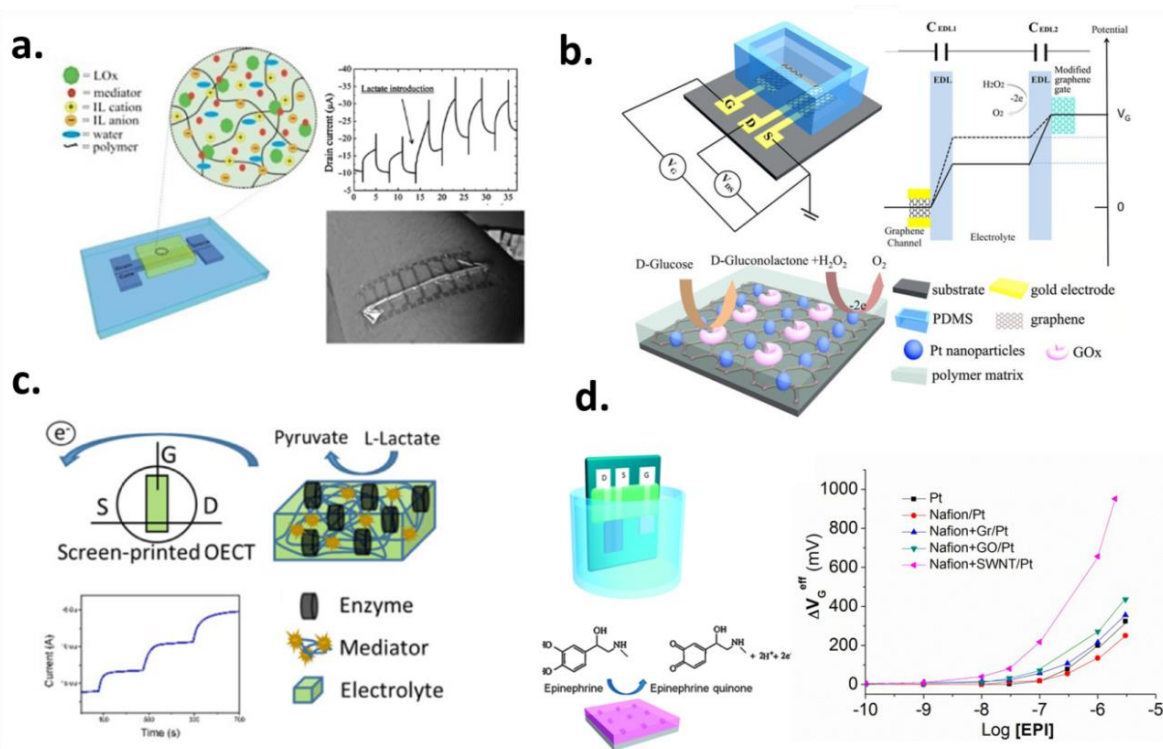


**Figure 2. Highly integrated electronic devices bearing organic materials as the transducing elements for metabolite detection.** (a) Schematic representation of the lactate OEET with an ionic gel solid state electrolyte, photograph of the actual flexible device and current modulation upon addition of lactate. Copyright © 2012 Royal Society of Chemistry (b) Illustration of the whole graphene solution gated transistor, showing the sensing electrode (gate) functionalization. Copyright © 2015, Rights Managed by Nature Publishing Group (c) Schematic diagram of the screen printed OEET and illustration showing the gate electrode functionalization, comprised of a mediator as well as current response for the enzymatic determination of lactate. Copyright © 2011, Materials Research Society (d) Schematic representation of the epinephrine OEET based sensor bearing functionalized gate electrodes and potential drop at the gate electrode upon different concentrations of epinephrine dependent on the different functionalization schemes. Copyright © 2012 Royal Society of Chemistry

Organic electronics have been used for enhancing biosensors thanks to distinct materials properties, however they can themselves constitute the active material of the transducer resulting in highly integrated devices. Forzani et al developed a glucose sensing device comprised of interdigitated nanoelectrodes, bridged by PANI/GOx nanojunctions. The transduction mechanism relied on the glucose oxidation inducing changes in the polymer redox state. Due to the small size of the nanojunction sensor, the enzyme was naturally regenerated without the need of redox mediators allowing for very fast responses and minimal oxygen consumption, a prerequisite for future *in vivo* applications. [51] **Mixed conduction** in CPs is a key property that has enabled several new modes of operation and devices including the organic electrochemical transistor (OEET), a rising star in terms of biosensing applications [52, 53]. After the first work on glucose sensing with OEETs in 1998, based on the CP PANI, using

tetrathiafulvalenium as an electron transfer mediator,[54] many have followed, mainly aiming at detecting the H<sub>2</sub>O<sub>2</sub> catalyzed oxidation at a Pt gate. [55] The integration of an ionic liquid as electrolyte [56] or the incorporation of carbon-based nanomaterials (graphene oxide), at the gate and channel electrode [57] represent interesting attempts to improve the stability and sensitivity respectively, of such devices (**Figure 2 a,b**). OEECT-based sensors have been also screen-printed and functionalised using a chitosan hydrogel matrix, incorporating a ferrocene electron transfer mediator along with the corresponding oxidase enzyme for the detection of glucose and lactate on artificial sweat samples (**Figure 3c**). [58] Epinephrine, a key neurotransmitter, has been also detected using solution processed OEECTs with remarkable sensitivities (sub nM) owing to a Nafion anti-interference layer and carbon-based nanomaterials co-immobilized on the gate electrodes (**Figure 3d**) [59].

### 3. Highly integrated Organic Electronic Devices for Point of Care Metabolite Sensing

#### 3.1 In vitro metabolite biosensors

##### 3.1.1 Metabolite sensing from bodily fluids/ gases

Blood is the most commonly used bodily fluid for metabolite level monitoring, however, due to the abundance of electroactive species, electrochemical detection methods become somewhat challenging not to mention the commonly observed biofouling of the sensing electrodes posing further restrictions. [60] CPs bearing appropriate surface modifications (i.e., incorporation of electron mediators, permselective membranes etc) can offer valuable tools towards novel, more accurate diagnostic devices. An antibody-mediated amperometric system developed by Wei et al was designed to avoid the interfering signals often encountered in complex matrices such as whole blood due to the need to use high potentials. Their 6-array gold electrochemical sensor coated with creatinine embedded in a PPy matrix thus allowed for rapid and accurate creatinine detection from whole blood resulting in a POC assay for allograft dysfunction (**Figure 3a**). [61]

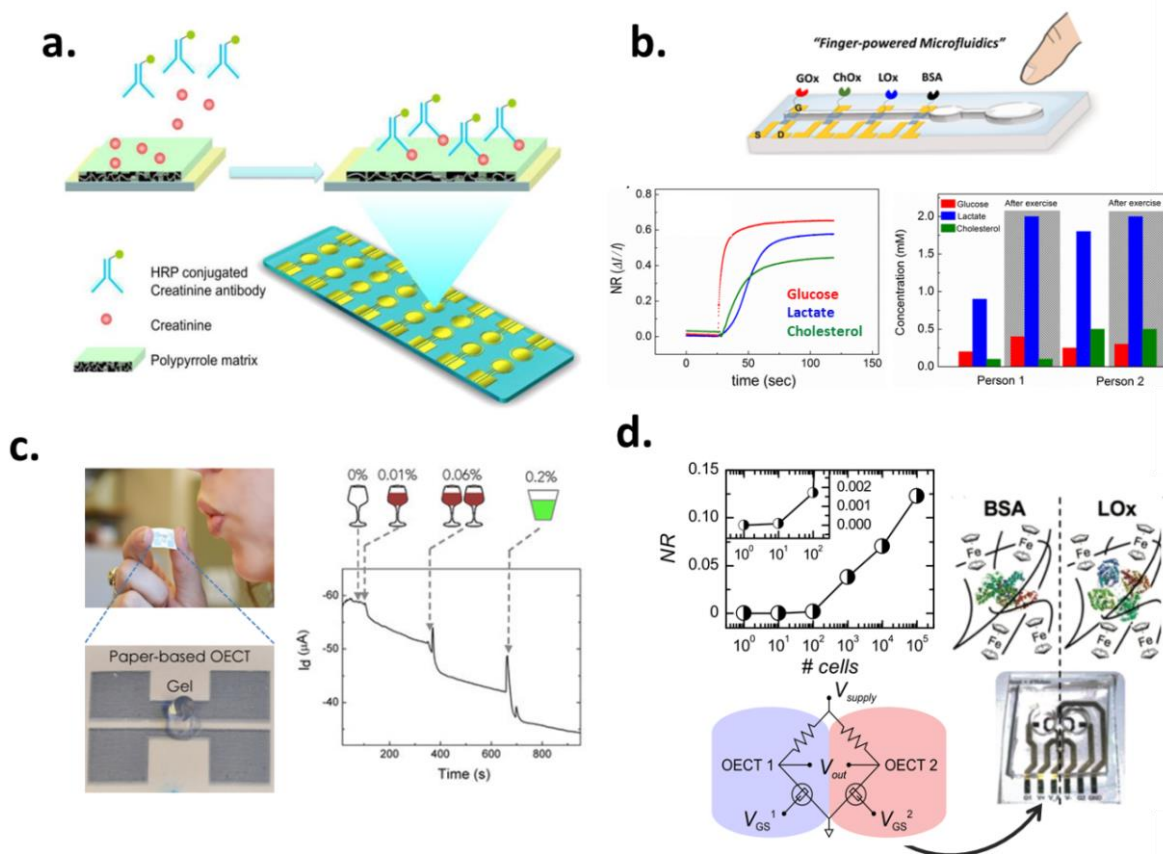


**Figure 3. Fully integrated point-of-care platforms based on organic electronics for in vitro detection of metabolites and used in real world applications.** (a) Illustration of the CP electrochemical sensor array for the direct measurement of creatinine from serum Copyright © 2013 American Chemical Society (b) Schematic showing the OECD-based multianalyte platform, simultaneous measurement of the three metabolites and the metabolites' levels of two healthy volunteers before and after exercise as measured by the proposed device. lens Copyright © 2016 WILEY-VCH Verlag GmbH & Co. KGaA, Weinheim (c) Photograph of the paper OECD- breathalyzer and curve showing the detection sensitivity. (d) Schematic of the sensitive reference-based OECD lactate sensing platform and lactate titration curve in different amounts of cells. lens Copyright © 2017 WILEY-VCH Verlag GmbH & Co. KGaA, Weinheim

Liao et al recently developed a flexible OECD platform based on PEDOT:PSS for the selective detection of urea and glucose in saliva samples. [62] To eliminate electrochemical interference in saliva, thus enhancing sensitivity and selectivity, the gate electrodes were modified with oppositely charged bilayer polymeric films for both anionic and cationic charge exclusion of interferents. Moving towards multiplexing, a PEDOT:PSS based OECD biosensing platform integrated with microfluidics, was developed for the simultaneous screening of glucose, lactate and cholesterol in human saliva samples. The interference issues were resolved by operating the device at a bias far below the oxidation potential of the electroactive species present in biofluids, by using ferrocene derivatives as a mediator. The final



device was tested with human volunteers before and after exercise to show relative variations of the metabolite profiles under stimuli (**Figure 3b**). [63] In a similar approach, simultaneous sensing of lactate and glucose was demonstrated by integrating two OECT-based devices each with a separate microfluidic channel. They generated a prototype portable glucose sensor by linking a smartphone with the device through Bluetooth connection, highlighting the ease of integration of such devices for POC systems.[64]

Electronic devices, (e-noses) have emerged as excellent candidates for the detection of breath volatile biomarkers compared with conventional methods used to date. Pavlou et al, were the first to detect the pathogen *Mycobacterium tuberculosis* both in vitro and in situ using a 14 gas-sensor array which consisted of a set of specifically tailored CPs which physically interact with volatile compounds produced by the in vitro cultures or the sputum samples, resulting in a change in electrical resistance. [65] In another study chemically-polymerized PPy films on-chip were used to capture absorbing and desorbing breath volatiles for subsequent chemical analysis from both environmental air samples as well as directly from exhaled human breath, paving the way for lab-on-a-chip-based environmental and health monitoring systems. [66] Bihar et. al recently developed a printed disposable breath analyser based on an all-PEDOT:PSS printed OECT, for the detection of blood alcohol levels from breath. The sensing platform, tested on human volunteers, showed remarkable sensitivity in detecting the consumption of even one glass of wine. (**Figure 3c**). [67]

### 3.1.2 Metabolite sensing from whole cells

Detection of cellular metabolites under different stimuli or environmental conditions can give useful insights for drug discovery and toxicology, particularly with the advent of organ-on-chip technologies. Larsen et al, used PEDOT:tosylate microelectrodes as an all polymer electrochemical chip for simple detection of potassium-induced transmitter release from neuron-like cells, demonstrating the potential of the method for drug screening applications. [68] To improve electrocatalytic activity of the sensing electrode, the PEDOT:PSS gate may also be decorated, with electrodeposited Pt nanoparticles (NPs). [69] Due to the high surface area of the NPs and the enzymes' specificity the authors achieved very sensitive determination of the critical metabolites glucose and lactate from live cells. Lactate production in tumor cell cultures derived from real patients was also measured using an OECT circuit. To circumvent the issue of interference in such samples, the proposed reference based sensor circuit design allowed for inherent background subtraction. Lactate production could be measured from a few

cells underlying the sensitivity of the device over a highly complex milieu and thus illustrating its potential for its use in *in vivo* applications for cancer diagnostics (**Figure 3d**). [70] In a more recent study, Curto et al demonstrated a multiparametric on-chip platform integrated with microfluidics for cell cultures, using among other in-line methods, the OECT-based detection of glucose produced by the cells as a measure to validate their improved differentiation under stimuli conditions. [71]

### 3.2 Wearable Metabolite Biosensors

**Box 3. Wearable metabolite sensors**

The diagram illustrates the field of wearable metabolite sensors, centered around a human figure. A vertical bar on the left indicates the level of invasiveness, ranging from high (red) to low (yellow). Six types of sensors are shown, each with a representative image and a line connecting it to the central figure:

- Saliva-based sensors:** A blue mouthpiece device.
- Tear-based sensors:** A small, circular device on a purple lens.
- Breath-based sensors:** A small white device held near a person's mouth.
- Sweat-based sensors:** A small device attached to a smartphone.
- Implantable sensors:** A small, circular device on a person's arm.
- ISF-blood based sensors:** A small, circular device on a person's skin.

**Overview of the rapidly growing field of wearable biosensors:** An undeniable trend in biosensor technology is on-body continuous monitoring of metabolites using wearable devices.[13] In parallel with the emergence of wearable electronics, wearable sensor-based systems for healthcare applications have attracted significant interest both in industrial and academic research.[72] Wearable biosensor applications aim to transform centralized hospital-based care systems to home-based personal medicine, reducing healthcare cost and time for diagnosis. Electrochemical transducers offer many advantages for wearable sensors for physiological monitoring, and can be easily integrated onto textile materials or directly on the skin. **Saliva-based: Copyright © 2016 Elsevier B.V., Implantable sensors: Copyright © 2013 WILEY-VCH Verlag GmbH & Co. KGaA, Weinheim, Tear-based: © 2016 WILEY-VCH Verlag GmbH & Co. KGaA, Weinheim, Sweat-based: © 2016 WILEY-VCH Verlag GmbH & Co. KGaA, Weinheim, ISF-blood based: Copyright © 2014 American Chemical Society**

The move towards biosensor technology for on-body continuous metabolite monitoring and the advancements in wearable electronics [13] have inevitably lead to wearable sensors for healthcare applications (see **Box 3**) [6, 72]. Although organic electronic materials have been successfully implemented into wearable sensors for electrophysiological measurements [73, 74], there are few examples of metabolite sensors using this technology as yet [75]. As we expect this area to trend rapidly, we present here some examples of current technologies used for metabolite sensing in wearable formats and illustrate progress towards this goal using organic electronic materials.

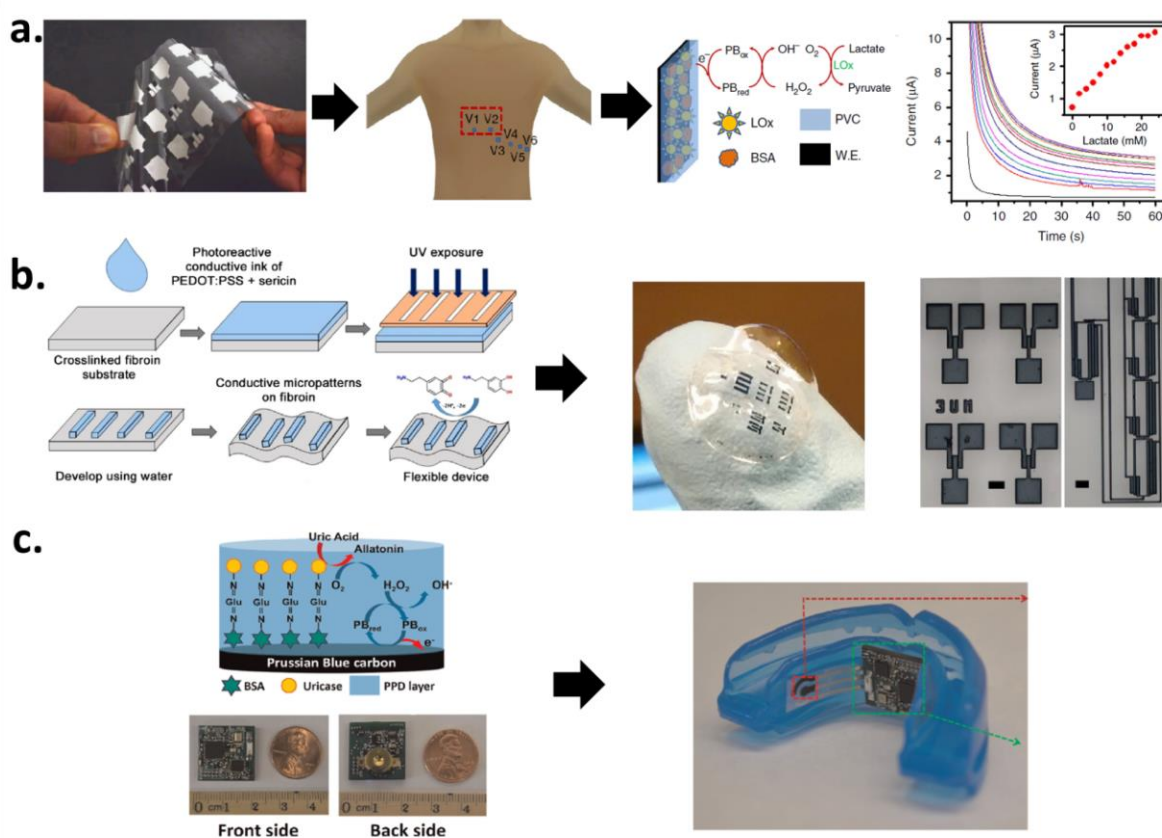


**Figure 4.** (a) Schematics of screen printed electrode, enzymatic sensing mechanism and amperometric response of wearable sweat-based lactate biosensor, [Copyright © 2016, Rights Managed by Nature Publishing Group](#) (b) schematic of fabrication steps on conductive micropattern on a flexible substrate, and large area micro patterns of flexible PEDOT:PSS on silk fibroin sheets with optical micrograph (Scalebars: 100 μm), [Copyright © 2016 Elsevier B.V.](#) (c) Saliva-based mouthguard uric acid biosensor and its various components with sensing principles. [Copyright © 2016 Elsevier B.V.](#)

Sweat-based wearable sensor systems, although mostly focused on a small number of physical or electrophysiological parameters, can yield significant information about a patient's

health status based on levels of the critical metabolites. [76] Wearable biosensors can be either textile/plastic based or epidermal (tattoo)-based systems.[77] Epidermal biosensors provide better contact with skin; but usually exhibit shorter life-time compared to textile based systems. Such biosensors were first developed in 2009 by the Rogers' group for continuous monitoring of physical parameters [78] and shortly after, Wang's group combined this approach with biorecognition elements towards the first printed tattoo-based biosensor.[79] A screen-printed electrode on temporary tattoo paper was developed with carbon and Ag/AgCl serving as working and reference electrode, respectively. The working electrode was also modified with CNTs carrying a mediator together with lactate oxidase (LOx) for continuous monitoring of lactate in sweat during exercise.[79] The same group later introduced a fully integrated sensor (comprising the sensory part, the microcontroller, the wireless communication system and the acquisition system) in an epidermal patch. The sensory part was composed of a screen-printed three electrode-based amperometric sensor and two carbon-based electrocardiogram electrodes for the simultaneous measurement of lactate and electrophysiological parameters (**Figure 4a**).[80]

CPs are especially advantageous for wearable sensor technology due to their compatibility with fabrication on flexible substrates.[56] In a very interesting approach, Pal. *et al* developed PEDOT:PSS electrodes on flexible fully biodegradable silk protein fibroin supports using a simple photolithographic process and an aqueous ink composed of the CP and carrier proteins. (**Figure 4b**).[81] The silk provided excellent mechanical and optical properties together with biocompatibility and controllable degradation. In a similar approach by the same group, silk proteins including fibroin and sericin were modified with photoreactive methacrylate groups to be used as substrate inks for the water-dispersible PEDOT:PSS that was micropatterned to develop biodegradable bioelectrode, for glucose sensing *in vitro* [82]. This opens up a new direction for the fabrication of an entirely organic, free-standing device with controllable biodegradability including scalability and processability, leading to applications in wearable or implantable bioelectronics with “wear/implant and forget” functionality[83] .

Complementing to recent progress on *in vitro* salivary diagnostics, wearable salivary sensing has also been reported, dating back to the 60s, where pH and other important electrolytes were measured on a partial denture.[84, 85] However, the focus now is on the development of wearable sensors for the early diagnosis of important metabolic diseases.[13, 86] An early example is a non-invasive mouthguard biosensor for continuous monitoring of uric acid, the end product of purine metabolism in the human body, developed by Wang *et al.*

al.[87] In this study, a screen-printed amperometric enzyme-based biosensor together with an integrated wireless transmitter were developed. As for their sweat sensors, carbon electrode containing mediators were printed as transducing elements on a plastic substrate and crosslinked uricase enzyme was electropolymerized to serve as the biorecognition element. A wireless amperometric circuit coupled with a Bluetooth low energy communication system was integrated on the mouthguard biosensor as shown in **Figure 4c**. [87] The advantages of this mouthguard sensor over in-dwelling type of devices are wearability, ease of operation and renewability.

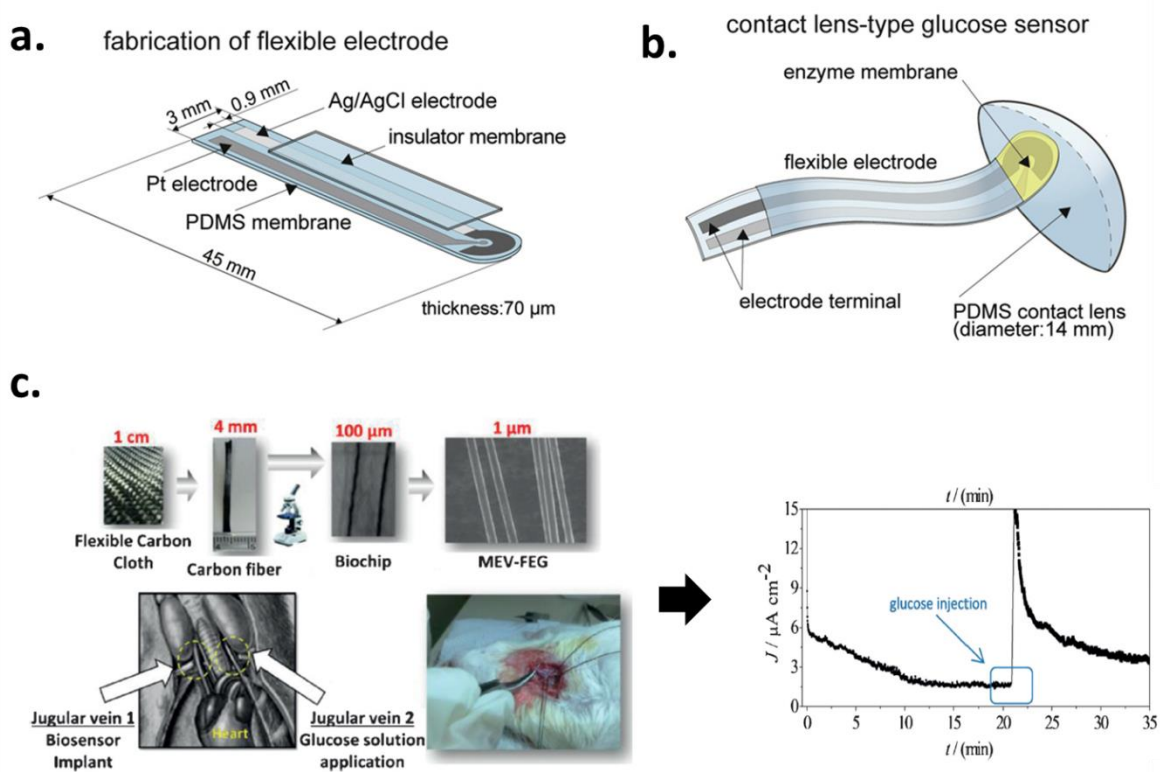


**Figure 5.** (a) The fabrication method of the contact lens biosensor on a flexible electrode and (b) integration of this electrode to the contact lens. Copyright © 2016 WILEY-VCH Verlag GmbH & Co. KGaA, Weinheim (c) Images showing the device fabrication steps and implantation in a rat vein, and *in vivo* chronoamperometry measurements with Glucose injection after 20 min (zoomed region). Copyright © 2015 WILEY-VCH Verlag GmbH & Co. KGaA, Weinheim

The very first successful prototype of electronic contact lenses was developed by Parviz *et. al.* in 2009, showing the first *in vivo* test of wirelessly powered contact lens display placed on a live, anesthetized rabbit's eye.[88] Later, they developed the first metabolite sensor in human tear fluid using the same contact lens approach by integrating a three- electrode

amperometric sensor system consisting of a Pt working electrode with immobilized GOx, and an external Ag/AgCl reference electrode on plastic films in an electrochemical cell again detecting H<sub>2</sub>O<sub>2</sub> catalysis.[89, 90] A lactate biosensor was developed in the same manner replacing GOx with LOx (Figure 1c).[91] Mitsubayashi *et. al.* developed an interesting strategy to produce enzyme-based glucose biosensors by integrating a polydimethyl siloxane (PDMS) membrane onto a contact lens. The counter/reference electrodes were fabricated by successively sputtering Ag and Pt metal onto a 70 μm thick PDMS substrate (**Figure 5a-b**).[92] Flexible electrodes were then bonded onto the surface of the contact lens using PDMS, and GOx was immobilized on the sensing region of the electrode. This integrated biosensor was successfully tested using a rabbit model.[92] Progress is moving towards integration of organic electronic materials into metabolite sensors from tears; a recent study by Lee et al has illustrated the potential for integration of graphene into contact lenses [93], while Tehrani et al are working towards a rapid detection of glucose on CuNP decorated graphene electrodes. [94]

Even though there has been no commercial success as yet in non-invasive wearable metabolite sensing using saliva, tears or sweat, limited commercial success has been achieved with interstitial fluid (ISF) based biosensors.[20] One of the most well-known examples is The GlucoWatch Biographer™ (Cygnus, Inc.). Having initially attracted considerable attention in the early 2000s, it was quickly withdrawn due to significant inaccuracies, sampling errors, skin irritation problems and frequent calibration needs.[19] Recently, Abbott launched the FreeStyleLibre as a new wearable continuous glucose monitoring device, [95] showing more promise in terms of comfort and user interface; the sensor can be used for 14 days and does not require any finger-stick calibration while its small sensory part (0.2 inches long) directly connects to a plastic patch that can be easily placed on the upper arm The glucose concentration is transferred in real-time to an external reader wirelessly *via* a near infra-red identification tag. [95] This recent progress on ISF based biosensor further expands the wearable biosensor market, and is anticipated to extend to other types of biosensors in the near future.

### 3.3 Implantable Biosensors

The concept of implantable metabolite sensors was first proposed by Leyland C. Clark in his seminal paper in 1962,[1] but was put into practice by Shichiri *et. al* in the early 80s.[96] There have been many different research efforts since then, mostly focusing on developing continuous glucose monitoring systems.[97] In one prominent study, an implantable 100 mm flexible

biochip for intravenous glucose sensing in rat blood was described.[98] The fabricated microelectrode was modified with a carbon-based composite consisting of flexible carbon fibres, neutral red as a mediator and GOx as an enzyme layer. The device was inserted in the thoracic region of a living rat for glucose measurements, simulating diabetic conditions by injecting glucose intravenously (**Figure 5c**). [98]

Despite limited progress in academic studies, considerable success has been achieved in industrial research and the implantable biosensor market has begun to expand in the last decade. In 2005, Medtronic (USA) launched the first implantable continuous glucose monitoring device for personal use.[6, 19] The self-implanted sensor was based on the amperometric determination of H<sub>2</sub>O<sub>2</sub> produced by the oxidation of glucose in the presence of glucose oxidase. Despite the commercial and medical success, there are still restrictions that limit to some extent the use of such devices. For instance, FDA still stipulates that the finger stick blood test must be performed in parallel when using these self-implantable biosensors. In addition issues such as biocompatibility, reliability, and powering all crucial aspects for implantable, long life-time devices still remain.[19] While it is impossible to include all successful devices in this review, there are other reviews for the reader interested in learning more about the historical evolution and development of commercialised implantable biosensors.[6, 19-21, 99]

## 4. Conclusions

Despite the significant progress in biosensor development, successfully commercialized devices are still scarce, with glucose sensors a notable exception. The dual market demands of high analytical performance and cheap, easy-to-use, long-lasting devices often render their clinical implementation beyond the reach of current technologies. Organic electronics is a field of research that has rapidly come to the fore for biological applications, despite its beginnings in areas such as large area, flexible applications embodied by devices such as the organic light emitting diode or organic photovoltaics. One of the factors credited for the success of organic electronics in biosensing applications is the literal flexibility and tunability of these materials to adapt to challenging performance requirements in biological milieux. Organic electronics may therefore represent the ideal technology to meet the market demands. Indeed, in cases of bioelectrocatalytic detection methods –such as those described in this review- we show examples where their organic, often polymeric in nature structure can allow for molecular wiring with the enzyme's active site and thus achieve high sensitivities without the need of

artificial electron mediators. Bearing in mind commonly raised issues in terms of stability and lifetime of the enzymes, future trends in this dynamic fast moving field of organic electronic biocatalytic sensors are anticipated towards the development of biomimetic architectures (i.e., molecular imprinted structures) harnessing the versatility in synthesis of such electronic materials. Transducer and biorecognition element can be sought as a single active component, combining electronic functionalities and the best features of the biological reagent in a more stable matrix, opening up new exciting directions in biosensor technology from both fundamental and practical aspect.

## Acknowledgements

A.M.P and R.O gratefully acknowledge the support by the Marie Curie ITN project OrgBio No. 607896. O.P. gratefully acknowledges support from the Knut and Alice Wallenberg Foundation (KAW 2014.0387) for postdoctoral research at Stanford University.

## References

- [1] Clark, L.C., Jr. and Lyons, C. (1962) Electrode systems for continuous monitoring in cardiovascular surgery. *Annals of the New York Academy of Sciences* 102, 29-45
- [2] Shukla, S.K., et al. (2014) Self-Reporting Micellar Polymer Nanostructures for Optical Urea Biosensing. *Industrial & Engineering Chemistry Research* 53, 8509-8514
- [3] Parlak, O., et al. (2017) Structuring Au nanoparticles on two-dimensional MoS<sub>2</sub> nanosheets for electrochemical glucose biosensors. *Biosensors & Bioelectronics* 89, 545-550
- [4] Parlak, O., et al. (2014) Two-Dimensional Gold-Tungsten Disulphide Bio-Interface for High-Throughput Electrocatalytic Nano-Bioreactors. *Advanced Materials Interfaces* 1
- [5] Scheller, F. and Schubert, F. (1991) *Biosensors*. Elsevier Science
- [6] Turner, A.P.F. (2013) Biosensors: sense and sensibility. *Chemical Society Reviews* 42, 3184-3196



- [7] Bard, A.J. and Faulkner, L.R. (2000) *Electrochemical Methods: Fundamentals and Applications*. Wiley
- [8] Jay, C.R.G.W., et al. (2013) *Electrochemistry*. Royal Society of Chemistry
- [9] Kleijn, S.E.F., et al. (2014) *Electrochemistry of Nanoparticles*. *Angewandte Chemie-International Edition* 53, 3558-3586
- [10] Parlak, O., et al. (2013) Template-directed hierarchical self-assembly of graphene based hybrid structure for electrochemical biosensing. *Biosensors & Bioelectronics* 49, 53-62
- [11] Osikoya, A., et al. (2016) Acetylene Sourced CVD synthesized catalytically active graphene for electrochemical biosensing. *Biosensors and Bioelectronics*
- [12] Kimmel, D.W., et al. (2012) *Electrochemical Sensors and Biosensors*. *Analytical Chemistry* 84, 685-707
- [13] Sekretaryova, A.N., et al. (2016) Bioelectrocatalytic systems for health applications. *Biotechnology Advances* 34, 177-197
- [14] Sekretaryova, A.N., et al. (2014) Unsubstituted phenothiazine as a superior water-insoluble mediator for oxidases. *Biosensors & Bioelectronics* 53, 275-282
- [15] Palazzo, G., et al. (2015) Detection Beyond Debye's Length with an Electrolyte-Gated Organic Field-Effect Transistor. *Advanced Materials* 27, 911-916
- [16] Kim, S.H., et al. (2013) Electrolyte-Gated Transistors for Organic and Printed Electronics. *Advanced Materials* 25, 1822-1846
- [17] Rivnay, J., et al. (2015) High-performance transistors for bioelectronics through tuning of channel thickness. *Science Advances* 1
- [18] Inal, S., et al. (2014) A High Transconductance Accumulation Mode Electrochemical Transistor. *Advanced Materials* 26, 7450-7455
- [19] Gifford, R. (2013) Continuous Glucose Monitoring: 40 Years, What Weve Learned and What's Next. *Chemphyschem* 14, 2032-2044

- [20] Newman, J.D. and Turner, A.P.F. (2005) Home blood glucose biosensors: a commercial perspective. *Biosensors & Bioelectronics* 20, 2435-2453
- [21] Wilson, G.S. and Gifford, R. (2005) Biosensors for real-time in vivo measurements. *Biosensors & Bioelectronics* 20, 2388-2403
- [22] Owens, R.M. and Malliaras, G.G. (2010) Organic Electronics at the Interface with Biology. *Mrs Bulletin* 35, 449-456
- [23] Rivnay, J., et al. (2014) The Rise of Organic Bioelectronics. *Chemistry of Materials* 26, 679-685
- [24] Mathieson, K., et al. (2012) Photovoltaic Retinal Prosthesis with High Pixel Density. *Nat Photonics* 6, 391-397
- [25] Someya, T., et al. (2016) The rise of plastic bioelectronics. *Nature* 540, 379-385
- [26] Lanzani, G. (2014) Materials for bioelectronics: organic electronics meets biology. *Nat Mater* 13, 775-776
- [27] Pitsalidis, C., et al. (2016) High mobility transistors based on electro-spray-printed small-molecule/polymer semiconducting blends. *Journal of Materials Chemistry C* 4, 3499-3507
- [28] Bettinger, C.J. and Bao, Z. (2010) Organic thin-film transistors fabricated on resorbable biomaterial substrates. *Adv Mater* 22, 651-655
- [29] Takamatsu, S., et al. (2016) Wearable Keyboard Using Conducting Polymer Electrodes on Textiles. *Adv Mater* 28, 4485-4488
- [30] Adhikari, B.R., et al. (2015) Carbon Nanomaterials Based Electrochemical Sensors/Biosensors for the Sensitive Detection of Pharmaceutical and Biological Compounds. *Sensors (Basel)* 15, 22490-22508
- [31] Yang, W., et al. (2010) Carbon Nanomaterials in Biosensors: Should You Use Nanotubes or Graphene? *Angewandte Chemie International Edition* 49, 2114-2138

- [32] Chiang, C.K., et al. (1977) Electrical Conductivity in Doped Polyacetylene. *Physical Review Letters* 39, 1098-1101
- [33] Bredas, J.L. and Street, G.B. (1985) Polarons, bipolarons, and solitons in conducting polymers. *Accounts of Chemical Research* 18, 309-315
- [34] Crispin, X., et al. (2006) The Origin of the High Conductivity of Poly(3,4-ethylenedioxythiophene)-Poly(styrenesulfonate) (PEDOT-PSS) Plastic Electrodes. *Chemistry of Materials* 18, 4354-4360
- [35] Malhotra, B.D., et al. (2006) Prospects of conducting polymers in biosensors. *Anal Chim Acta* 578, 59-74
- [36] Vallejo-Giraldo, C., et al. (2014) Biofunctionalisation of electrically conducting polymers. *Drug Discov Today* 19, 88-94
- [37] Schuhmann, W. (2002) Amperometric enzyme biosensors based on optimised electron-transfer pathways and non-manual immobilisation procedures. *J Biotechnol* 82, 425-441
- [38] Schuhmann, W., et al. (2000) Electron-transfer pathways between redox enzymes and electrode surfaces: reagentless biosensors based on thiol-monolayer-bound and polypyrrole-entrapped enzymes. *Faraday Discuss*, 245-255; discussion 257-268
- [39] Swann, M.J., et al. (1997) The role of polypyrrole as charge transfer mediator and immobilization matrix for d-fructose dehydrogenase in a fructose sensor. *Biosensors and Bioelectronics* 12, 1169-1182
- [40] Pud, A.A. (1994) Stability and degradation of conducting polymers in electrochemical systems. *Synthetic Metals* 66, 1-18
- [41] Kros, A., et al. (2005) Poly(pyrrole) versus poly(3,4-ethylenedioxythiophene): implications for biosensor applications. *Sensors and Actuators B: Chemical* 106, 289-295
- [42] Kros, A., et al. (2001) Poly(3,4-ethylenedioxythiophene)-Based Glucose Biosensors. *Advanced Materials* 13, 1555-1557

- [43] Thompson, B.C., et al. (2010) Conducting Polymer Enzyme Alloys: Electromaterials Exhibiting Direct Electron Transfer. *Macromolecular Rapid Communications* 31, 1293-1297
- [44] Wang, J.-Y., et al. (2013) Synthesis of Redox Polymer Nanobeads and Nanocomposites for Glucose Biosensors. *ACS Applied Materials & Interfaces* 5, 7852-7861
- [45] Pan, L., et al. (2012) Hierarchical nanostructured conducting polymer hydrogel with high electrochemical activity. *Proceedings of the National Academy of Sciences* 109, 9287-9292
- [46] Mano, N., et al. (2007) An Electron-Conducting Cross-Linked Polyaniline-Based Redox Hydrogel, Formed in One Step at pH 7.2, Wires Glucose Oxidase. *Journal of the American Chemical Society* 129, 7006-7007
- [47] Li, L., et al. (2015) A nanostructured conductive hydrogels-based biosensor platform for human metabolite detection. *Nano Lett* 15, 1146-1151
- [48] Centonze, D., et al. (1992) Interference-free glucose sensor based on glucose-oxidase immobilized in an overoxidized non-conducting polypyrrole film. *Fresenius' Journal of Analytical Chemistry* 342, 729-733
- [49] Xue, H., et al. (2001) Polyaniline-polyisoprene composite film based glucose biosensor with high permselectivity. *Synthetic Metals* 124, 345-349
- [50] Yang, G., et al. (2014) High-Performance Conducting Polymer Nanofiber Biosensors for Detection of Biomolecules. *Advanced materials (Deerfield Beach, Fla.)* 26, 4954-4960
- [51] Forzani, E.S., et al. (2004) A Conducting Polymer Nanojunction Sensor for Glucose Detection. *Nano Letters* 4, 1785-1788
- [52] Strakosas, X., et al. (2015) The organic electrochemical transistor for biological applications. *Journal of Applied Polymer Science* 132
- [53] Pappa, A.-M., et al. (2017) Polyelectrolyte Layer-by-Layer Assembly on Organic Electrochemical Transistors. *ACS Applied Materials & Interfaces* 9, 10427-10434

- [54] N. Bartlett, P. (1998) Measurement of low glucose concentrations using a microelectrochemical enzyme transistor. *Analyst* 123, 387-392
- [55] Zhu, Z.-T., et al. (2004) A simple poly(3,4-ethylene dioxythiophene)/poly(styrene sulfonic acid) transistor for glucose sensing at neutral pH. *Chemical Communications*, 1556-1557
- [56] Khodagholy, D., et al. (2012) Organic electrochemical transistor incorporating an ionogel as a solid state electrolyte for lactate sensing. *Journal of Materials Chemistry* 22, 4440-4443
- [57] Zhang, M., et al. (2015) Highly sensitive glucose sensors based on enzyme-modified whole-graphene solution-gated transistors. *Scientific Reports* 5, 8311
- [58] Scheiblin, G., et al. (2015) Screen-printed organic electrochemical transistors for metabolite sensing. *MRS Communications* 5, 507-511
- [59] Mak, C.H., et al. (2015) Highly-sensitive epinephrine sensors based on organic electrochemical transistors with carbon nanomaterial modified gate electrodes. *Journal of Materials Chemistry C* 3, 6532-6538
- [60] Krishnan, S., et al. (2008) Advances in polymers for anti-biofouling surfaces. *Journal of Materials Chemistry* 18, 3405-3413
- [61] Wei, F., et al. (2012) Serum Creatinine Detection by a Conducting-Polymer-Based Electrochemical Sensor To Identify Allograft Dysfunction. *Analytical Chemistry* 84, 7933-7937
- [62] Liao, C., et al. (2015) Flexible organic electrochemical transistors for highly selective enzyme biosensors and used for saliva testing. *Adv Mater* 27, 676-681
- [63] Pappa, A.M., et al. (2016) Organic Transistor Arrays Integrated with Finger-Powered Microfluidics for Multianalyte Saliva Testing. *Adv Healthc Mater* 5, 2295-2302
- [64] Ji, X., et al. (2016) Highly Sensitive Metabolite Biosensor Based on Organic Electrochemical Transistor Integrated with Microfluidic Channel and Poly(N-vinyl-2-pyrrolidone)-Capped Platinum Nanoparticles. *Advanced Materials Technologies* 1, 1600042

- [65] Pavlou, A.K., et al. (2004) Detection of Mycobacterium tuberculosis (TB) in vitro and in situ using an electronic nose in combination with a neural network system. *Biosensors & bioelectronics* 20, 538-544
- [66] Strand, N., et al. (2010) Chemically Polymerized Polypyrrole for On-Chip Concentration of Volatile Breath Metabolites. *Sensors and actuators. B, Chemical* 143, 516-523
- [67] Bihar, E., et al. (2016) A Disposable paper breathalyzer with an alcohol sensing organic electrochemical transistor. *Scientific Reports* 6, 27582
- [68] Larsen, S.T., et al. (2012) Characterization of poly(3,4-ethylenedioxythiophene):tosylate conductive polymer microelectrodes for transmitter detection. *Analyst* 137, 1831-1836
- [69] Strakosas, X., et al. (2017) Catalytically enhanced organic transistors for in vitro toxicology monitoring through hydrogel entrapment of enzymes. *Journal of Applied Polymer Science* 134
- [70] Braendlein, M., et al. (2017) Lactate Detection in Tumor Cell Cultures Using Organic Transistor Circuits. *Advanced Materials*, 1605744
- [71] Curto, V., et al. (2017) A multi-parametric organic transistor toolbox with integrated microfluidics for in line in vitro cell monitoring. *Microsystems and Nanoengineering*
- [72] Khan, Y., et al. (2016) Monitoring of Vital Signs with Flexible and Wearable Medical Devices. *Advanced Materials* 28, 4373-4395
- [73] Takamatsu, S., et al. (2015) Direct patterning of organic conductors on knitted textiles for long-term electrocardiography. *5*, 15003
- [74] Bihar, E., et al. (2017) Fully Printed Electrodes on Stretchable Textiles for Long-Term Electrophysiology. *Advanced Materials Technologies* 2, 1600251
- [75] Gualandi, I., et al. (2016) Textile Organic Electrochemical Transistors as a Platform for Wearable Biosensors. *6*, 33637
- [76] Heikenfeld, J. (2016) Technological leap for sweat sensing. *Nature* 529, 475-476

- [77] Parrilla, M., et al. (2016) A Textile-Based Stretchable Multi-Ion Potentiometric Sensor. *Advanced Healthcare Materials* 5, 996-1001
- [78] Kim, D.H., et al. (2011) Epidermal Electronics. *Science* 333, 838-843
- [79] Jia, W.Z., et al. (2013) Electrochemical Tattoo Biosensors for Real-Time Noninvasive Lactate Monitoring in Human Perspiration. *Analytical Chemistry* 85, 6553-6560
- [80] Imani, S., et al. (2016) A wearable chemical-electrophysiological hybrid biosensing system for real-time health and fitness monitoring. *Nature Communications* 7
- [81] Pal, R.K., et al. (2016) Conducting polymer-silk biocomposites for flexible and biodegradable electrochemical sensors. *Biosensors & Bioelectronics* 81, 294-302
- [82] Kurland, N.E., et al. (2013) Precise Patterning of Silk Microstructures Using Photolithography. *Advanced Materials* 25, 6207-6212
- [83] Kurland, N.E., et al. (2014) Silk Protein Lithography as a Route to Fabricate Sericin Microarchitectures. *Advanced Materials* 26, 4431
- [84] Graf, H. and Muhleman, H.R. (1966) TELEMETRY OF PLAQUE PH FROM INTERDENTAL AREA. *Helvetica Odontologica Acta* 10, 94
- [85] Graf, H. and Muhlemann, H.R. (1969) ORAL TELEMETRY OF FLUORIDE ION ACTIVITY. *Archives of Oral Biology* 14, 259
- [86] Bandodkar, A.J. and Wang, J. (2014) Non-invasive wearable electrochemical sensors: a review. *Trends in Biotechnology* 32, 363-371
- [87] Kim, J., et al. (2015) Wearable salivary uric acid mouthguard biosensor with integrated wireless electronics. *Biosensors & Bioelectronics* 74, 1061-1068
- [88] Shum, A.J., et al. (2009) Functional modular contact lens. In *Biosensing II* (Razeghi, M. and Mohseni, H., eds)
- [89] Parviz, B.A. (2009) FOR YOUR EYE ONLY. *Ieee Spectrum* 46, 36-41

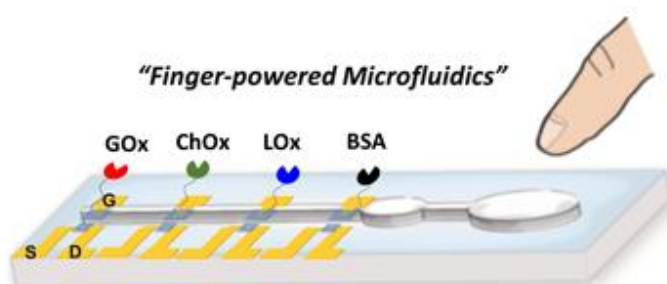
- [90] Yao, H., et al. (2011) A DUAL MICROSCALE GLUCOSE SENSOR ON A CONTACT LENS, TESTED IN CONDITIONS MIMICKING THE EYE. In 2011 Ieee 24th International Conference on Micro Electro Mechanical Systems, pp. 25-28
- [91] Thomas, N., et al. (2012) A contact lens with an integrated lactate sensor. *Sensors and Actuators B-Chemical* 162, 128-134
- [92] Chu, M.X., et al. (2011) Soft contact lens biosensor for in situ monitoring of tear glucose as non-invasive blood sugar assessment. *Talanta* 83, 960-965
- [93] Lee, S., et al. (2017) Smart Contact Lenses with Graphene Coating for Electromagnetic Interference Shielding and Dehydration Protection. *ACS Nano*
- [94] Tehrani, F., et al. (2015) Rapid Prototyping of a High Sensitivity Graphene Based Glucose Sensor Strip. *PLoS ONE* 10, e0145036
- [95] <http://www.freestylelibre.com/>.
- [96] Shichiri, M., et al. (1982) WEARABLE ARTIFICIAL ENDOCRINE PANCREAS WITH NEEDLE-TYPE GLUCOSE SENSOR. *Lancet* 2, 1129-1131
- [97] Katz, E. (2014) *Implantable Bioelectronics*. John Wiley & Sons
- [98] Iost, R.M., et al. (2015) Glucose Biochip Based on Flexible Carbon Fiber Electrodes: In Vivo Diabetes Evaluation in Rats. *Chemelectrochem* 2, 518-521
- [99] Vaddiraju, S., et al. (2010) Emerging synergy between nanotechnology and implantable biosensors: A review. *Biosensors & Bioelectronics* 25, 1553-1565



# Chapter 2

---

## Organic Transistor Arrays Integrated with Finger-Powered Microfluidics for Multianalyte Saliva Testing



The present Chapter is based on the following publication:

**“Organic Transistor Arrays Integrated with Finger-Powered  
Microfluidics for Multianalyte Saliva Testing”**

*A. M. Pappa, V. F. Curto, M. Braendlein, X. Strakosas, M.J. Donahue, M.*

*Fiocchi, G. G. Malliaras, R. M. Owens*

*Adv. Healthcare Mater. 2016, 5, 2295–2302*

## Abstract

We report a compact multianalyte biosensing platform, comprised of an organic electrochemical transistor (OECT) microarray integrated with a pumpless “finger-powered” microfluidic, for quantitative screening of glucose, lactate and cholesterol levels. A biofunctionalization method was designed which provides selectivity towards specific metabolites as well as minimization of any background interference. In addition, we developed a simple method to facilitate multi-analyte sensing and avoid electrical crosstalk between the different transistors by electrically isolating the individual devices. The resulting biosensing platform, verified using human samples, offers the possibility to be used in easy-to-obtain biofluids with low abundance metabolites, such as saliva. Based on our proposed method, other types of enzymatic biosensors can be integrated into the array to achieve multiplexed, non-invasive, personalized point-of-care diagnostics.

### Author’s contribution:

For the present publication, used as chapter 2 in this thesis my contribution was: the OECT fabrication and characterization, the development of the biofunctionalization strategy, and the biosensor characterization. Moreover, I prepared the manuscript, including the figures.

## 1. Introduction

Point-of-care testing (POCT), is one of the fastest growing sectors of medical diagnostics. However, effective POCT methods pose stringent requirements and challenges for biosensor development.<sup>[1-3]</sup> Multiplexed and compact devices for high throughput analysis in a cost-effective and time-saving manner, are urgently required for next generation biosensors, to provide more holistic and accurate understanding of the system under investigation. Advances in electronics and microfabrication have allowed the miniaturization of various optical and electronic transducers allowing for faster and more sensitive devices for diagnostics.<sup>[4,5]</sup> Despite these developments, it remains challenging to develop portable, low-cost biosensing platforms that are able to detect multiple metabolites simultaneously with high sensitivity and selectivity.

Lactate, glucose and cholesterol are metabolites of critical importance in healthcare. Although cellular metabolic pathways are somewhat complex, quantification of such key markers in normal and under different conditions, as well as assaying their relative abundance compared to other metabolites, can provide useful insights for the health status of an individual. For example, due to the close metabolic relationship between glucose and lactate, fluctuations of their absolute or relative concentrations, along with cholesterol quantification, can be correlated with certain medical conditions such as heart disease and diabetes.<sup>[6,7]</sup> Commercialized metabolite sensor chips rely mainly on finger-stick blood draws. However, the intrusiveness and inconvenience of such blood – sampling methods as well as the stringent requirements for continuous real-time sampling and screening (for example in areas as diverse as critical healthcare units to sports medicine) emphasize the importance of non-invasive biosensing technologies using alternative biofluids such as saliva.<sup>[8]</sup>

Organic electrochemical transistors (OECTs) represent a very promising class of organic thin film transistors (OTFTs) that have recently fueled scientific interest as especially performant transducers in sensing applications. OECTs couple the advantages of OTFTs<sup>[9]</sup> (i.e., simple electrical readout, inherent signal amplification, ease of fabrication and straightforward miniaturization), with electrochemically driven operation in aqueous solutions, thereby establishing a conduit between electronics and biology.<sup>[10]</sup> OECTs, unlike the vast majority of OTFTs, comprise an organic active layer which is in direct contact with the biological milieu of interest. The working principle relies on the electrochemical doping/de-doping of the organic semiconductor upon application of a small gate bias.<sup>[11,12]</sup> As amplifying transducers of ionic-to-electronic signals, OECTs can also be integrated with microfluidic channels, toward lab-on-a-chip applications.<sup>[13,14]</sup>

Poly(3,4-ethylene-dioxythiophene):poly(styrene sulfonic acid) (PEDOT:PSS) has emerged as the benchmark material of organic bioelectronics<sup>[15-17]</sup> and is typically employed as the active layer of OECTs. Such devices have been used as ion-selective sensors,<sup>[18,19]</sup> cell-based sensors<sup>[20,21]</sup> and when coupled with redox enzymes, as biocatalytic sensors for the detection of metabolites (i.e., glucose, lactate, etc),<sup>[22-24]</sup> the latter showing great potential for POCT applications. Kergoat et al recently reported on the use of PEDOT:PSS based OECTs for single- analyte detection of critical neurotransmitters such as glutamate and acetylcholine,<sup>[25]</sup> while Liao et al demonstrated sensitive and selective single-analyte detection of key metabolites such as glucose and urea in saliva samples, as a potential POCT system.<sup>[26]</sup> In those studies, as in most cases of amperometric biosensors using an oxidase type of enzyme, the sensing mechanism relies on the detection of hydrogen peroxide (H<sub>2</sub>O<sub>2</sub>), a by-product of the enzymatic reactions. In practical applications, such approaches suffer from several constraints related to the selectivity of the device, mainly due to the existence of electro-active compounds in complex media. Specifically, the relatively high potential (0.6 V vs. Ag/AgCl reference) required for the oxidation of H<sub>2</sub>O<sub>2</sub> increases significantly the level of interference from endogenous electroactive species (e.g., uric acid, dopamine, and ascorbic acid) that are present in bodily fluids, leading to misinterpretation of the recorded signals. One possible strategy to reduce or eliminate electrochemical interference of endogenous species is through the use of permselective membranes such as nafion and poly-lysine for size or charge based exclusion of the interferents.<sup>[26]</sup>

In the case of multianalyte detection from a single biological sample, diffusion of H<sub>2</sub>O<sub>2</sub> between adjacent biosensors may also lead to signal misinterpretation. Notably, two kinds of “cross-talk” should be considered, electrical and chemical. The former results primarily from capacitive coupling and the latter from diffusion of H<sub>2</sub>O<sub>2</sub>.<sup>[27]</sup> Arguably, a more elegant alternative to the detection of H<sub>2</sub>O<sub>2</sub> is the use of mediators as a strategy to improve selectivity and performance of such amperometric biosensors. Indeed, as we show in this study, by using a novel biofunctionalisation scheme incorporating an electron mediator (ferrocene), molecular wiring of the enzyme active site to the electrode is achieved, thus lowering the working potential of the electrodes, and reducing background signal.

We report here, for the first time, the development of a compact biosensing platform consisting of multiplexed OECTs for the simultaneous detection of three critical biomarkers: glucose, lactate and cholesterol. The real-time detection of a combination of analytes from human saliva samples is achieved in a non-invasive and label-free manner with high selectivity

and sensitivity in the relevant physiological ranges. Additionally, this versatile platform is integrated with a simple pumpless poly(dimethylsiloxane) (PDMS) - based microfluidic towards the realization of POCT devices.

## 2. Results and discussion

### 2.1 OECT biofunctionalization and use for enzymatic sensing

**Figure 1a** shows a schematic illustration of the device structure of a single OECT fabricated on a glass substrate, as well as the generic biofunctionalization scheme at the planar gate electrode of each transistor, based on the method of Strakosas et al.<sup>[28]</sup> Briefly, by blending PEDOT:PSS with polyvinyl alcohol (PVA), we introduce free hydroxyl groups on the surface of the conducting polymer, a functionality subsequently used for covalent attachment of a heterobifunctional silane (3-glycidoxypropyltrimethoxysilane, GOPS) via a condensation reaction. A different protein was then immobilized on each gate electrode of the four transistors, namely glucose oxidase (GOx), lactate oxidase (LOx) and cholesterol oxidase (ChOx) for the respective detection of glucose, lactate and cholesterol. Bovine serum albumin (BSA) was immobilized on the fourth electrode serving as the control.

The first generation of enzymatic biosensors, in which the co-substrate for the enzyme is oxygen, suffer from several disadvantages, principally oxygen dependence and interference from electro-oxidizable compounds. Indeed, when we used a highly complex biological matrix, i.e., whole blood, we observed a significant decrease in the background signal when the same device was operated at low potential (0.2 V) compared to a higher potential (0.4 V) (**Supplementary Figure S1**). To circumvent this issue, other types of redox active molecules have been used as an alternative co-substrate for the enzyme (known as electrochemical mediators), to reduce the applied potential to near - zero values.<sup>[29,30]</sup>

Among the electron mediators used in biosensing applications, ferrocene (Fc), a stable organometallic compound, is frequently used due to its favorable intrinsic properties (i.e., low molecular mass, good electrochemical stability and reversibility at low potentials and formation of stable redox states).<sup>[31]</sup> However, Fc absorbs weakly onto metal electrodes due to its small size and low affinity with such surfaces, leading to leaching of Fc, with subsequent concerns for toxicity. A solution to this issue is to provide a supporting matrix to improve the stability of the system.



the modified electrode in PBS are characteristic of the immobilized Fc group, whereas the drastic increase of the current in the presence of glucose in the buffer solution indicates the effective immobilization of GOx and the expected enzymatic reaction.

The sensing mechanism of our platform, based on the enzyme/mediator complex functionalized gate electrode is illustrated in **Figure 1c**. Upon addition of a sample containing the substrate of interest, an enzymatic reaction occurs, the enzyme is reduced and cycles back via the ferrocene/ferricenium (Fc/Fc<sup>+</sup>) ion couple which mediates electron transfer between the redox enzyme and the PEDOT: PSS gate electrode, due to its low oxidation potential. The resulting change in the gating of the channel is proportional to the concentration of the analyte allowing its quantification. The reaction cycles at the gate electrode specifically for each of the three analytes along with the subsequent reactions at the channel are shown in **Supplementary Figure S2a**.

## 2.2 Characterization of biofunctionalised OECTs

OECTs have proven to exhibit the highest transconductance ( $g_m$ ) among electrolyte-gated transistors of comparable geometry,<sup>[11]</sup> defined as  $g_m = \partial I_D / \partial V_G$ . Transconductance is the figure of merit for biosensing applications as it sensitively quantifies the current flowing in the channel ( $I_D$ , drain current), in response to a change ( $V_G$ , gate voltage), and is thus a measure of the “efficiency” of transduction of a biological event. Rivnay et al, recently demonstrated that the transconductance of an OECT can be tuned by not only changing the channel geometry but also the conducting polymer film thickness.<sup>[34]</sup> We customized the channel geometry in order to obtain the highest transconductance value at the applied gate bias of 0.1- 0.2 V which coincides with the working potential of our enzymatic sensors (0.2 V). **Figure 2a**, shows the transfer characteristics of such an OECT, before and after the gate biofunctionalization. These characteristics demonstrate typical low voltage operation ( $V_G, V_D < |1 \text{ V}|$ ) in the depletion mode. The corresponding  $g_m$  exhibits its maximum value of 16 mS at  $V_G = 0.15 \text{ V}$  and  $V_D = -0.6 \text{ V}$ . Notably, the biofunctionalization process doesn't lead to any significant alterations in the device performance.

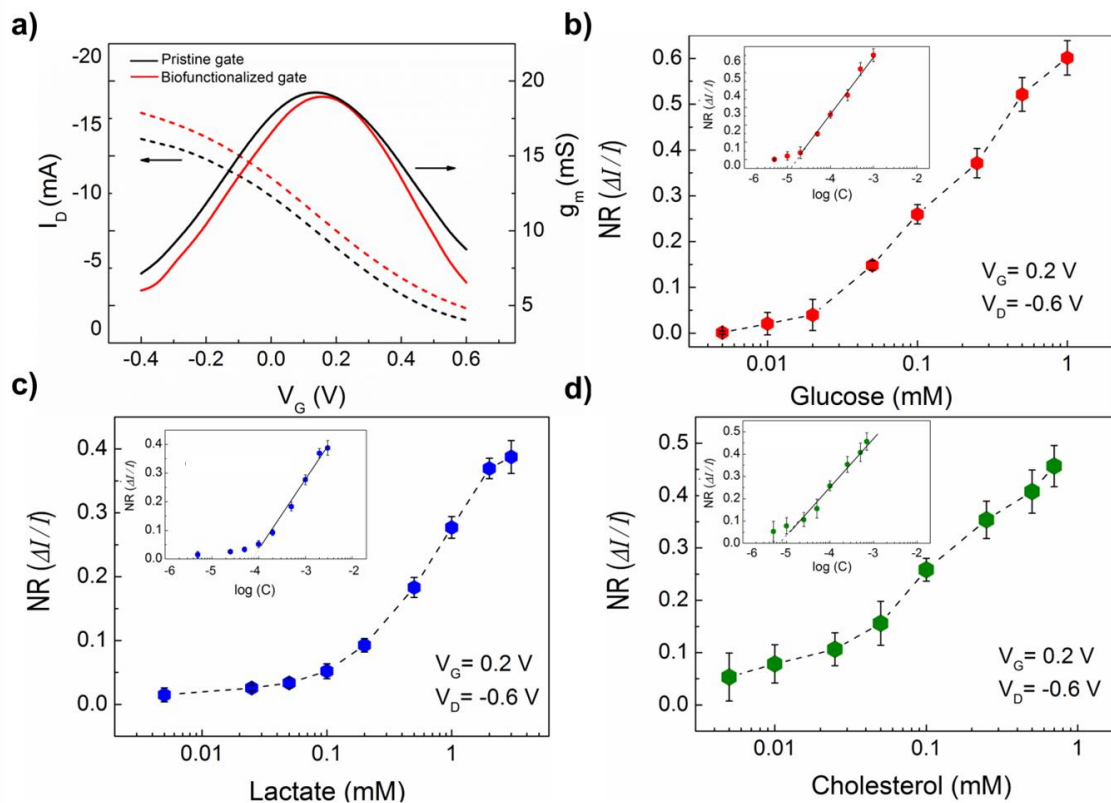


**Figure 2. Characterization of biofunctionalised OECTs.** (a) Steady state characteristics of a representative OECT: transfer curve and its corresponding transconductance (dashed line indicates the working point of OECTs for signal acquisition), before and after biofunctionalization. (b), (c) and (d) Normalized calibration curves derived from the chronoamperometric response of the OECTs after successive additions of increasing concentrations of the analytes glucose (b), lactate (c) and cholesterol (d) respectively. Insets of (b)-(d) show the corresponding linear parts of the calibration curves.

For the calculation of sensitivity and linear range, two vital indicators of the sensing performance of any sensor, chronoamperometric (CA) measurements were performed on the differently functionalized transistors after successive additions of increasing concentrations of corresponding analytes. **Figures 2b-d** show the calibration curves, deduced from the CA measurements after performing each experiment at least three times (**Supplementary Figure S2b**). In order to compare the responses of different devices the current outputs were normalized as described in the Experimental section.

The logarithmic plot of current response vs. analyte concentration yields a linear behavior in the concentration range of 0.02 – 1 mM for glucose, 0.1 – 2 mM for lactate and 0.01 - 0.7 mM for cholesterol, while all coincide with the corresponding physiological levels in saliva, ranging typically from 0.1 - 0.5 mM, 0.1 - 2.5 mM and 0.1 - 0.45 mM of glucose,



lactate, and cholesterol respectively.<sup>[35]</sup> The OECTs show excellent sensitivities in the  $\mu\text{M}$  range and lower limits of quantification (LOQ) of 10  $\mu\text{M}$  for glucose, 50  $\mu\text{M}$  for lactate and 10  $\mu\text{M}$  for cholesterol as determined from the calibration curves.

For the bio-sample tested here, we show detection in the relevant physiological range, however as might be expected, changes in the enzyme loading can be used as a method to alter the dynamic range.<sup>[36]</sup> Upon increasing the enzyme loading we observed no noticeable change in the biosensors' analytical characteristics, probably due to limitations in the diffusion of the analytes. After a certain threshold of enzyme concentration, the response of the device became relatively independent of changes in enzyme activity, an observation that is in accordance with previous studies.<sup>[36]</sup> We determined the critical enzyme concentrations for the three different enzymes and used it throughout as described in the Experimental section. Increasing the CS-Fc concentration in our biocomplex on the other hand, resulted in a significant shift towards higher upper limits in the linear range (**Supplementary Figure S3**). This is attributed to an increase in the CS film thickness, which acts as a diffusion limiting barrier for the analyte. However, the increase of the CS film thickness inevitably extends the response time of the device. Overall, by fine tuning the enzyme/mediator complex loading we can rather easily adjust our sensor's analytical characteristic to the needs of a specific analytical task.

### 2.3 Selective multianalyte detection in complex media using the OECT array

In this work an array of analyte -specific OECTs, operated in a common electrolyte, i.e., the relevant biological sample, was fabricated, therefore electrical crosstalk between the different transistors was typically an issue to troubleshoot. In a common-source configuration and in the presence of a common electrolyte, the individual transistor gating will induce changes in each of the separate sensing circuits due to polarization. To circumvent this issue we ensured a closed electrical loop for each of the sensors by isolating the individual grounds (in our case the source) as shown schematically in **Figure 3a**. The current output of two adjacent transistors in the same electrolyte after a DC sequential pulsing at the gate electrode of each OECT demonstrated no evidence of electrical cross-talk between individual OECTs (**Figure 3b**). **Figure 3c** shows the normalized current response of the three differently functionalized transistors operated simultaneously after successive additions of the corresponding analytes in known concentrations. Each device operates independently and specifically for the relevant analyte, without any biological crosstalk (**Figure 3c**). When a mixture containing all analytes was added

on the OECT array, the current-response times of each transistor differed. This can be related to the spatial position of each device with respect to the central addition of the metabolite mixture as well the different kinetic properties of each enzyme (**Figure 3d**).

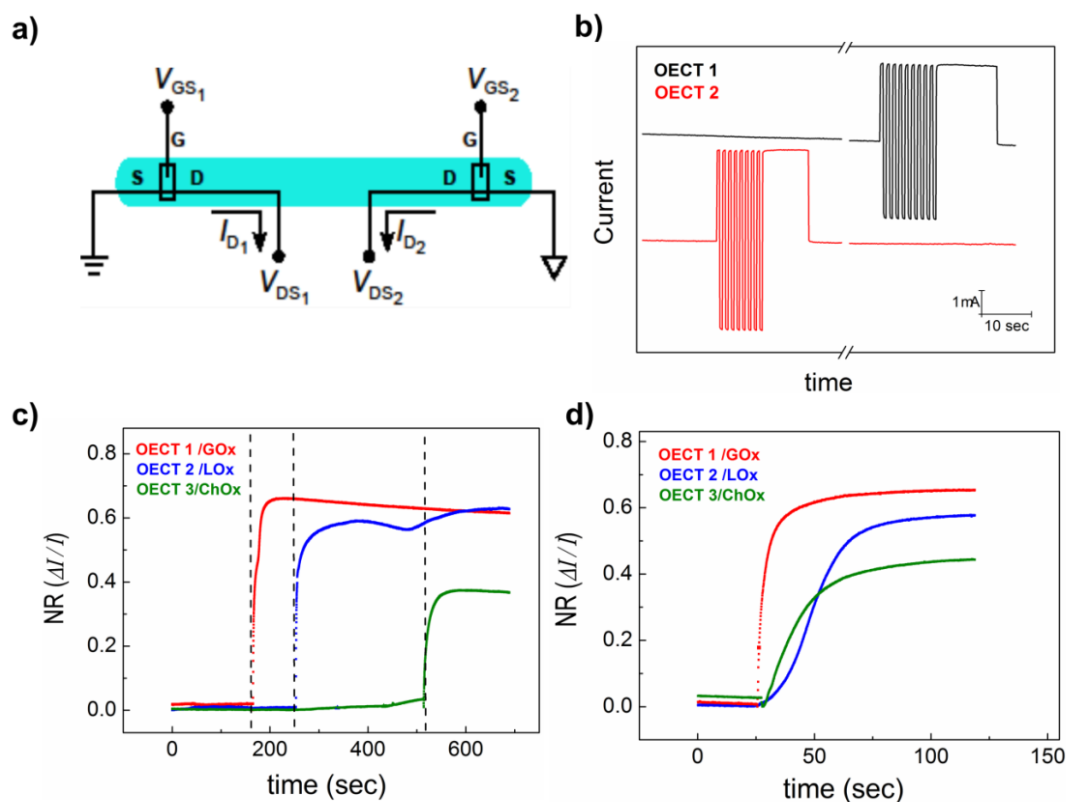


**Figure 3. Selective multianalyte detection in complex media using the OECT** (a) A schematic circuit diagram of two OECTs on the array (b) CA response of the channels of two OECTs after sequential pulsing of the gates showing the absence of electrical cross-talk. CA response of three differently functionalized OECTs after (c) successive additions of known concentrations of the three analytes and (d) addition of a mixture of the three analytes.

## 2.4 On-chip multianalyte detection in saliva using the OECT

The use of biological samples such as blood and saliva is known to increase background interference. One strategy used predominantly in *in vivo* biosensing applications to improve biosensor signal-to-noise ratio (SNR) with respect to electrochemical interference present in biological media, is the use of a “blank electrode”. This identical electrode that lacks the selectivity towards a specific analyte, is utilized in extracting any background signal related to

unspecific reactions and thus to improve the sensitivity of the biosensor.<sup>[37,38]</sup> To this end, we incorporated an extra OECT into the microarrays, which was functionalized with a non-specific protein, BSA. Interference studies with respect to the detectable analytes were also performed with our reference transistor, to further ensure specificity and sensitivity of our system. The device showed no response to the presence of these analytes in the medium, further confirming its non-specific nature (data not shown).

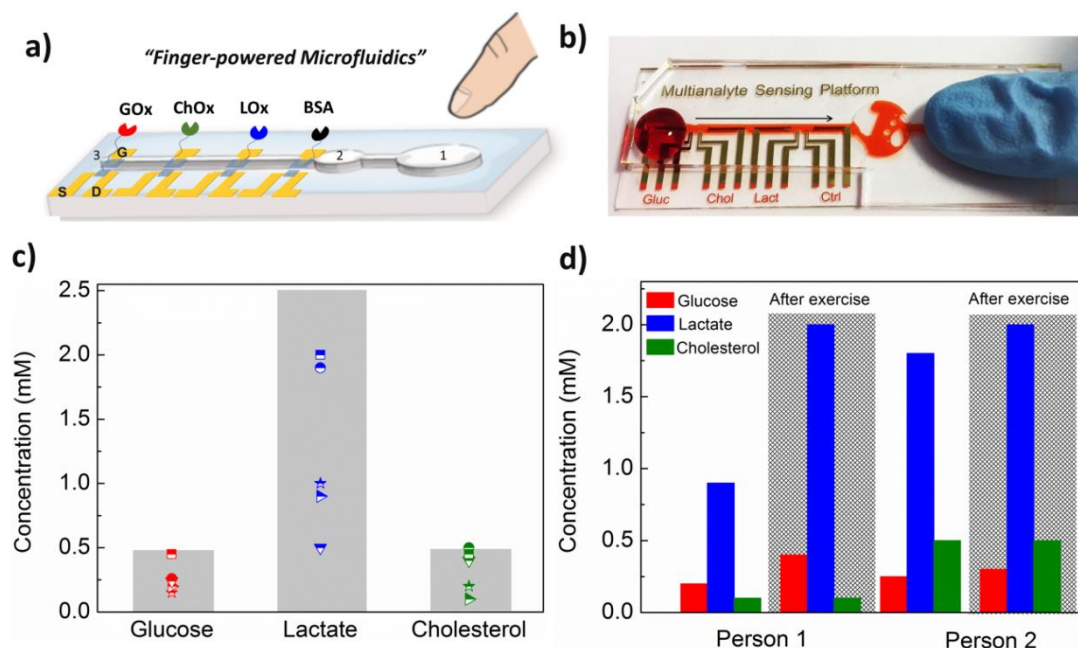


**Figure 4. Selective multianalyte detection in complex media using the OECT array** (a) Schematic illustration of the biosensing multiplatform with the embedded "finger-powered" PDMS microfluidic showing the 1) activation "button", 2) the liquid reservoir and 3) the punched inlet and (b) photograph of the actual device used for the measurements, showing droplet (for illustration purposes, a red-coloured solution) that was pushed from the large round area serving as activation "button", on the right of the device, through the sensing areas to the outlet as the arrow indicates (c) Salivary metabolite levels of 5 healthy volunteers as measured with our setup (the marked areas represent the physiological ranges of concentrations for each analyte) and (d) relative salivary metabolite variations of two healthy volunteers before and after intense physical exercise.

Furthermore, we integrated a versatile, portable and easy-to use "human-powered", PDMS-based microfluidic in the OECT array. Microfluidics allow for laminar flow, ultra-small sample volumes, faster analysis, portability, miniaturization and automation.<sup>[39]</sup> In our approach, the human finger, serving as the pumping actuation force, provides the pressure to

drive the liquid inside the microchannel.<sup>[40]</sup> The microfluidic device consists of a straight channel and two large round areas (**Figure 4a**). Simply, the larger round area is used as the activation “button” for the microfluidics by depressing the PDMS layer. The applied pressure results in a decrease in the total volume of the microchannel. After pipetting the specimen on top of the punched inlet, the pressure is released and the liquid starts to flow inside the microchannel due to re-expansion. Since this process is reversible, the smaller round region is used as a liquid reservoir (dead volume) to avoid complete emptying of the microchannel, which can result in faulty operation of the transistors. It should be mentioned that physiological solution (PBS) was flowed in all the experiments prior to the detection media in order to obtain our baseline and thus avoid any possible signal misinterpretation due to contamination from the previous samples. A photograph of the resulting portable biosensing set up embedded within the microfluidic is provided in **Figure 4b**. Although the measurement set up utilized herein is a custom lab-based multi-valent measuring system (described in the Experimental section) which is not portable, once specific requirements are outlined for electronic acquisition, portable embedded electronics can be tailored to the application at hand to be compatible with POCT.

It is believed that salivary metabolite levels can reflect the corresponding blood concentrations since saliva is an ultra-filtrate of plasma. In particular, most metabolites can be detected in saliva due to their passive diffusion from blood and subsequent secretion from salivary glands.<sup>[41,42]</sup> **Figure 4c** shows the salivary metabolite levels of five healthy volunteers as measured by our device. For the calculation of the analyte concentrations the current normalized responses of the OECTs were correlated with the calibration curves for each metabolite that are shown in **Figures 2b-d**. All metabolite levels were found to be within the physiological range (shaded areas in the graph), indicating the relevance of the measurements. In order to examine the relative variations of those metabolites under different physiological conditions, we collected samples from two healthy volunteers before and after intense physical exercise and the results are summarized in **Figure 4d**. Monitoring of metabolite levels in sports medicine has been extensively employed as a means of determining the athlete’s health status during exercise. Lactate is a crucial intermediary in numerous cellular, localized and whole body metabolic processes and the balance of its production and removal is highly dependent on a multitude of parameters. Lactate is known to be formed by skeletal muscle when the rate of glycolysis exceeds the metabolic rate of the citric acid cycle and oxidative phosphorylation (i.e., during intense exercise). However, given the multivariate mechanisms of energy metabolism

that are involved, the levels of other associated metabolites need to be concurrently measured in order to obtain a more holistic understanding of the rather complicated bioenergetic pathways. With our platform we anticipate meeting such requirements that can facilitate simultaneous identification of informative biomarkers in particular healthcare applications.

### 3. Conclusions

In this work, key challenges in continuous multi-analyte biosensing such as analyte specificity and elimination of electrical and biological cross-talk were successfully addressed. A multiplexed OECT platform integrated with a portable “finger-powered” microfluidic was developed, allowing for the detection of several critical biomarkers simultaneously. Measurements were performed with this prototype device in human saliva, to detect three clinically relevant biomarkers, glucose, lactate and cholesterol. The biosensors achieved excellent analytical performance with detection ranges that covered the physiological ranges in saliva. This versatile and easy-to-handle platform enables the implementation of any type of enzymatic biosensors toward accurate, rapid, non- invasive and portable next generation healthcare monitoring. Finally, the solution processability of our main material (PEDOT:PSS) and the simple planar fully integrated design renders the process easily scalable for high throughput production of disposable sensors.

### 4. Experimental Section

*Device Fabrication:* The devices are fabricated photolithographically using a parylene-C lift-off process.<sup>[17]</sup> Patterned gold lines served as source, drain, and gate electrodes. PEDOT:PSS blended with PVA was employed as the active layer of the OECT and also deposited on the gate. The overall device architecture consists of four  $\mu\text{m}$ -sized OECTs, each of them with a channel of Width-to-Length (W/L) of 100/10 ( $\mu\text{m}/\mu\text{m}$ ) and a planar gate of  $500 \times 500 \mu\text{m}^2$ . The metal contacts and interconnects were patterned using Shipley 1813 photoresist, exposed to UV light with a SUSS MJB4 contact aligner, developed in MF-26 followed by thermal evaporation of chromium (10 nm) and gold (100 nm) and metal lift-off in acetone/isopropanol. Two  $2 \mu\text{m}$  thick parylene C layers (SCS Coating) separated by an anti-adhesive (industrial cleaner, Micro-90) were successively deposited using a SCS Labcoater 2. The first parylene layer, was attached to the substrate using 3 (trimethoxysilyl)propyl methacrylate (A-174 Silane) as an adhesion promoter. For the patterning of the PEDOT:PSS channel, AZ9260 photoresist was spin casted,

exposed, and developed in AZ developer (AZ Electronic Materials) followed by reactive ion etching by O<sub>2</sub> plasma (Oxford 80 Plasmalab plus) of the unprotected layers of parylene. For the deposition of the PEDOT:PSS/PVA films, a formulation of the commercial aqueous dispersion PH-1000 (Heraeus Clevios GmbH), consisting of 5% V/V ethylene glycol, 0.4% V/V dodecyl benzene sulphonic acid and 25% wt of polyvinyl alcohol was sonicated before spin-casting (2.500rpm / 35sec, for a thickness of 90 nm). The resulting devices were subsequently baked at 110 °C for 1 h followed by 2 rinsing/soaking cycles in deionized water to remove any excess of low molecular weight compounds.

*Device functionalization:* For the gate electrode functionalization, 3 glycidoxypropyltrimethoxysilane (GOPS) was deposited by vapor deposition at 90°C for 1h under vacuum and baked after washing with ethanol (15 sec), for the formation of the epoxy-modified gate electrode surface. The three enzyme solutions were prepared in 1X PBS (Phosphate Buffered Saline) in their optimum concentrations, 2mg/ml for glucose oxidase (from *Aspergillus Niger*, ≥100 U/mg, Sigma) 10 mg/ml lactate oxidase (from *Aerococcus viridans*, ≥55 U/mg, Roche) and 5 mg/ml for cholesterol oxidase (from *Streptomyces sp.* ≥20 U/mg, Sigma). Chitosan – Ferrocene (CS-Fc) 4 mg/ml was diluted in a 1% v/v acetic acid aqueous solution. Prior to CS-Fc /enzyme complex formation, the enzyme solutions were mixed with EDC:NHS (1:1) 100 mM in 2-(N-morpholino)ethanesulfonic acid (MES) buffering agent in a 4:1 enzyme: reaction mixture ratio and left for 30 min to react.

Subsequently, the CS-Fc/enzyme complex was formed by mixing the activated enzyme solution with the CS-Fc solution in a 1:1 ratio and left for 30 min. Following that, the mixture was drop-casted selectively onto the epoxy- modified gate electrodes and left overnight in a humid environment to avoid evaporation.

*Device characterization:* All characterization was performed using 1X PBS. The cyclic voltammograms of the biofunctionalized electrodes were recorded using a potentiostat-galvanostat (Autolab, PGSTAT128N) with a Ag/AgCl reference electrode and a platinum counter electrode. The electrical characterization of the OECT (IV curves and calibration curves) was performed using a Keithley 2612A dual SourceMeter with customized LabVIEW software. The chronoamperometric measurements were recorded using a National Instruments PXIe-1062Q system. For this, the channel and the gate of the OECT were biased using an isolated analog output model, NI PXIe-4322, with 300 V CAT II channel to channel isolation. The current output of each OECT was recorded with a separate digital multimeter card, PXI-

4071, mounted in the same chassis. A customized LabVIEW software was used to address each hardware component.

*Chronoamperometric measurements for calibration of metabolites and multianalyte testing:*

Glucose and lactate were dissolved as stock solutions in PBS 1X, while cholesterol was dissolved in a PBS 1X solution containing 2% v/v Triton X-100, followed by heating until a clear solution was obtained. The stock analyte solutions were subsequently diluted in PBS 1X to perform calibration curves. Each measurement was conducted by consecutive additions of increasing concentrations of the analyte solutions after baseline (steady current) in PBS 1X was reached to our devices. The readout signal at zero analyte concentration is determined by the steady current obtained in PBS solution. The device response for each metabolite concentration was subtracted after the current output reached steady state and was normalized according to the following equation:

$$NR = \left| \frac{I_{conc} - I_{conc=0}}{I_{conc=0}} \right| \quad (1)$$

where  $I_{conc=0}$ ,  $I_{conc}$  are the current outputs in the absence of any analyte (baseline) and after the addition of a specific concentration of analyte respectively. For multianalyte measurements in PBS or saliva, the transistors were operated simultaneously and current outputs of each transistor were recorded individually with a separate digital multimeter card as described above. In the particular case of saliva samples our background signal is given by the readout signal (current output) of the control device (BSA functionalized device) in the presence of the saliva.

*Microfluidic fabrication:* The fabrication of the microfluidics master mold was carried out by pasting a 50  $\mu\text{m}$  thick double-sided pressure sensitive adhesive film, PSA (AR8890, Adhesives Research, Ireland) onto a plastic petri dish. The desired microfluidic pattern was created by cutting the PSA with a cutting plotter (Large Flatbed plotter - FC2250 series). For the formation of the polydimethylsiloxane (PDMS) microfluidics, PDMS was prepared by mixing PDMS elastomer with the curing agent from Sylgard 184 kit at a weight ratio of 10:1. After mixing and centrifugation, the PDMS was poured onto the master mold, and cured in an oven at 60  $^{\circ}\text{C}$  overnight. Following curing, the PDMS layer was peeled from the master and the inlet was made using a metal punch (2 mm in diameter). Finally, the PDMS microfluidics was placed on top of the OECTs device that were previously fabricated and functionalized on conventional microscope glass slide. By mean of optical microscope, successful alignment of the microchannel and the OECTs was performed.

*Saliva sampling:* Saliva samples were collected from 15 healthy volunteers and 5 of them were randomly chosen for the experiments. Saliva sampling was performed at fasting conditions (at

least 3h) using a direct expectoration method the so called “spitting method”. Subjects were asked to collect saliva in their mouths and to spit it into a sterile plastic tube with a diameter of 6 cm for 5 min, based on existing protocol. <sup>[43]</sup> Saliva sampling was done according to ethics principles set out by the biosafety committee at Ecole des Mines de St. Etienne and consent forms were signed by all donors.

## Acknowledgements

We are grateful to A. Hama and Dr. S. Inal for their valuable advice. This work was supported through grants by the Marie Curie ITN OrgBIO Project No. 607896 (A-M. P and M.B) and the Marie Curie IEF In Time Project No. 624673 (V.F.C). We also acknowledge the valuable assistance of Thomas Lonjaret in the development of the electronic acquisition systems

## References

- [1] Y. Liu, Z. Matharu, M. C. Howland, A. Revzin, A. L. Simonian, *Anal. Bioanal. Chem.* **2012**, *404*, 1181.
- [2] S. Kumar, S. Kumar, M. A. Ali, P. Anand, V. V. Agrawal, R. John, S. Maji, B. D. Malhotra, *Biotechnol. J.* **2013**, *8*, 1267.
- [3] Y. Wan, Y. Su, X. Zhu, G. Liu, C. Fan, *Biosens. Bioelectron.* **2013**, *47*, 1.
- [4] I. Willner, *Rev. Mol. Biotechnol.* **2002**, *82*, 325.
- [5] A. P. F. Turner, *Science.* **2000**, *290*, 1315.
- [6] C. Wang, *J. Diabetes Res.* **2013**, *2013*, 390534.
- [7] S. K. Arya, M. Datta, B. D. Malhotra, *Biosens. Bioelectron.* **2008**, *23*, 1083.
- [8] Y.-H. Lee, D. T. Wong, *Am. J. Dent.* **2009**, *22*, 241.
- [9] L. Torsi, M. Magliulo, K. Manoli, G. Palazzo, *Chem. Soc. Rev.* **2013**, *42*, 8612.
- [10] X. Strakosas, M. Bongo, R. M. Owens, *J. Appl. Polym. Sci.* **2015**, *132*, 41735-41749.
- [11] D. Khodagholy, J. Rivnay, M. Sessolo, M. Gurfinkel, P. Leleux, L. H. Jimison, E. Stavrinidou, T. Herve, S. Sanaur, R. M. Owens, G. G. Malliaras, *Nat. Commun.* **2013**, *4*, 2133.



- [12] D. A. Bernardis, G. G. Malliaras, *Adv. Funct. Mater.* **2007**, *17*, 3538.
- [13] J. T. Mabeck, J. A. DeFranco, D. A. Bernardis, G. G. Malliaras, S. Hocdé, C. J. Chase, *Appl. Phys. Lett.* **2005**, *87*, 013503.
- [14] S. Y. Yang, J. A. DeFranco, Y. A. Sylvester, T. J. Gobert, D. J. Macaya, R. M. Owens, G. G. Malliaras, *Lab Chip* **2009**, *9*, 704.
- [15] G. Lanzani, *Nat. Mater.* **2014**, *13*, 775.
- [16] D. T. Simon, S. Kurup, K. C. Larsson, R. Hori, K. Tybrandt, M. Goiny, E. W. H. Jager, M. Berggren, B. Canlon, A. Richter-Dahlfors, *Nat. Mater.* **2009**, *8*, 742.
- [17] M. Sessolo, D. Khodagholy, J. Rivnay, F. Maddalena, M. Gleyzes, E. Steidl, B. Buisson, G. G. Malliaras, *Adv. Mater.* **2013**, *25*, 2135.
- [18] M. Sessolo, J. Rivnay, E. Bandiello, G. G. Malliaras, H. J. Bolink, *Adv. Mater.* **2014**, *26*, 4803.
- [19] P. Lin, F. Yan, H. L. W. Chan, *ACS Appl. Mater. Interfaces* **2010**, *2*, 1637.
- [20] S. A. Tria, M. Ramuz, L. H. Jimison, A. Hama, R. M. Owens, *J. Vis. Exp.* **2014**, e51102.
- [21] J. Rivnay, M. Ramuz, P. Leleux, A. Hama, M. Huerta, R. M. Owens, *Appl. Phys. Lett.* **2015**, *106*, 043301.
- [22] D. A. Bernardis, D. J. Macaya, M. Nikolou, J. A. DeFranco, S. Takamatsu, G. G. Malliaras, *J. Mater. Chem.* **2008**, *18*, 116.
- [23] D. Khodagholy, V. F. Curto, K. J. Fraser, M. Gurfinkel, R. Byrne, D. Diamond, G. G. Malliaras, F. Benito-Lopez, R. M. Owens, *J. Mater. Chem.* **2012**, *22*, 4440.
- [24] H. Tang, F. Yan, P. Lin, J. Xu, H. L. W. Chan, *Adv. Funct. Mater.* **2011**, *21*, 2264.
- [25] L. Kergoat, B. Piro, D. T. Simon, M.-C. Pham, V. Noël, M. Berggren, *Adv. Mater.* **2014**, *26*, 5658.
- [26] C. Liao, C. Mak, M. Zhang, H. L. W. Chan, F. Yan, *Adv. Mater.* **2015**, *27*, 676.
- [27] G. S. Wilson, R. Gifford, *Biosens. Bioelectron.* **2005**, *20*, 2388.
- [28] X. Strakosas, M. Sessolo, A. Hama, J. Rivnay, E. Stavrinidou, G. G. Malliaras, R. M. Owens, *J. Mater. Chem. B* **2014**, *2*, 2537.
- [29] G. Scheiblin, A. Aliane, X. Strakosas, V. F. Curto, R. Coppard, G. Marchand, R. M. Owens, P. Mailley, G. G. Malliaras, *MRS Commun.* **2015**, *5*, 507.

- [30] N. Y. Shim, D. A. Bernardis, D. J. Macaya, J. A. Defranco, M. Nikolou, R. M. Owens, G. G. Malliaras, *Sensors*. **2009**, *9*, 9896.
- [31] L. Fernández, H. Carrero, *Electrochim. Acta* **2005**, *50*, 1233.
- [32] W. Yang, H. Zhou, C. Sun, *Macromol. Rapid Commun.* **2007**, *28*, 265.
- [33] F. Quignard, A. Choplin, A. Domard, *Langmuir* **2000**, *16*, 9106.
- [34] J. Rivnay, P. Leleux, M. Sessolo, D. Khodagholy, T. Hervé, M. Fiocchi, G. G. Malliaras, *Adv. Mater.* **2013**, *25*, 7010.
- [35] R. S. P. Malon, S. Sadir, M. Balakrishnan, E. P. Córcoles, *Biomed Res Int.* **2014**, 962903.
- [36] E. M. Durso, P. R. Coulet, *Anal. Chim. Acta* **1993**, *281*, 535.
- [37] C. G. J. Schabmueller, D. Loppow, G. Piechotta, B. Schütze, J. Albers, R. Hintsche, *Biosens. Bioelectron.* **2006**, *21*, 1770.
- [38] A. Weltin, J. Kieninger, B. Enderle, A.-K. Gellner, B. Fritsch, G. A. Urban, *Biosens. Bioelectron.* **2014**, *61*, 192.
- [39] S. Nahavandi, S. Baratchi, R. Soffe, S.-Y. Tang, S. Nahavandi, A. Mitchell, K. Khoshmanesh, *Lab Chip* **2014**, *14*, 1496.
- [40] K. Iwai, R. D. Sochol, L. Lin, in *2011 IEEE 24th Int. Conf. Micro Electro Mech. Syst.*, IEEE, **2011**, pp. 1131–1134.
- [41] A. Aguirre, L. A. Testa-Weintraub, J. A. Banderas, G. G. Haraszthy, M. S. Reddy, M. J. Levine, *Crit. Rev. Oral Biol. Med.* **1993**, *4*, 343.
- [42] J. Kim, G. Valdés-Ramírez, A. J. Bandodkar, W. Jia, A. G. Martinez, J. Ramírez, P. Mercier, J. Wang, *Analyst* **2014**, *139*, 1632.
- [43] R. M. Nagler, O. Hershkovich, *Arch. Oral Biol.* **2005**, *50*, 7.

## Supporting Information

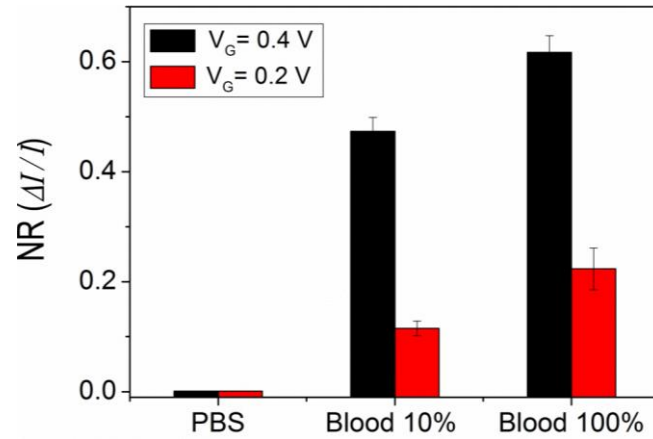
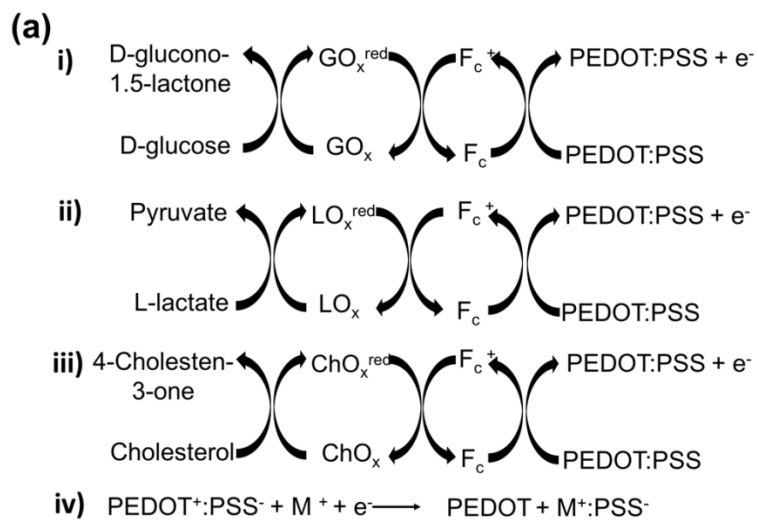


**Figure S1:** Normalized response of the OECT under different gate bias in the presence of complex media (whole blood) in a diluted (10%) and undiluted form.



(b)

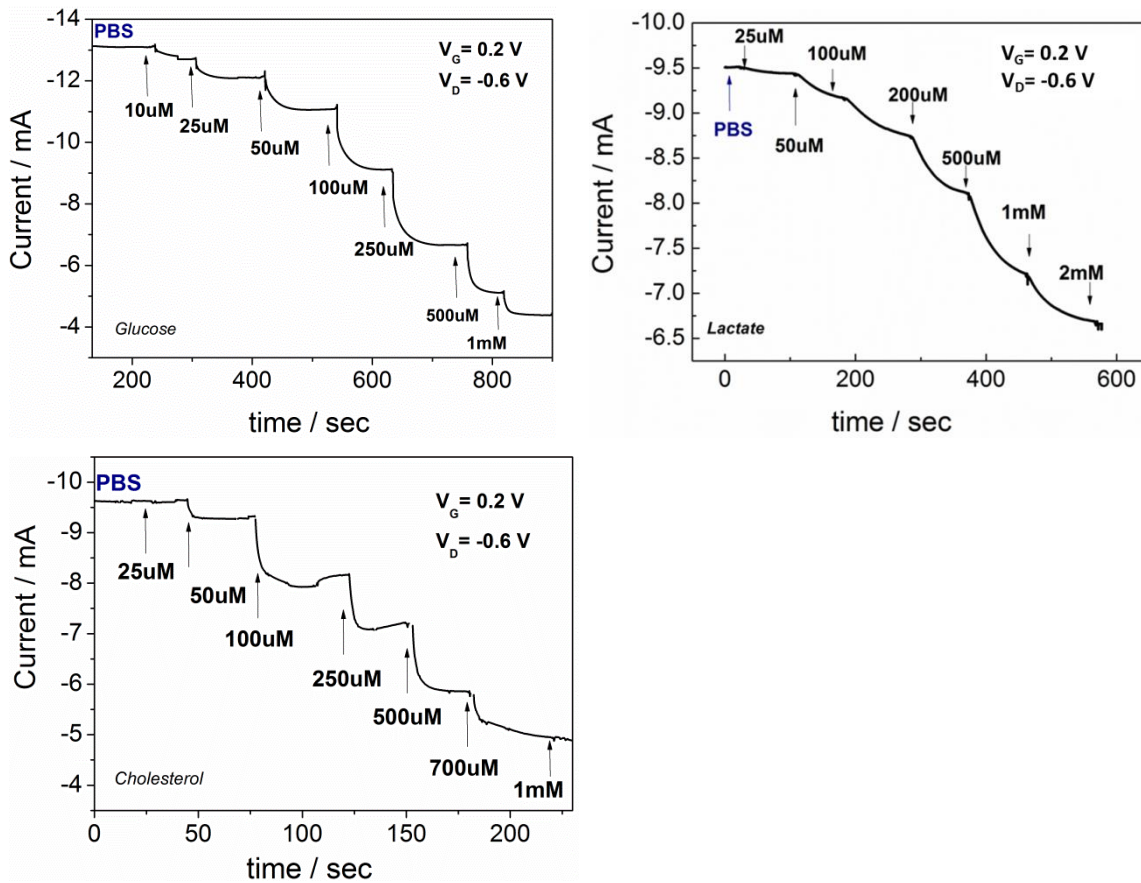


**Figure S2:** Chronoamperometric detection of glucose, lactate and cholesterol. a) Reaction mechanisms at the gate electrode for detection of i) glucose, ii) lactate and iii) cholesterol respectively as well as iv) the subsequent reactions at the channel b) Typical chronoamperometric responses of the three analyte-specific OECTs after successive additions of increasing concentrations of the corresponding analytes

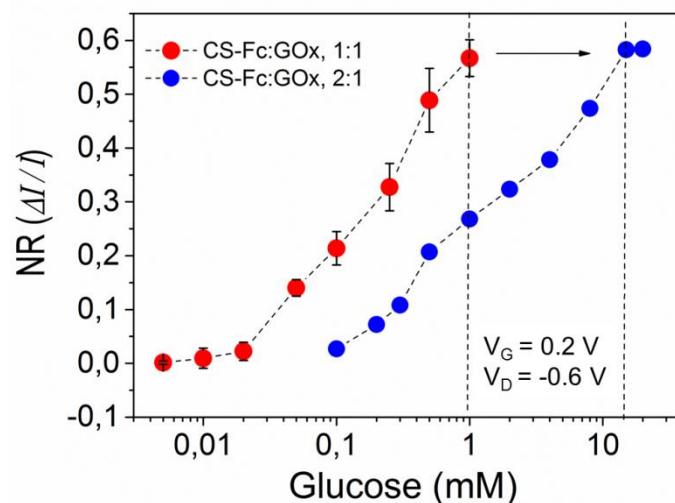
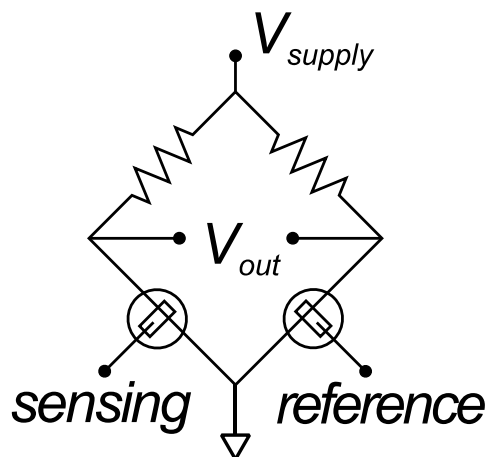


**Figure S3:** Comparative calibration curves of glucose with different enzyme: mediator ratio

# Chapter 3

---

## Lactate Detection in Tumor Cell Cultures Using Organic Transistor Circuits



The present Chapter is based on the following publication:

**“Lactate Detection in Tumor Cell Cultures Using Organic  
Transistor Circuits”**

*M. Braendlein\*, A.-M. Pappa\*, M. Ferro, A. Lopresti, C. Acquaviva, E.*

*Mamessier, G. G. Malliaras, R. M. Owens*

*Adv. Mater. 2017, 29, 1605744*

*\*equal contribution*

## **Abstract**

**A biosensing platform based on an organic transistor circuit for metabolite detection in highly interferent biological media is introduced.** The sensor circuit provides inherent background subtraction allowing for highly sensitive lactate detection in tumor cell cultures. The proposed sensing platform paves the way toward rapid, label-free and cost-effective clinically relevant *in vitro* diagnostic tools.

### Author's contribution:

For the present publication, used as chapter 3 in this thesis my contribution was: the OECT functionalization and characterization, the development of the sensing strategy the and performance of the lactate detection experiments in the biological samples. Also, I contributed equally in the preparation of the manuscript.

## 1. Introduction

Rapid and early diagnosis of disease is known to be a significant factor in treatment and improved prognosis, notably in cancer. From the first commercialized device based on the “enzyme electrode”, introduced by Clark and Lyons, able to measure accurately glucose concentrations in whole blood samples,<sup>[1,2]</sup> to research prototypes of miniaturized epidermal sensor chips able to measure real-time multiple analytes,<sup>[3]</sup> biosensors have evolved significantly and become invaluable tools for diagnosis of many pathologies from infections to heart disease. Remarkably, little of the progress in the field of biosensing has translated to improved diagnosis of cancer.<sup>[4]</sup>

Use of biosensors in diagnostic applications requires identification of a biomarker (to confer specificity) while the sensitivity is mostly related to the intimate coupling of a reaction involving the biomarker, with a transducer. In cancer diagnostics, clinicians are highly dependent on the identification of biomarkers that will reliably predict occurrence and recurrence of cancerous cell populations, however such reliable biomarkers are few and far between, perhaps explaining the dearth of cancer biosensing devices.<sup>[5,6]</sup> One marked feature of cancer however, is the increased glycolytic activity associated with highly proliferative aggressive cell growth.<sup>[7]</sup> In recent years, increased metabolic activity has been suggested as a biomarker for cancer. This idea is not new, having been introduced over 60 years ago by Warburg, who predicted enhanced uptake and usage of glucose and thus production of lactate.<sup>[8]</sup> Lactate has proven to be a prognostic indicator of the degree of malignancy in primary tumors as well as of the probability of metastasis.<sup>[9]</sup>

Electrical, label-free biosensing of metabolites such as glucose and lactate is known to be advantageous with regards to speed and sensitivity, and indeed the integration of biosensors with microelectronic devices has brought about multiplexed capabilities as well as enabled miniaturization and automation.<sup>[10–12]</sup> However, some key issues still impede their practical implementation in a clinical setting. These issues include signal drift due to environmental changes (e.g. electrolyte evaporation, temperature changes, instability of transducer), as well as signal misinterpretation due to interference (e.g. charged species or oxidizable compounds in complex media).<sup>[13]</sup> Sensor circuits represent an elegant alternative solution, departing from a single sensor and focusing on a more complete system that can be readily intercepted with simple acquisition tools, as demonstrated by Svensson et. al.<sup>[14]</sup>

Recently, the organic electrochemical transistor (OECT) has drawn considerable attention as sensing element.<sup>[15–17]</sup> In a three terminal configuration, the active material, being

comprised of an organic semiconductor, can be electrochemically doped or dedoped through an ionic current from the electrolyte into the polymer, thereby changing its conductivity.<sup>[18]</sup> The possibility for low voltage gating provides devices sensitive to biological signals that may consist of minute ionic currents.<sup>[19]</sup> OECTs have proven to outperform state-of-the-art devices such as electrodes,<sup>[20]</sup> and have been used in a wide variety of biological applications, including metabolite sensing.<sup>[21–23]</sup>

## 2. Results and Discussion

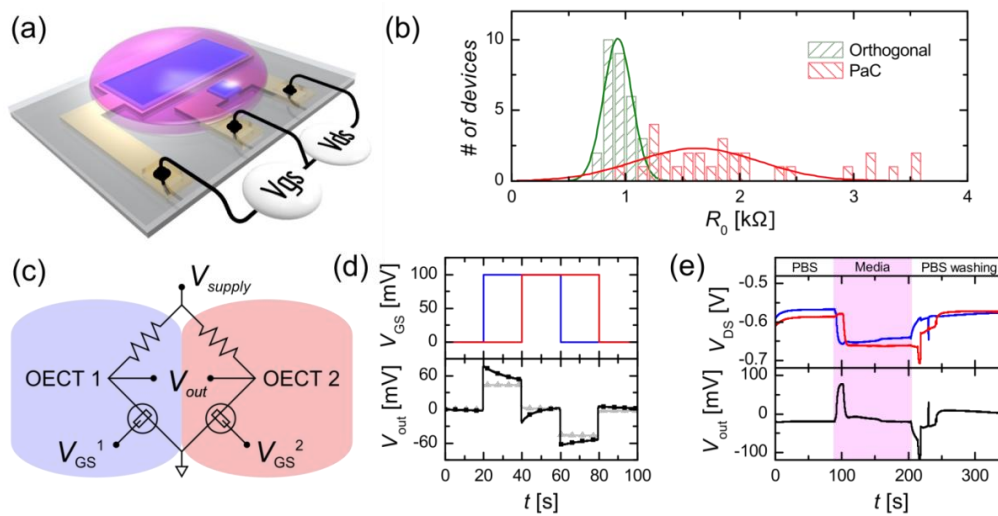


**Figure 1.** (a) Depiction of a planar OECT (blue: PEDOT:PSS, pink: electrolyte). The voltage supplies for the gate ( $V_{GS}$ ) and the source-drain bias ( $V_{DS}$ ) are depicted as white spheroids connected to the gold leads. (b) Comparison of channel resistance at  $V_{GS} = 0$  V and  $V_{DS} = -0.1$  V of 32 devices fabricated with orthogonal resist (green) against 32 devices with Parylene-C peel-off method (red). The bin size is  $0.1$  k $\Omega$ . The bold lines show a Gaussian fit. The distribution is much narrower for the orthogonal method, indicating a much better device to device homogeneity. The device geometry is  $W/L = 0.6$  and  $d = 100$  nm. (c) Schematic circuit layout of the Wheatstone bridge sensor circuit. The load resistors are on the drain side of the OECT. The electrolyte of the two OECTs is physically separated, ensuring a disjointed gating. The two branches of the bridge are highlighted in blue and red. (d) Chronopotentiometric recording upon pulsing the gate of each OECT for different values of the drain load resistor (gray triangles:  $R_{load} = 70$   $\Omega$  and  $V_{supply} = -1.5$  V; black squares:  $R_{load} = 190$   $\Omega$  and  $V_{supply} = -2.7$  V). The pulse pattern is shown in the upper graph for the left (blue) and the right (red) branch of the Wheatstone bridge. The results have been offset corrected  $V_{out} - V_{out}(t = 0)$ . (e) Chronopotentiometric recording upon changing the electrolyte. The upper graph shows the floating voltage point of each branch of the Wheatstone bridge circuit. The lower graph shows the output voltage, i.e. the voltage difference between the two floating points. The electrolyte is changed from 1X PBS (white) to DMEM cell culture media supplemented with FBS (pink) and then consecutively washed again with 1X PBS (three times). The spikes in the curves are due to pipetting effects. The supply voltage is  $V_{supply} = -2.5$  V for load resistors of  $R_{load} = 190$   $\Omega$ . The gate voltage is kept constant at  $V_{GS} = 200$  mV.



Bearing in mind the complex issues related to sensitive and specific detection of metabolites of interest in pathologies such as cancer, in this article, we present an *in vitro* electronic platform for sensitive and accurate metabolite sensing in highly interfering samples, such as cell culture media. In particular, we developed a reference-based sensor circuit, by integrating two differently functionalized OEECTs, comprised of the well-known organic p-type semiconductor poly(3,4-ethylenedioxythiophene):poly(styrene sulfonate) (PEDOT:PSS),<sup>[24]</sup> into a Wheatstone bridge layout.

The planar all-PEDOT:PSS configuration of the channel and the gate (**Figure 1a**) facilitates the device biofunctionalization<sup>[23]</sup> and also allows for future integration with microfluidics. For the device fabrication, a new lithographic approach based on a fluorinated photoresist, that allows for direct patterning of spun-cast PEDOT:PSS, was employed in this work (**Figure S1**). Starting from a homogeneously coated PEDOT:PSS film and ablatively patterning the active areas,<sup>[25,26]</sup> a greater device homogeneity can be achieved (**Figure 1b** and **Figure S2c**), contrary to the conventional Parylene-C peel-off technique.<sup>[27]</sup> According to the output and transfer characteristics of the OEECTs (**Figure S2a-b**), the maximum transconductance<sup>[28]</sup>  $g_m = \Delta I_D / \Delta V_{GS}$  of 6.4 mS is obtained at  $V_{GS} = 200$  mV, which coincides with the sensor's working potential, to ensure maximum sensitivity. By adding a drain load resistor in series with the OEECT, a floating voltage point  $V_{float}$  is created which depends on the drain current  $I_D$  and is set by the supply voltage  $V_{supply}$ .

$$V_{float} = V_{supply} - R_{load} \cdot I_D(V_{GS}, V_{float}) \quad 1$$

To a first order,  $V_{float}$  depends linearly on the applied gate bias and can thus be used as a reference to the signal of interest. By connecting two such branches in parallel, a full Wheatstone bridge is provided (**Figure 1c**), where one OEECT is used as a reference and the other can be functionalized, to respond specifically to a given target analyte. The difference between the two floating voltage points, the output voltage  $V_{out}$ , gives an intrinsically background subtracted response to any change in the gating of the sensing OEECT. In addition, the response starts at low amplitudes and increases with the gate voltage. This so called signal-ON response is generally easier to detect with simple data acquisition tools. The magnitude of the drain load resistor sets the inherent gain of the device  $\Delta V_{out} / \Delta V_{GS}$  and shifts the transconductance depending on the operation regime.<sup>[29]</sup> Specifically, the gain scales linearly when operating the device in the saturation regime. We thus herein set the operation point of both OEECTs to  $OP = -0.6$  V. This voltage value is not sufficient to reach full saturation in our

device, but gives a good compromise between linearity in the gain and a sufficient dynamic range for the sensing mechanism to avoid electrolysis in the water based electrolyte.<sup>[30]</sup>

We demonstrate the working principle of our Wheatstone bridge platform upon the application of a voltage pulse at both gates (**Figure 1d**). The electrolyte of the reference OECT is physically separated from the sensing OECT. As expected,  $V_{\text{out}}$  remains zero when equal voltages are applied to both gates, after a certain stabilization time. The observed difference in the response time for the different drain load values is related to their respective aspect ratio ( $W/L = 5$  for  $R_{\text{load}} = 70 \Omega$  vs  $W/L = 1.7$  for  $R_{\text{load}} = 190 \Omega$ ). The changing voltage drop across the resistor and the resulting change in the current needs to equilibrate accordingly inside the conductive polymer. The gain can be extracted as  $\Delta V_{\text{out}} / \Delta V_{\text{GS}} = 0.4$  for  $R_{\text{load}} = 70 \Omega$  and  $\Delta V_{\text{out}} / \Delta V_{\text{GS}} = 0.5$  for  $R_{\text{load}} = 190 \Omega$ . For our enzymatic sensing approach, higher sensitivity (i.e. higher gain) is more important than high speed, thus we chose the higher drain load for the remainder of this study.

One key advantage of the Wheatstone bridge sensor circuit is the inherent background subtraction. When working with low volume samples, evaporation of the liquid results in a drift in  $I_{\text{D}}$ . Additionally, electro-oxidizable compounds present in the sample, as in the case of cell culture media, can induce changes in  $I_{\text{D}}$  due to direct electron transfer at the gate thus leading to an effective dedoping of the PEDOT:PSS material.<sup>[31]</sup> When changing the sample from a phosphate-buffered saline solution (PBS) to cell culture media, the response of the single OECTs in our device is in the range of 100 mV (corresponding to a change of  $\Delta I_{\text{D}} \approx 0.5$  mA), whereas the baseline of the bridge remains fairly constant (**Figure 1e**). The observed spikes are due to electrolyte perturbation as a result of consecutive pipetting of the two wells. After rinsing with PBS, the original operation point of each individual OECT is retrieved. Note also the stability in  $V_{\text{out}}$ , while the single OECTs haven't reached steady state operation yet (0 s to 50 s).

**Figure 2a** shows a depiction of our Wheatstone bridge lactate sensor. The dashed line indicates the reference (left) and the sensing (right) branch of the bridge. To render our sensor specific to lactate, we employed a biofunctionalization scheme at the gate of the sensing OECT based on our previous work,<sup>[10]</sup> by using an oxidase type enzyme (lactate oxidase) along with an electrochemical mediator. The enzyme/mediator complex is immobilized at the gate electrode of the OECT. An identical biofunctionalization scheme is applied to the gate electrode of the reference OECT by replacing the specific oxidase with a non-specific protein (bovine serum albumin), thus ensuring a similar surface environment and response time.

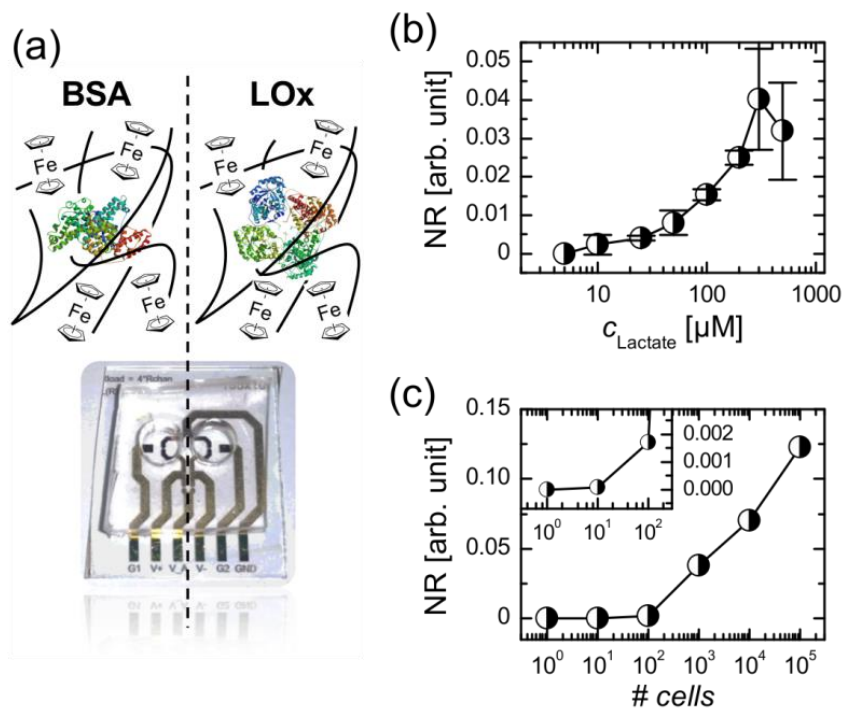


**Figure 2.** (a) Schematic depiction of the biofunctionalization approach using lactate oxidase. Ferrocene is attached to a polymeric supporting matrix, chitosan. The chitosan-ferrocene/lactate oxidase complex is immobilized on the sensing OECT using epoxy terminated self-assembled monolayers. On the reference OECT the same complex is used, where the specific enzyme is substituted by a non-specific protein BSA to ensure equality in the two devices. (b) Calibration curve of the Wheatstone bridge lactate sensor for three different devices. The data points are extracted upon consecutive addition of 1X PBS containing increasing lactate concentrations. The normalized response is  $NR = \Delta V_{\text{out}} / \Delta V_{\text{out,max}}$ . The supply voltage is  $V_{\text{supply}} = -2.3$  V for load resistors of  $R_{\text{load}} = 180 \Omega$ . The gate voltage is kept constant at  $V_{\text{GS}} = 200$  mV. (c) Titration curve of one selected Wheatstone bridge lactate sensor after successive addition of media collected from cells cultured at different concentrations for 24 hours (from  $10^1$  to  $10^5$  PBMC, the point at  $10^0$  corresponds to fresh culture media). The inset shows the a zoom in of the same data to highlight the onset of lactate detection.

A calibration curve of lactate in buffer (1X PBS) is derived from the chronopotentiometric response of the Wheatstone bridge sensor after successive additions of increasing concentrations into the wells of both OECTs (**Figure 2b**). For ease of comparison between different devices, we normalize our response as the change in  $V_{\text{out}}$  divided by the maximum possible change, i.e., when  $I_D$  drops to zero and all potential would drop on the OECT. The calibration curve shows a linear behavior in the range of  $30 \mu\text{M}$  to  $300 \mu\text{M}$  and a detection limit of down to  $10 \mu\text{M}$  can be extracted.

To demonstrate the sensitivity of our device, we performed a titration curve (**Figure 2c**), assessing the response of the device to an accumulation of lactate in cell media, collected after

incubation with increasing numbers of peripheral blood mononuclear cells (PBMC) for 24 h. As baseline, fresh cell culture media is used. In one chronopotentiometric measurement, we successively add samples harvested from a different number of cells, starting from the lowest concentration. The titration curve shows an onset of response from medium incubated between 10-100 cells. From this, we can estimate a detection limit of lactate produced by a few  $10^5$  of cells (estimated to be  $\sim 10 \mu\text{M}$  from the calibration curve) The background concentration of lactate in fresh media is estimated to be about  $50 \mu\text{M}$  (**Figure S3**) but this is not perceptible in the measurements due to the reference based sensing mechanism of our circuit.

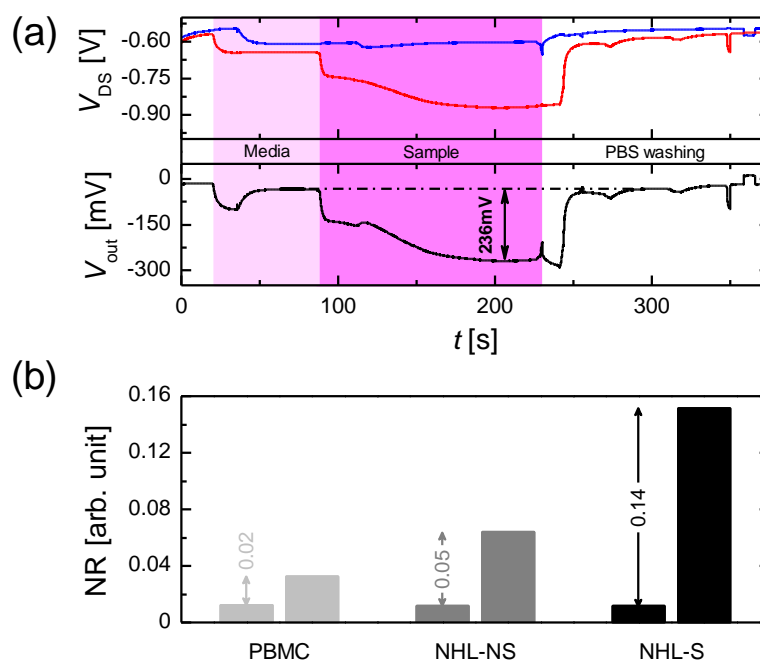


**Figure 3.** (a) Typical chronopotentiometric recording for lactate analysis with the Wheatstone bridge sensor. The addition of media before incubation (light pink) and after incubation with cells of interest (dark pink) and the washing with 1X PBS solution is indicated in the center of the graph. The difference between the baseline of bare media and the response due to the sample reflects the lactate amount produced by the cells. The red (blue) line shows the operation point of the sensing (reference) OECT. (b) Comparison of lactate production from peripheral blood mononuclear cells versus unstimulated and stimulated primary non-Hodgkin’s lymphoma cells (left to right). The left bar corresponds to media before incubation with cells and the right bar to media in which cells grew for 24 hours. The supply voltage  $V_{\text{supply}} = -2.3 \text{ V}$  for load resistors of  $R_{\text{load}} = 180 \Omega$ .

**Figure 3a** represents a typical chronopotentiometric recording in cell-derived samples. On the top is shown the individual response of each branch of the bridge and on the bottom the subtraction of those signals. Due to the two separate wells, a short delay between the exchanges

of the sample electrolyte in both wells is observed, which leads to a temporary rise in  $V_{\text{out}}$ . This does not reflect any biological activity. As each cell line requires specific culture media that contains different nutrients (including lactate) in various concentrations, for each measurement we use the corresponding culture media as a baseline. The difference in the baseline of the media vs the sample gives a direct measure of the lactate produced by the cells. Note that  $V_{\text{out}}$  returns to its initial value, once the device is rinsed with PBS, indicating that the device operation is not affected by the addition of complex media and the sensor can be reused for several measurements.

As already mentioned, a common feature of cancer cells is the enhanced rate of glycolysis, where glucose gets converted into pyruvate, and is aerobically fermented into lactic acid even under normoxia.<sup>[32,33]</sup> Indeed, Brand et al. recently showed that human melanoma metastases were found to exhibit a “Warburg phenotype” with high lactate measured both intracellularly and extracellularly.<sup>[34]</sup> This reinforces our hypothesis that electronic detection methods may be used in the future for cancer diagnostics, for example for predicting metastatic potential. The advantage of our reference based sensor circuit is in providing higher sensitivity for such kind of *in vitro* applications, while allowing for a more accurate lactate production analysis, even in the harsh sensing milieu that is provided by complex cell media. We thus used our platform to investigate the lactate produced by cancer cells and normal cells grown under similar conditions. **Figure 3b** shows the measured lactate, produced from malignant samples, specifically samples from a non-Hodgkin’s lymphoma (NHL) patient. These are composed of lymphocytes, notably malignant B lymphocytes known to secrete a high amount of lactate in comparison to normal PBMCs.<sup>[35]</sup> For the analysis, we use culture media incubated with a population of  $10^4$  cells for 24 hours. We compare both the unstimulated as well as the stimulated samples, where the stimulus promotes lymphocyte proliferation. The reference is a non-cancerous PBMC culture, mainly composed of lymphocytes, under similar conditions ( $10^4$  cells, 24 hrs). The normalized response for the PBMC is  $NR = 0.02$ , which from a linear interpolation of the calibration curve in Figure 2 (**Figure S4**) can be estimated to a lactate concentration of  $c_{\text{lactate}} \approx 140 \mu\text{M}$ . The unstimulated lymphoma cells show a normalized response of  $NR = 0.05$ , hence more than twice the lactate concentration  $c_{\text{lactate}} \approx 370 \mu\text{M}$ . Finally, the stimulated lymphoma cells show  $NR = 0.14$ , which correlates with a lactate concentration of  $c_{\text{lactate}} \approx 1 \text{ M}$  (the raw data of this measurement are shown in Figure 3a), however we note that this lies beyond the measured range of the calibration curve and saturation of our enzyme-based sensor device is to be expected. Nonetheless, this value lies significantly

above the unstimulated lymphoma cells, which can be explained by the fact that the stimulation process significantly enhanced cell proliferation and thus metabolic activity. We also measured more samples with the Wheatstone bridge sensor set at a lower operation point and we could see a similar trend for the unstimulated and stimulated samples, even though the absolute values of the device recordings are much lower (**Figure S5**). This emphasizes the fact that a proper operation point of the device is needed in order to achieve the desired amplification.

### 3. Conclusions

In conclusion, the sensitivity of the device presented in this paper allows for *ex vivo* detection of a broad range of lactate concentrations, from as little as  $10^5$  of non-malignant cells in “resting” conditions, i.e. cells with basal metabolic activity, to cells with strong metabolic activity, here stimulated tumor cells. The OECT has proven to provide highly sensitive metabolite detection due to its high current modulation in response to a change in the gate bias while the Wheatstone bridge sensor circuit provides an inherent background subtraction, thus ensuring elimination of any interference arising from other factors (i.e., electro-oxidizable compounds, electrolyte evaporation etc). As a proof-of-concept, the lactate produced from cultures of healthy PBMC and malignant non-Hodgkin’s lymphomas was compared. An elevated lactate production was indeed monitored in the cancer cells, confirming their intrinsic enhanced glycolytic metabolic activity, even in unstimulated conditions. To our knowledge, this is the first time that such a miniaturized sensor circuit has been applied to clinically relevant testing protocols that are important to follow tumor evolution or treatment efficiency in cancer patients.<sup>[36]</sup>

### 4. Experimental Section

*Device fabrication:* (a) The Parylene-C devices in Figure 1b are fabricated according to reference [29]. (b) For the Wheatstone bridge sensor, a lift-off process using photolithographic patterning (plastic mask, Selba S.A.) of negative photoresist (S1813, 3500 rpm, 35 s; softbake 110 °C, 60 s; SUSS MJB4 i-line 65 mJ/cm<sup>2</sup>; MF-26 developer, 30 s) and metal evaporation of chromium (10 nm) and gold (160 nm) defines the connection pads and interconnects. PEDOT:PSS solution (19 ml Clevios PH-1000, Heraeus Holding GmbH; 1 ml ethylene glycol, Sigma Aldrich; 50 µl dodecyl benzene sulfonic acid, Acros Organics; 1 wt% (3-

glycidyoxypropyl) trimethoxysilane, Sigma Aldrich) is spuncast (1500 rpm, 30 s) and hardbaked (125 °C, 60 min) to generate a homogeneous film (100 nm). PEDOT:PSS was patterned using a fluorinated negative photoresist (OSCoR 5001, Orthogonal Inc.) that does not degrade the polymer during fabrication. We spuncast the photoresist (1 ml per glass slide, 1200 rpm, 35 s), softbaked (65 °C, 60 s), exposed (i-line 63 mJ/cm<sup>2</sup>), post-exposure baked (90 °C, 60 s) and developed (Developer 100, Orthogonal Inc., double puddle 2 x 25 s). Dry etching (150 W, O<sub>2</sub> 50 sccm, CHF<sub>3</sub> 5 sccm, 90 s) and stripping (Stripper 903, Orthogonal Inc., double puddle 2 x 60 s) defines channel and drain load resistors. An insulator (DE1 Orthogonal Inc.) is patterned via spincasting (2000 rpm, 60 s), softbaking (90 °C, 60 s), exposing (i-line 149 mJ/cm<sup>2</sup>), post-exposure bake (90 °C, 60 s) and develop (developer 100, Orthogonal Inc., double puddle 2 x 45 s).

*Device characterization:* IV curves were recorded using a Keithley 2612A dual SourceMeter. All other recordings were done with a National Instruments PXIe-1062Q system at 50 Hz sampling rate (isolated analog output NI PXIe-4322 for supply and gate voltage, digital multimeter NI PXI-4071 for measuring output voltage).

*Biofunctionalization and Sensing Mechanism:* We used a protocol of enzyme/mediator (lactate oxidase/chitosan-ferrocene) immobilization on the PEDOT:PSS gate as shown in an earlier publication.<sup>[10]</sup> The enzyme-mediator complex is covalently attached to the gate via epoxy terminated self-assembled monolayers ((3-glycidyoxypropyl)trimethoxysilane) on top of the oxygen plasma treated PEDOT:PSS surface. In the presence of the analyte (lactate), catalysis at the enzyme (lactate oxidase) results in the generation of an electron and a further dedoping of the PEDOT:PSS channel (**Figure S6**).

*Lactate measurements:* We apply  $V_{GS} = 200$  mV on both OECT gates and a constant supply voltage for a target operation point of  $OP = -600$  mV. 30  $\mu$ l 1X PBS solution is added into each well and when the output signal is stable, PBS is substituted by an equal amount of cell culture media (this sets the baseline of the measurement). After signal stabilization ( $\sim 1$  min), the solution is substituted with the sample of interest. Finally, the device is rinsed by consecutively exchanging the liquid in each well with 30  $\mu$ l of fresh 1X PBS until the device reaches the initial operation point.

*Sample preparation:* PBMCs were obtained from volunteers and anonymous donors of *Etablissement Français du Sang*. Peripheral leukocytes were isolated by Ficoll density gradient centrifugation (Axis-Shield PoC AS, Norway). The mononuclear cells were washed twice, counted and conserved in RPMI 1640 (GIBCO, InvitroGen) supplemented with 10% heat-

inactivated fetal calf serum (Lonza, Belgium) at a concentration of  $1.10 \times 10^6$  Cells/ml. Lymph node biopsies, from B-NHL patients, were mechanically disrupted and passed through a  $100 \mu\text{m}$  nylon filter (BD Bioscience) to obtain a suspension of mononuclear cells. Cells were washed twice, counted and conserved in RPMI1640 supplemented with 10% heat-inactivated fetal calf serum at a concentration of  $1.10 \times 10^6$  Cells/ml. Cells suspension (PBMC or B-NHL cells) were used in culture experiments in RPMI 10 % FCS with or without PolyIg mix ( $2 \mu\text{g/ml}$ ) and CpG ( $1.25 \mu\text{g/ml}$ ) stimuli. The supernatants were harvested after incubation of 24 h at  $37^\circ\text{C}$  in 5%  $\text{CO}_2$ . Supernatants were briefly spun ( $> 20\,000 \text{ G}$ ) then filtered through a  $0.2 \mu\text{m}$  mesh. All samples have been diluted 1:1 in 1X PBS. The study was approved by the ethical board of the Paoli-Calmettes institute (Comité d'Orientation Stratégique, Marseille, France). Patients provided informed consent in accordance with the Declaration of Helsinki.

## Acknowledgements

M.B. and A-M.P. contributed equally to the present work. This work was supported by the Marie Curie ITN project OrgBio No. 607896. The authors would like to thank Dr. Vincenzo Curto for the chemical synthesis of Chitosan-Ferrocene. The authors are deeply grateful to Aimie Pavia, Magali Ferro, and Dr. Pierre Leleux for their help with the conducting polymer patterning process.

## References

- [1] L. C. Clark, C. Lyons, *Ann. N. Y. Acad. Sci.* **1962**, *102*, 29.
- [2] S. J. Updike, G. P. Hicks, *Nature* **1967**, *214*, 986.



- [3] W. Gao, S. Emaminejad, H. Y. Y. Nyein, S. Challa, K. Chen, A. Peck, H. M. Fahad, H. Ota, H. Shiraki, D. Kiriya, D.-H. Lien, G. A. Brooks, R. W. Davis, A. Javey, *Nature* **2016**, 529, 509.
- [4] Y. Liu, Z. Matharu, M. C. Howland, A. Revzin, A. L. Simonian, *Anal. Bioanal. Chem.* **2012**, 404, 1181.
- [5] N. L. Henry, D. F. Hayes, *Mol. Oncol.* **2012**, 6, 140.
- [6] M. Kalia, *Metabolism* **2015**, 64, S16.
- [7] S. Walenta, M. Wetterling, M. Lehrke, G. Schwickert, K. Sundfjør, E. K. Rofstad, W. Mueller-Klieser, *Cancer Res.* **2000**, 60, 916.
- [8] O. Warburg, *Science* **1956**, 123, 309.
- [9] S. Walenta, T. Schroeder, W. Mueller-Klieser, *Biomol. Eng.* **2002**, 18, 249.
- [10] A.-M. Pappa, V. F. Curto, M. Braendlein, X. Strakosas, M. J. Donahue, M. Fiocchi, G. G. Malliaras, R. M. Owens, *Adv. Healthc. Mater.* **2016**, DOI 10.1002/adhm.201600494.
- [11] J. P. Lafleur, A. Jönsson, S. Senkbeil, J. P. Kutter, *Biosens. Bioelectron.* **2016**, 76, 213.
- [12] G. Luka, A. Ahmadi, H. Najjaran, E. Alocilja, M. DeRosa, K. Wolthers, A. Malki, H. Aziz, A. Althani, M. Hoorfar, *Sensors* **2015**, 15, 30011.
- [13] H. Deng, A. K. L. Teo, Z. Gao, *Sens. Actuators B Chem.* **2014**, 191, 522.
- [14] P.-O. Svensson, D. Nilsson, R. Forchheimer, M. Berggren, *Appl. Phys. Lett.* **2008**, 93, 203301.
- [15] J. Rivnay, R. M. Owens, G. G. Malliaras, *Chem. Mater.* **2014**, 26, 679.
- [16] C. Liao, C. Mak, M. Zhang, H. L. W. Chan, F. Yan, *Adv. Mater.* **2015**, 27, 676.
- [17] M. Sessolo, J. Rivnay, E. Bandiello, G. G. Malliaras, H. J. Bolink, *Adv. Mater.* **2014**, 26, 4803.
- [18] G. P. Kittlesen, H. S. White, M. S. Wrighton, *J. Am. Chem. Soc.* **1984**, 106, 7389.
- [19] L. Kergoat, B. Piro, M. Berggren, G. Horowitz, M.-C. Pham, *Anal. Bioanal. Chem.* **2012**, 402, 1813.
- [20] D. Khodagholy, J. Rivnay, M. Sessolo, M. Gurfinkel, P. Leleux, L. H. Jimison, E. Stavrinidou, T. Herve, S. Sanaur, R. M. Owens, G. G. Malliaras, *Nat. Commun.* **2013**, 4, 2133.
- [21] D. Khodagholy, T. Doublet, P. Quilichini, M. Gurfinkel, P. Leleux, A. Ghestem, E. Ismailova, T. Hervé, S. Sanaur, C. Bernard, G. G. Malliaras, *Nat. Commun.* **2013**, 4, 1575.
- [22] N. Y. Shim, D. A. Bernards, D. J. Macaya, J. A. DeFranco, M. Nikolou, R. M. Owens, G. G. Malliaras, *Sensors* **2009**, 9, 9896.

- [23] X. Strakosas, M. Sessolo, A. Hama, J. Rivnay, E. Stavrinidou, G. G. Malliaras, R. M. Owens, *J Mater Chem B* **2014**, *2*, 2537.
- [24] J. Rivnay, P. Leleux, M. Ferro, M. Sessolo, A. Williamson, D. A. Koutsouras, D. Khodagholy, M. Ramuz, X. Strakosas, R. M. Owens, C. Benar, J.-M. Badier, C. Bernard, G. G. Malliaras, *Sci. Adv.* **2015**, *1*, e1400251.
- [25] P. G. Taylor, J.-K. Lee, A. A. Zakhidov, M. Chazichristidi, H. H. Fong, J. A. DeFranco, G. G. Malliaras, C. K. Ober, *Adv. Mater.* **2009**, *21*, 2314.
- [26] S. Zhang, E. Hubis, C. Girard, P. Kumar, J. DeFranco, F. Cicoira, *J Mater Chem C* **2016**, *4*, 1382.
- [27] M. Sessolo, D. Khodagholy, J. Rivnay, F. Maddalena, M. Gleyzes, E. Steidl, B. Buisson, G. G. Malliaras, *Adv. Mater.* **2013**, *25*, 2135.
- [28] J. Rivnay, P. Leleux, M. Sessolo, D. Khodagholy, T. Hervé, M. Fiochi, G. G. Malliaras, *Adv. Mater.* **2013**, *25*, 7010.
- [29] M. Braendlein, T. Lonjaret, P. Leleux, J.-M. Badier, G. G. Malliaras, *Adv. Sci.* **2016**, 1600247.
- [30] E. Zoulias, E. Varkaraki, N. Lymberopoulos, C. N. Christodoulou, G. N. Karagiorgis, *TCJST* **2004**, *4*, 41.
- [31] X. Strakosas, M. Huerta, M. J. Donahue, A. Hama, A.-M. Pappa, M. Ferro, M. Ramuz, J. Rivnay, R. M. Owens, *J. Appl. Polym. Sci.* **2016**, DOI 10.1002/app.44483.
- [32] J. R. Doherty, J. L. Cleveland, *J. Clin. Invest.* **2013**, *123*, 3685.
- [33] M. V. Liberti, J. W. Locasale, *Trends Biochem. Sci.* **2016**, *41*, 211.
- [34] A. Brand, K. Singer, G. E. Koehl, M. Kolitzus, G. Schoenhammer, A. Thiel, C. Matos, C. Bruss, S. Klobuch, K. Peter, M. Kastenberger, C. Bogdan, U. Schleicher, A. Mackensen, E. Ullrich, S. Fichtner-Feigl, R. Kesselring, M. Mack, U. Ritter, M. Schmid, C. Blank, K. Dettmer, P. J. Oefner, P. Hoffmann, S. Walenta, E. K. Geissler, J. Pouyssegur, A. Villunger, A. Steven, B. Seliger, S. Schreml, S. Haferkamp, E. Kohl, S. Karrer, M. Berneburg, W. Herr, W. Mueller-Klieser, K. Renner, M. Kreutz, *Cell Metab.* **2016**, DOI 10.1016/j.cmet.2016.08.011.
- [35] V. Jurišić, G. Konjević, R. Jančić-Nedeljkov, M. Sretenović, B. Banićević, M. Colović, I. Spužić, *Med. Oncol.* **2004**, *21*, 179.
- [36] S.-C. Lee, M. Marzec, X. Liu, S. Wehrli, K. Kantekure, P. N. Rangunath, D. S. Nelson, E. J. Delikatny, J. D. Glickson, M. A. Wasik, *NMR Biomed.* **2013**, *26*, 106.



## Supporting Information

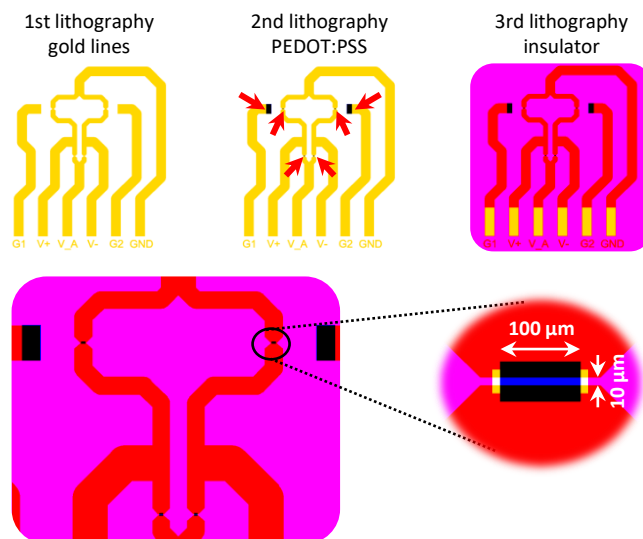


**Figure S1.** Fabrication layout for photolithography of the Wheatstone bridge sensor. The different colors indicate UV exposure for the different lithography steps. The first lithography step defines the lead lines with a lift-off process of a positive photoresist (Shipley S1813). The second lithography step defines the PEDOT:PSS active area via dry etching while protecting the gate, the channel and the drain load resistor with a negative fluorinated photoresist (Orthogonal OSCOR 5001). The red arrows indicate the two OECT channels (top) and drain load resistors (bottom). The third lithography step patterns the insulator to open the gate, the channel, the drain load resistor and contact pads (Orthogonal Neg1). The zoomed images depict the planar configuration of the OECT as well as the geometry of the active area. The channel of the OECT is defined as  $W/L = 100 \mu\text{m} / 10 \mu\text{m}$  with an overlap of  $20 \mu\text{m}$  between gold and PEDOT:PSS. The insulator window, that defines the area of the PEDOT:PSS in contact with electrolyte, has a dimension of  $120 \mu\text{m}$  by  $30 \mu\text{m}$  to allow for good alignment during fabrication. The whole device is covered with a 5 mm layer of polydimethylsiloxane (PDMS), within which we introduced two wells for the two OECTs. This allows for separate gating of both OECTs, and encapsulation of the drain load resistors.

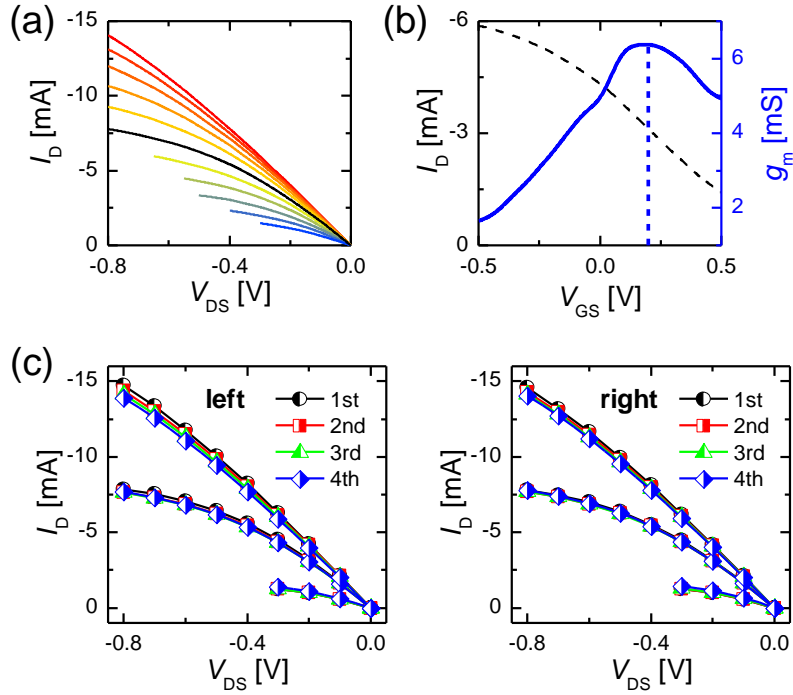


**Figure S2.** (a) Output characteristics of the OECTs used in the Wheatstone bridge sensor. The aspect ratio of the channel is  $W/L = 10$  and thickness is  $d = 100$  nm. The gate voltage  $V_{GS}$  is varied from  $-0.5$  V (red curve) to  $+0.5$  V (blue curve) in steps of  $100$  mV. The drain voltage is ramped from  $0$  V to a maximum voltage difference between source to drain and gate to drain of no more than  $-0.8$  V to avoid water electrolysis. The output curve at  $V_{GS} = 0$  V is highlighted (black). (b) Transfer characteristics of the same OECT at  $V_{DS} = -0.3$  V. The maximum transconductance is at  $V_{GS} = 0.2$  V (dashed blue line). (c) Consecutive IV curves for the OECTs of the left and the right branch in the Wheatstone bridge configuration for one selected device. The gate voltages from top to bottom are  $V_{GS} = [-0.5$  V,  $0$  V,  $+0.5$  V]. The OECTs have been measured as is after finishing the fabrication process. It can be seen that the output characteristics are fairly stable with consecutive cycling, indicating good device stability. Also, the drain current is almost identical for both OECTs over the whole voltage ramp, showing a good device homogeneity.

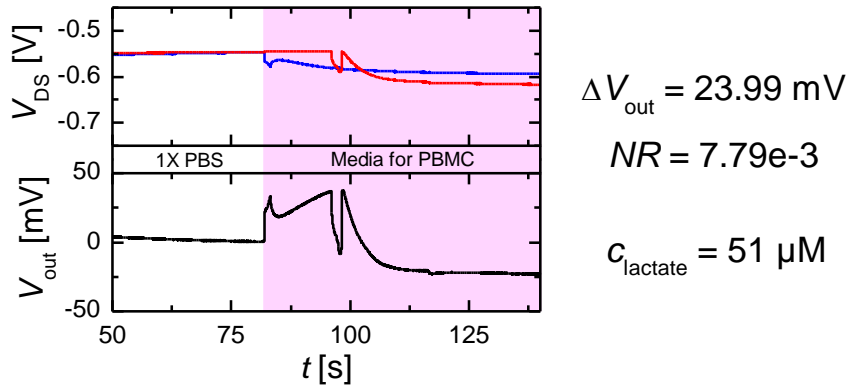


**Figure S3.** Estimation of the lactate concentration present in media for peripheral blood mononuclear cells. The lactate concentration is extracted from the normalized response via a linear interpolation of the calibration curve (see **Figure S4**).

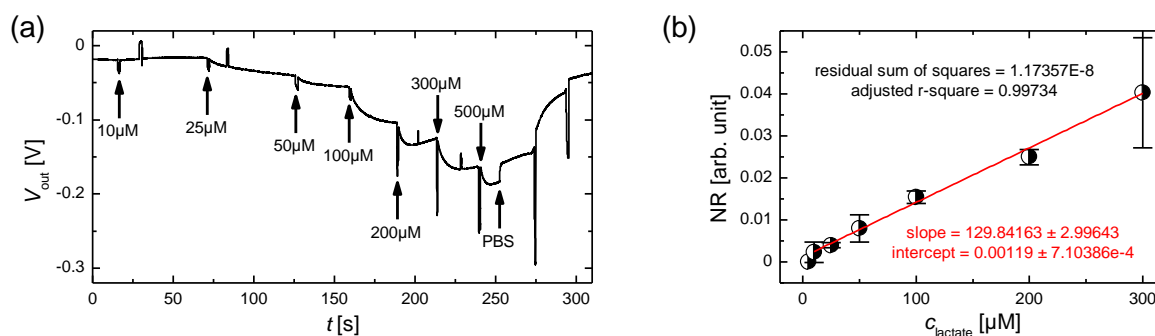


**Figure S4.** (a) Raw data for one selected calibration curve. The addition of the different lactate concentrations is indicated with arrows. After washing with PBS, the initial value of the output voltage is almost retrieved. (b) Linear interpolation of the calibration curve. The adjusted R-squared value indicates a clear linear regression. This is used to calculate the lactate concentration from the normalized response of the Wheatstone bridge sensor.

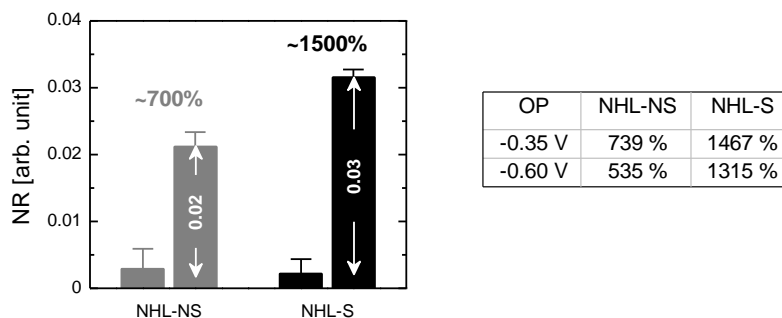


**Figure S5.** Normalized response for medium from unstimulated (NS) and stimulated (S) non Hodgkin's lymphoma samples recorded at a lower operation point ( $OP = -0.35$  V). The left column shows the lactate concentration of fresh medium and the right column the lactate concentration of the sample. The overall response is much lower due to the decreased amplification at the lower operation point. However, the percentage-wise increased lactate production of sample versus reference media are comparable to the data recorded at higher operation point (extracted from Figure 3b).

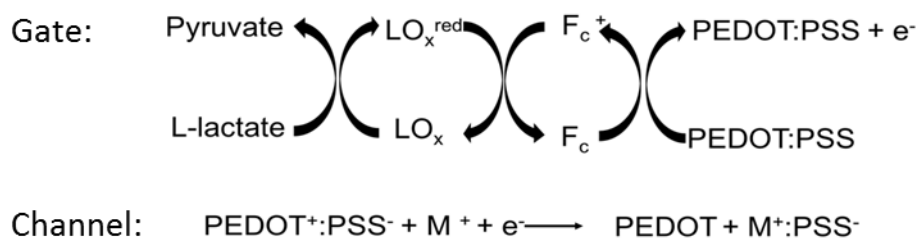
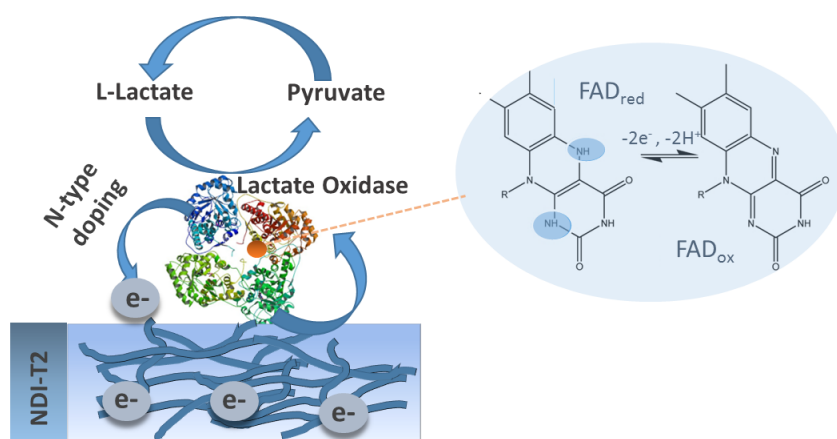


**Figure S6.** Reaction cycles at the enzyme/mediator functionalized gate electrode, in the presence of the analyte (lactate) and the subsequent reaction at the channel.

# Chapter 4

---

## Metabolite detection with an N-type accumulation mode organic electrochemical transistor



The present Chapter is based on the following publication:

**“Metabolite detection with an N-type accumulation mode organic electrochemical transistor”**

*A.-M. Pappa, A. Giovannitti, D. Ohayon, I. Uguz, I. McCulloch, R. M. Owens\*  
and S. Inal\**

*In preparation*

## Abstract

Organic electrochemical transistors (OECTs) are electrolyte gated organic thin film transistors that can transduce, as well as amplify, ionic signals of biological origin into electronic ones. The vast majority of OECTs operate in the depletion regime, switch off upon application of a gate voltage. This poses, specific disadvantages when it comes to biosensing as compared to accumulation mode devices that switch on upon detection/transduction of a biological event. Herein, for the first time, an accumulation mode OECT is presented, comprising an N-type organic semiconductor in the channel, for enzymatic detection of lactate. Without the need for an electron-transfer mediator, the channel conductance is modulated when lactate is oxidised by the enzyme lactate oxidase present in the electrolyte, leading to a sensor with high sensitivity ( $10 \mu\text{A}/\mu\text{M}$ ) in a wide concentration range ( $10 \mu\text{M}$  -  $10 \text{mM}$ ) in physiologically relevant electrolytes such as blood and sweat. This is due to the operation principle of this transistor type which allows for the bioelectrocatalytic reactions to occur at the channel, as well as to the excellent communication network between the organic semiconductor and the enzyme that results in the electronic doping of the semiconductor as a consequence of the direct charge transfer from the enzyme. Taken together, these results highlight the versatility of the synthesis and processing of organic electronic materials enabling high degree of customization based on the needs of a specific application towards high-performance, simple-to-fabricate, low-cost point-of-care sensors.

### Author's contribution:

For the present publication, used as chapter 5 in this thesis my contribution was: the OECT fabrication and characterization, the development of the biofunctionalization strategy, and the lactate sensing experiments. Moreover, I prepared the manuscript, including the figures.



## 1. Introduction

Rapid and early diagnosis of disease plays a major role in preventative healthcare and constitutes the driving force for the significant advances in biosensors technology [1,2]. Enzyme-based electrocatalysis represents today the most efficient label-free and rapid tool for the detection of critical metabolites including glucose, lactate, cholesterol etc [3]. due to the high selectivity, catalytic activity and fast acting properties of the enzymes at the interface with the electrode [4].

To date, the most commonly studied enzyme-based biosensors rely on the amperometric detection of hydrogen peroxide, which is formed when the molecular oxygen gets reduced when the enzyme cycles back and gets re-oxidised. Poor sensitivity due to the especially high potentials required for hydrogen peroxide oxidation (and thus detection) and the subsequent interference due to the electro-oxidizable compounds present in complex milieu, have placed a focus on the direct electrochemistry between the enzyme and the electrode. In most cases, the distance between the active site of the enzyme and the electrode surface is too long for direct electron transfer (DET) due to the protein shielding of the enzyme [5]. This is more apparent in traditional electrode materials (of inorganic nature) where electron transfer via a tunneling mechanism is rather tedious if not implausible thus necessitating the use of electron transfer mediators (e.g., ferrocene derivatives, ferrocyanide, conducting organic salts and quinones). Such small molecules can provide the required electron tunneling between the enzyme and the electrode and facilitate charge transfer.

The emergence of polymeric materials that conduct electricity, has not only revolutionised the landscape of traditional electronic applications [6,7] but has also entered the biomedical arena aiming to bridge the gap between electronics and biology [8–10]. Conjugated polymers (CPs), apart from their apparent merits such as chemical structure tunability, low-temperature and low-cost processing and integration with flexible technologies, constitute, at a molecular level, more efficient electrode materials for biosensing due to their polymeric structure and electron conducting behaviour. For example, in bioelectrocatalytic sensing, CPs can provide themselves efficient electron relays allowing for fast electron transfer, avoiding free-diffusing redox species between the electrode and the enzyme. Indeed, polypyrrole was the first CP that was shown to provide an electron relay between the surface of the electrode and the active site of the enzyme, significantly enhancing the biosensors analytical characteristics [11]. Following on this, PEDOT- based glucose sensors with potential for long-term measurements, were presented by Kros et al.[12], by physically incorporating a positively

charged polymer in the conducting polymeric matrix of the biosensor, allowing for more efficient ET due to the increased electrostatic interaction of the positively charged entrapped polymer with the negatively charged enzyme .

Alongside the distinct material properties, CPs enable novel and highly integrated device configurations, such as the organic electrochemical transistor (OECT). OECTs are electrolyte gated organic thin film transistors that can transduce and amplify ionic signals of biological origin into electronic ones [13-15]. One major advantage of the OECT technology is the especially high amplification of the transduced signals [16], as reflected by their transconductance values which are among the highest reported for organic transistors [17,18]. Poly(3,4-ethylenedioxythiophene) polystyrene sulfonate (PEDOT:PSS), an intrinsically doped organic semiconductor, represents to date the workhorse material of OECTs used in numerous biological applications including metabolite monitoring [19–21]. These transistors operate in the depletion regime meaning that they switch off upon application of a gate voltage. This poses specific disadvantages when it comes to biosensing as compared to accumulation mode devices that switch on upon detection or transduction of a biological event [22]. In principal, the accumulation mode transistors are identified with a large operation window, a high signal on/off response and a low-power operation [23].

We show for the first time, an accumulation mode electrochemical transistor comprising an N-type organic semiconductor in the channel, for enzymatic detection of lactate. Without the need for an electron-transfer mediator, the channel is doped when lactate is oxidised by the enzyme lactate oxidase present in the electrolyte, leading to a sensor with superior sensitivity and detection range compared to PEDOT:PSS analogues. This is due to the operation principle of this transistor type which allows for the bioelectrocatalytic reactions to occur at the channel. By fine tuning the semiconductor to improve its interactions with the enzyme, we can detect lactate with high sensitivity ( $10 \mu\text{A}/\mu\text{M}$ ) and in a wide concentration range ( $10 \mu\text{M} - 10 \text{mM}$ ) within the physiologically relevant concentrations in blood and sweat. The device exhibits a linear detection range from  $10 \mu\text{M}$  to  $1 \text{mM}$  and a very fast response (ca. 2 sec) for low metabolite concentrations ( $<0.3 \text{mM}$ ) due to the efficient electron transfer from the enzyme to the channel, as evidenced by cyclic voltammetry and optical measurements.

## 2. Results and Discussion

## 2.1 Characterization of the N-type organic semiconductor and proposed sensing mechanism

**Figure 1a** represents the proposed mechanism of an enzyme electrode for lactate sensing based on the N-type organic semiconductor. The concept of an enzyme coupled biosensing electrode involves the following; the enzyme catalyzes a reaction which either involves consumption or generation of electroactive species and then the depletion or production process of such species can be monitored to give a direct measurement of the analyte concentration. Our goal is thus to fabricate a mediatorless lactate sensor where, upon the reduction of the biocatalyst (the enzyme lactate oxidase, LOx) in the presence of lactate, the generated electron(s) will directly get transferred to the redox active polymer increasing its carrier density and thus the current that is flowing. In order to achieve that, it is essential to establish good electrochemical coupling between the enzyme and the electrode surface.

The design criteria for N-type organic semiconductors compatible with OECT operation, typically involve a narrow band gap donor-acceptor copolymer with polar side chains[24]. **Figure 1b** shows the molecular structure of the organic semiconductor employed in this work, comprised of the highly electron-deficient 2,6-dibromonaphthalene-1,4,5,8-tetracarboxylic diimide (NDI) monomer which can easily be copolymerized with electron-rich thiophene based co-monomers following a procedure for semiconducting polymers with polar side chains [25]. The solubility of the polymer in polar solvents increases with the amount of glycol side chains and the same applies for its swelling in aqueous. In this case, the organic semiconductor is comprised of 90% glycol and 10% alkyl chains.

**Figure 1c** presents the cyclic voltammetry (CV) measurements of thin films comprising the NDI-T2 on indium tin oxide (ITO)-coated glass substrates. As shown, the attachment of polar glycol chains at the polymer backbone enables reversible electrochemical switching between the reduced and neutral states. During the reduction (n-type doping process) sodium ions drift into the thin film to stabilize the negative charge on the polymer backbone. The redox reactions in 0.1 M sodium chloride (NaCl) aqueous solution are stable exhibiting reversible doping and de-doping over multiple cycles. It is worth noting that the measurements were performed under ambient conditions, without removing oxygen. The absorption onset is found around 817 nm which is consistent with an increased donor strength of the glycol-bithiophene unit. The initial UV-Vis spectrum shows two absorption peaks, a  $\pi$ - $\pi^*$  transition located between 350 and 450 nm and a broader absorption band from an intramolecular charge transfer complex between 550 and 800 nm.

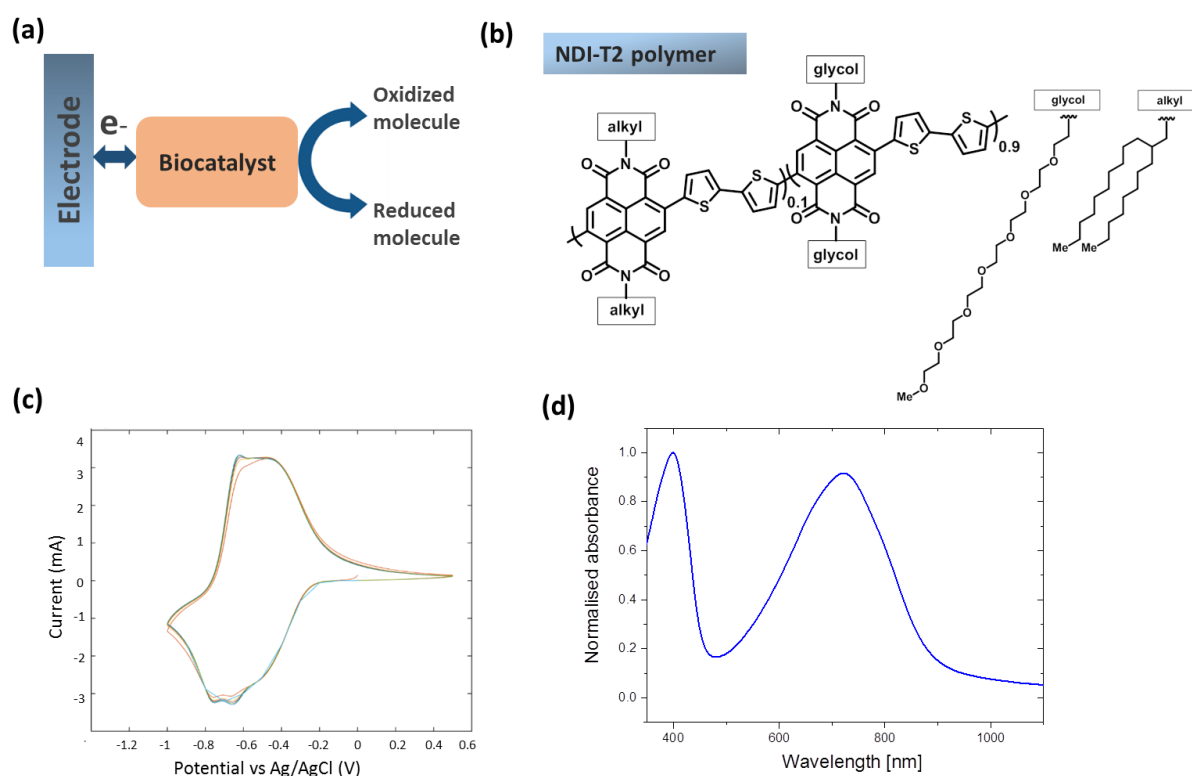


**Figure 1:** (a) schematic of the lactate oxidase redox reactions at the NDI-T2 electrode proposing a direct charge transfer on the OSC (b) Structure of the N-type semiconductor (NDI-T2) employed in this work. (c) Cyclic Voltammetry of the NDI-T2 on ITO-coated glass substrates in 0.1 M NaCl aqueous solution (40 cycles) and (d) normalized UV-VIS NIR absorption spectra.

## 2.2 Accumulation mode N-type OECTs

The OECT configuration, comprising of the NDI-T2 both in the channel and the planar gate electrode, is shown in Figure 2a. Such all-planar configuration (Vs the typical OECT structures involving an external top gate electrode) are preferred for future applications since they are compatible with large area processes such as printing and also provides ease for integration with microfluidics. For the device fabrication, gold contacts (source drain and gate electrodes) and interconnects were patterned on a glass substrate and an additional layer of Parylene C was used to insulate the gold interconnects. The CP, here the NDI-T2, is spin cast directly from solution without any annealing steps and serves as both channel and gate electrode. The device is operated in an aqueous 0.1 M Phosphate Buffer Saline solution (PBS) which is the physiologically relevant electrolyte.

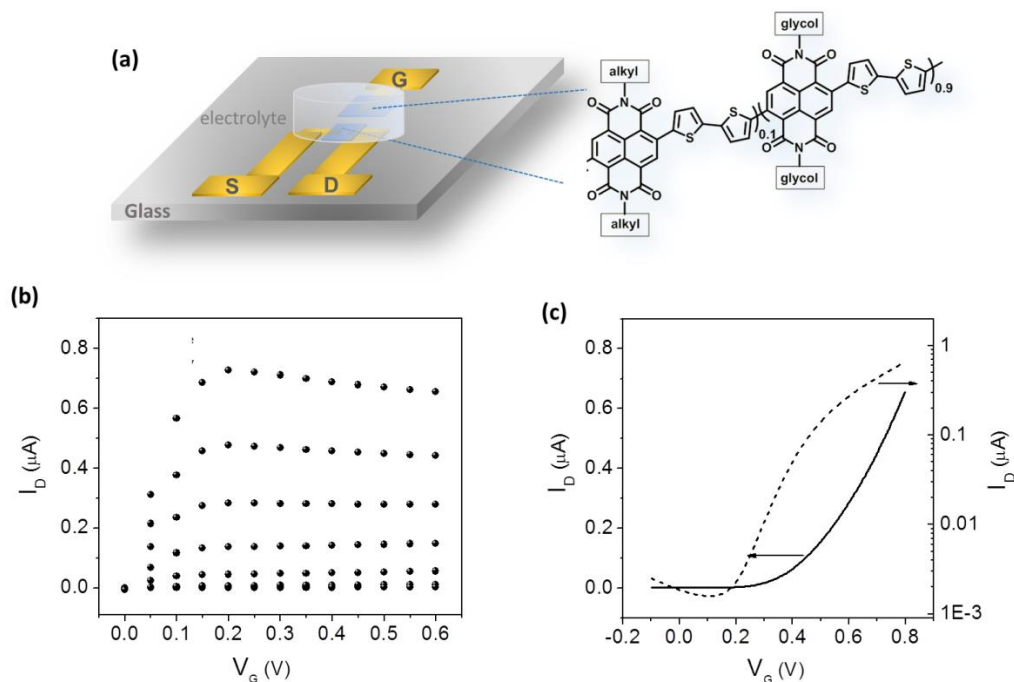


**Figure 2:** OECT characteristics based on the NDI-T2 OSC both on the channel and on the gate (a) Schematic representation of the all-planar OECT configuration (b) IV output characteristics and (c) transfer characteristics of the N-type OECT gated by the same gate material

Typically, in electrochemical transistors operating in accumulation mode, the application of a positive or negative gate bias triggers electrochemical redox reactions resulting in the reduction (n-type doping) or oxidation (p-type doping) of the organic semiconductor respectively, thus increasing its conductivity. Given that such systems operate in aqueous electrolytes, the gate potential that can be applied to dope the semiconductor is limited to the value that results in water electrolysis. **Figure 2b** shows typical output (drain bias vs drain current when increasing gate bias with a step of 0.1V) characteristics of the N-type OECT for a channel length of 10  $\mu\text{m}$  and a width of 100  $\mu\text{m}$ . **Figure 2c**, shows typical transfer characteristics (gate bias vs drain current) for a fixed drain bias of 0.5 V. As can be seen, the n-type device with the given channel length typically exhibits a peak current of around 0.7  $\mu\text{A}$  (at  $V_G=0.8$  V) and a peak transconductance of 8  $\mu\text{S}$  (at  $V_G=0.8$  V) as calculated from the slope of the transfer curve.

### 2.3 Highly sensitive mediator-free lactate detection with the N-type OECTs

Lactate is a metabolite that has evoked great interest due to its association with critical healthcare conditions such as hemorrhage, respiratory failure, hepatic disease, sepsis and tissue hypoxia. L-lactate oxidase is a globular flavoprotein usually obtained from various

microorganisms, such as *Aerococcus viridians* and is widely used for the electrochemical determination of lactate [26]. As can be seen in **Figures 3 a,b** the electrons that are involved in the enzymatic reaction are transferred from lactate to the oxidized form of the enzyme cofactor (Flavin Adenine Dinucleotide, FAD) present in the enzyme's structure.

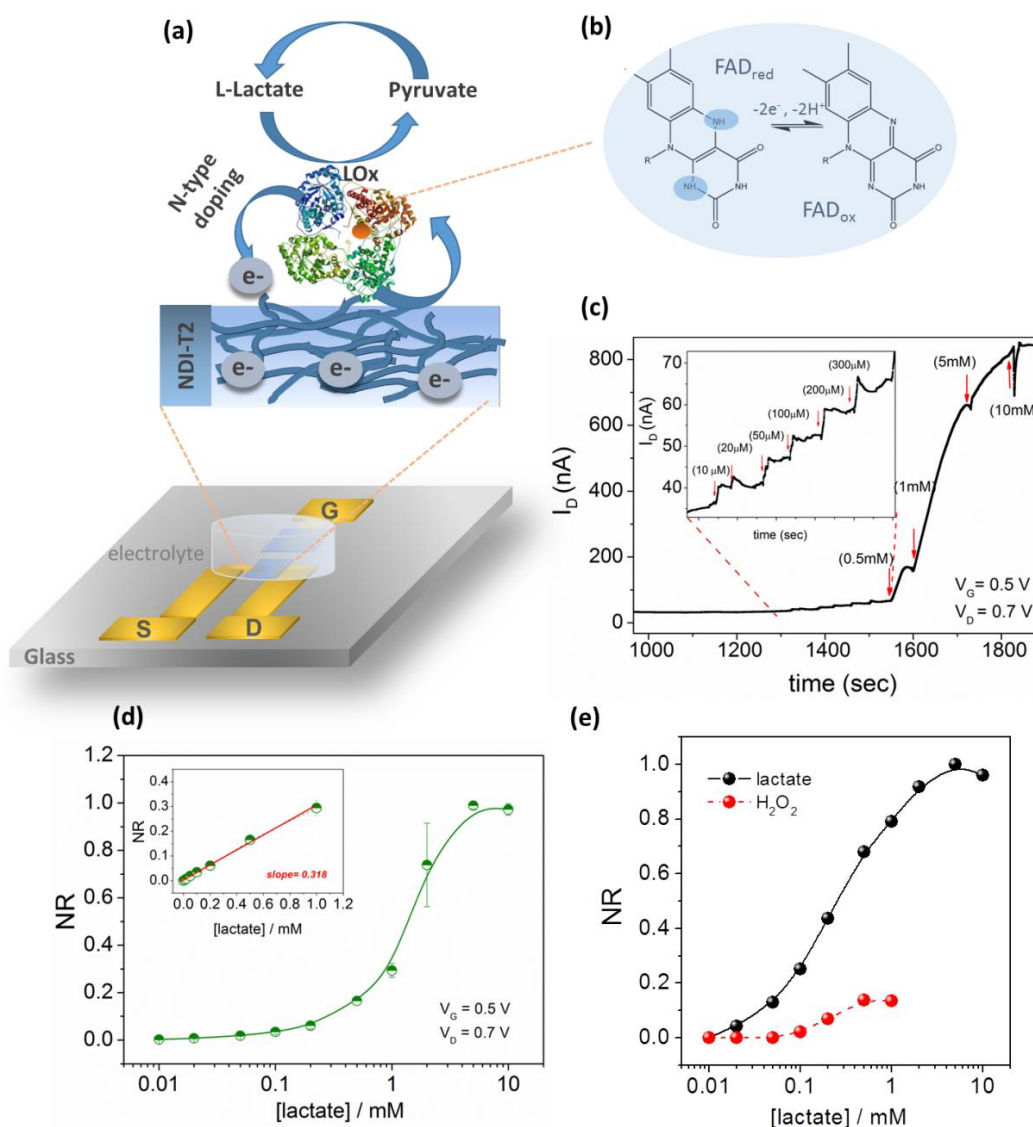


**Figure 3:** N-type OECT lactate sensor: (a) schematic of the OECT biosensor showing the device structure and the enzymatic reactions at the sensing electrode as well as (b) the enzyme cofactor redox reaction. (c) Real-time response of the OECT (drain current as a function of time) after the additions of increasing concentrations of lactate in the enzyme-containing PBS solution and (d) calibration curve of the lactate as extracted from the amperometric response measurements. (e) Device sensitivity with hydrogen peroxide (red line) vs lactate (black line) showing that the hydrogen peroxide oxidation is not the underlying mechanism behind the current increase.

In **Figure 1c**, the chronoamperometric response of the N-type OECT is shown as we increase the concentration of lactate in the presence of LOx and without the addition of any mediator, at a fixed gate bias of 0.5V and drain bias of 0.7V. By applying a higher source drain bias than the gate bias we ensure that the oxidation reaction is driven to the channel electrode which we use as our sensing element. The source-drain current is shown to increase with lactate concentration, suggesting that the enzymatic reactions somehow increase the conductivity of our semiconductor. The N-type OECT lactate biosensor yields excellent performance characteristics as shown from the lactate calibration curve of Figure 1d, such as high sensitivity values ( $10 \mu\text{A}/\mu\text{M}$ ) for a wide analyte concentration range ( $10 \mu\text{M} - 10 \text{mM}$ ) within the physiologically relevant concentrations in blood and sweat. Additionally the device exhibits a linear detection range from  $10 \mu\text{M}$  to  $1 \text{mM}$  and ultra fast response (ca. 2 sec) especially for low metabolite concentrations ( $<0.3 \text{mM}$ ). In order to compare the responses of different devices the current outputs were normalized (NR) as described elsewhere [20].

Generally, in enzyme biosensors, when the enzyme's cofactor is not sufficiently wired to the electrode and in the absence of an electron transfer mediator, the diffusing molecular oxygen takes the electrons from the reduced cofactor, transferring them to hydrogen peroxide. In order to rule out this possibility, we tested the device sensitivity to hydrogen peroxide, by adding the corresponding hydrogen peroxide concentrations in a similar manner to the lactate chronoamperometry measurements. **Figure 3e** shows clearly that peroxide has no effect on the OECT response, further suggesting that the proposed mechanism relies on charge transfer directly to the electrode from the enzyme. We thus can hypothesize that the enzyme added in the PBS solution, has a good electrochemical contact with our redox active electrode (the channel of the OECT) resulting in efficient electron wiring and subsequently n-type doping of the semiconductor. One question that remains to be answered relates to the nature of the interactions between the enzyme and the electrode that lead to such good electrochemical contact, and if this is bias-dependent mechanism or not. It is worth noting at this point that when the enzyme was covalently attached to the surface of the organic semiconductor, the biosensor response was very poor (data not shown) suggesting that the cofactor was far away from the electrode. Future experiments will thus focus on understanding the nature of the enzyme-electrode interactions that led to such good contact and also the underlying mechanism of electrode doping (i.e., electrostatic).

## 2.4 Device operation can tune sensor analytical characteristics

In order to get a better insight into the device (OECT) operation principle with respect to the biosensors analytical characteristics we also varied the device parameters (drain vs gate bias) and performed the chronoamperometric measurements as mentioned before. **Figure 4a** shows a comparative graph of the calibration curves obtained at different device operation parameters. As can be seen from the slope of the curves (at a linear scale) in **Figure 4b** the device that was operated at lower gate bias (0.5V) exhibited a wider linear lactate range but lower sensitivity compared to the devices operated at higher gate bias (0.6V) keeping the same drain bias (0.7 V). The highest sensitivity is attributed to the higher transconductance of the device at the higher gate bias and thus to the higher amplification of the signal. Interestingly, in the case where the gate bias is at its maximum (0.7 V) and equal to the drain bias we observe an intermediate response in terms of sensitivity but still lower linear range of detection. We believe that this might be due to overstressing of the device, given the very high overall potential applied, and we assume that this might lead to loss of sensitivity.

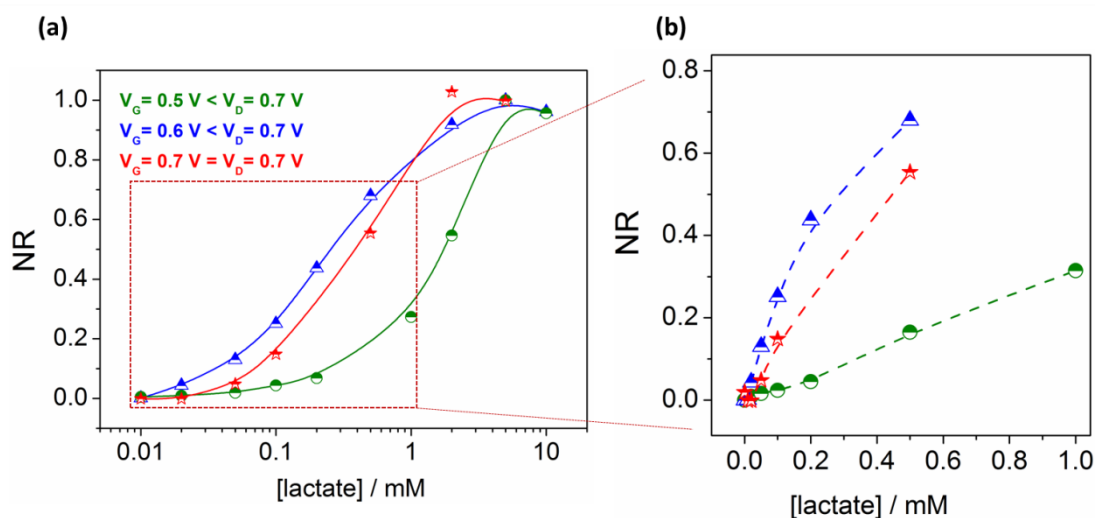


**Figure 4: Tuning OECT lactate sensor analytical characteristics** (a) Comparative graph of the calibration curves obtained at different different device operation parameters and the (b) linear scale response of the devices showing the sensitivities as the slope of the curves.

Taking all the above into account, our findings highlight the role of the OECT in biosensing applications serving as both amplifying and transducing element. By controlling the device parameters we not only fine tune the sensor's performance in terms of sensitivity and range of detection but we can also define the direction of the electric field and so the given redox reactions' direction (i.e., we can force the reactions to occur either at the channel or at



the gate electrode) favoring the biological system that is studied. More importantly this can be achieved just by controlling the set parameters and without the need to redesign anything *de novo*, highlighting the high versatility such systems can offer.

## Conclusions

Overall we showed herein, that the apparent advantages of the OECT technology for biosensing applications (sensitivity and compatibility with aqueous) extend to a new class of materials, organic semiconductors compatible with OECT operation (they swell in aqueous solutions and can be volumetrically doped by the application of a gate bias) that exhibit electron transport. Without the need for an electron-transfer mediator, the OECT channel (comprised of the N-type material) gets doped when lactate is oxidised by the enzyme lactate oxidase present in the electrolyte. This is hypothesized to be due to electron transfer at the electron transporting material which directly results in increase in its conductivity. This novel concept of using accumulation mode OECT devices with active materials that act simultaneously as electron acceptors opens up a wide range of possibilities in bioelectrocatalytic sensing and also in other fields such as biofuel cells.

## References

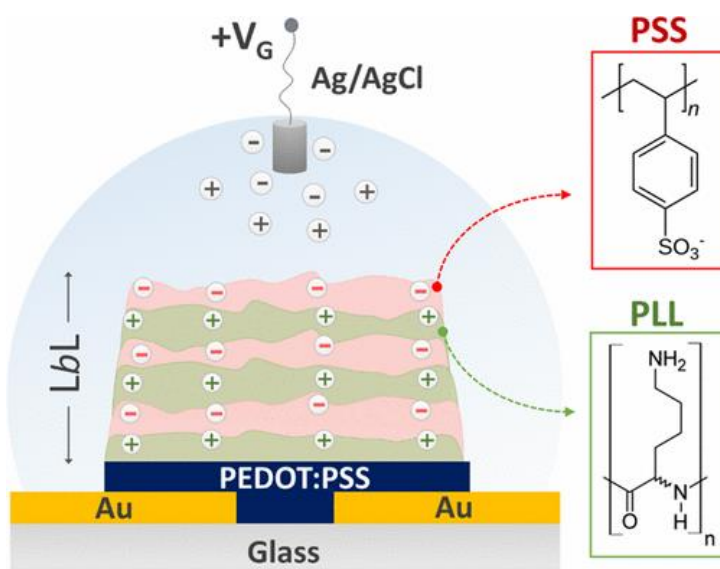
- [1] S. Sharma, J. Zapatero-Rodríguez, P. Estrela, R. O’Kennedy, *Biosensors* **2015**, *5*, 577.
- [2] C. Dincer, R. Bruch, A. Kling, S. Dittrich, G. A. Urban, *Trends Biotechnol.* **2017**, *xx*, 1.
- [3] A. N. Sekretaryova, M. Eriksson, A. P. F. Turner, *Biotechnol. Adv.* **2016**, *34*, 177.
- [4] Z. Zhao, H. Jiang, in *Biosensors*, InTech, **2010**.
- [5] R. S. Freire, C. A. Pessoa, L. D. Mello, L. T. Kubota, *J. Braz. Chem. Soc.* **2003**, *14*, 230.
- [6] W. Bru, T. D. Schmidt, B. J. Scholz, C. Mayr, **2013**, *65*, 44.
- [7] L. Lu, T. Zheng, Q. Wu, A. M. Schneider, D. Zhao, L. Yu, **2015**, DOI 10.1021/acs.chemrev.5b00098.
- [8] D. T. Simon, E. O. Gabrielsson, K. Tybrandt, M. Berggren, *Chem. Rev.* **2016**, acs.chemrev.6b00146.

- [9] R. M. Owens, G. G. Malliaras, *MRS Bull.* **2011**, 35, 449.
- [10] J. Rivnay, R. M. Owens, G. G. Malliaras, *Chem. Mater.* **2014**, 26, 679.
- [11] W. Schuhmann, *Biosens. Bioelectron.* **1995**, 10, 181.
- [12] A. Kros, R. J. M. Nolte, N. A. J. M. Sommerdijk, *J. Polym. Sci. Part A Polym. Chem.* **2002**, 40, 738.
- [13] G. Palazzo, D. De Tullio, M. Magliulo, A. Mallardi, F. Intranuovo, M. Y. Mulla, P. Favia, I. Vikholm-Lundin, L. Torsi, *Adv. Mater.* **2015**, 27, 911.
- [14] L. Kergoat, B. Piro, M. Berggren, G. Horowitz, M.-C. Pham, *Anal. Bioanal. Chem.* **2012**, 402, 1813.
- [15] A. Giovannitti, D. Sbircea, S. Inal, C. B. Nielsen, E. Bandiello, **2016**, DOI 10.1073/pnas.1608780113.
- [16] D. Khodagholy, J. Rivnay, M. Sessolo, M. Gurfinkel, P. Leleux, L. H. Jimison, E. Stavriniidou, T. Herve, S. Sanaur, R. M. Owens, G. G. Malliaras, *Nat. Commun.* **2013**, 4, 2133.
- [17] J. Rivnay, P. Leleux, M. Sessolo, D. Khodagholy, T. Hervé, M. Fiocchi, G. G. Malliaras, *Adv. Mater.* **2013**, 25, 7010.
- [18] J. Rivnay, P. Leleux, M. Ferro, M. Sessolo, A. Williamson, D. A. Koutsouras, D. Khodagholy, M. Ramuz, X. Strakosas, R. M. Owens, C. Benar, J. Badier, C. Bernard, G. G. Malliaras, **2015**.
- [19] M. Zhang, C. Liao, C. H. Mak, P. You, C. L. Mak, F. Yan, *Sci. Rep.* **2015**, 5, 8311.
- [20] A.-M. Pappa, V. F. Curto, M. Braendlein, X. Strakosas, M. J. Donahue, M. Fiocchi, G. G. Malliaras, R. M. Owens, *Adv. Healthc. Mater.* **2016**, 5, 2295.
- [21] M. Braendlein, A. Pappa, M. Ferro, A. Lopresti, C. Acquaviva, E. Mamessier, G. G. Malliaras, R. M. Owens, **2017**, DOI 10.1002/adma.201605744.
- [22] S. Inal, J. Rivnay, P. Leleux, M. Ferro, M. Ramuz, J. C. Brendel, M. M. Schmidt, M. Thelakkat, G. G. Malliaras, *Adv. Mater.* **2014**, 26, 7450.
- [23] C. B. Nielsen, A. Giovannitti, D.-T. Sbircea, E. Bandiello, M. R. Niazi, D. A. Hanifi, M. Sessolo, A. Amassian, G. G. Malliaras, J. Rivnay, I. McCulloch, *J. Am. Chem. Soc.* **2016**, 138, 10252.
- [24] A. Giovannitti, C. B. Nielsen, D. Sbircea, S. Inal, M. Donahue, M. R. Niazi, D. A. Hanifi, A. Amassian, G. G. Malliaras, J. Rivnay, I. McCulloch, *Nat. Commun.* **2016**, 7, 1.
- [25] A. Giovannitti, C. B. Nielsen, J. Rivnay, M. Kirkus, D. J. Harkin, A. J. P. White, H. Sirringhaus, G. G. Malliaras, I. McCulloch, *Adv. Funct. Mater.* **2016**, 26, 514.

[26] K. Rathee, V. Dhull, R. Dhull, S. Singh, *Biochem. Biophys. Reports* **2016**, 5, 35.

# Chapter 5

## Polyelectrolyte Layer by Layer Assembly on Organic Electrochemical Transistors



The present Chapter is based on the following publication:

**“Polyelectrolyte Layer by Layer Assembly on Organic Electrochemical Transistors”**

*A. M. Pappa, S. Inal, K. Roy, Y. Zhang, C. Pitsalidis, A. Hama, J. Pas, G. G.*

*Malliaras and R. M. Owens*

*ACS Appl. Mater. Interfaces, 2017, 9 (12), pp 10427–10434*

## **Abstract**

Oppositely charged polyelectrolyte multilayers (PEMs) were built-up in a layer-by-layer (LbL) assembly on top of the conducting polymer channel of an organic electrochemical transistor (OECT), aiming to combine the advantages of well-established PEMs with a high performance electronic transducer. The multilayered film is a model system to investigate the impact of biofunctionalization on the operation of OECTs comprising a poly(3,4-ethylenedioxythiophene) polystyrene sulfonate (PEDOT:PSS) film as the electrically active layer. Understanding the mechanism of ion injection into the channel that is in direct contact with charged polymer films provides useful insights for novel biosensing applications such as nucleic acid sensing. Moreover, LbL is demonstrated to be a versatile electrode modification tool enabling tailored surface features in terms of thickness, softness, roughness, and charge. LbL assemblies built-up on top of conducting polymers will aid the design of new bioelectronic platforms for drug-delivery, tissue engineering and medical diagnostics.

### Author's contribution:

For the present publication, used as the whole Chapter 6 in this Thesis my contribution was: the OECT fabrication and characterization, the development of the biofunctionalization strategy based on the layer-by layer assemblies of oppositely charged polyelectrolytes, and the nucleic acid experiments. Moreover, I prepared the biggest part of the manuscript, including the figures.

## 1. Introduction

The discovery of conducting polymers (CPs) has fueled research in multiple areas, and recently in the field of bioelectronics, coupling conventional electronics with biology.<sup>1,2</sup> The ability of CPs to conduct both electrons and ions, in combination with their soft nature and compatibility with biological species, are only some of the merits that render these materials a promising conduit between electronics and biology.<sup>3</sup> The field of organic bioelectronics leverages the properties of CPs to improve the biotic/abiotic interface, aiming to address unmet clinical needs.<sup>4</sup> For organic bioelectronic devices, the interface of the CP (the abiotic electronic component) with the biological milieu is of utmost importance, dictating most chemical, biological or electrical processes.<sup>5</sup> The ability to control and tailor this interface, either through post-processing or via synthesis, can endow devices with new functionalities, e.g. detection or stimulation of a biological process, which may otherwise be infeasible or inefficient with unmodified CP electrodes.<sup>6</sup> Synthetic routes are generally tedious, with the disadvantage of possibly interfering with the overall device performance, considering that electrical properties of CPs are often reported to be very sensitive to changes in the chemical structure.<sup>7</sup> Another point to take into account is that adsorption of a bio-active compound onto a solid substrate can introduce conformational changes in the molecule which may reduce, if not eliminate bioactivity.<sup>8</sup>

Layer-by-layer (LbL) assembly, first established by Decher et al,<sup>9</sup> is a bottom-up nanofabrication technique for multilayer formation on top of a desired substrate.<sup>10</sup> LbL assembly can generally be built up by alternating deposition of mutually interacting species such as oppositely charged polyelectrolytes, yielding polyelectrolyte multilayers (PEMs) that represent the majority of the LbL generated films studied to date.<sup>11</sup> Other PEM deposition techniques have been reported to be less versatile than LbL mostly due to limited type of assembly components (Langmuir-Blodgett type deposition is limited to amphiphilic molecules) and the requirement of certain chemical species on the surface for the attachment of the layers (e.g. self-assembled monolayers).<sup>10</sup> Given that most bioactive compounds have charged sites at their surfaces, LbL can also be applied to construct architectures including biological molecules.<sup>10</sup> The variety of materials that can be deposited as thin films using this technique, the mild processing conditions compatible with physiological conditions and its cost-effectiveness, as well as the control and tunability of the film properties, render LbL ideal for functionalizing surfaces with biological compounds.<sup>12,13</sup> Moreover, the use of the LbL technique for deposition/encapsulation of electroactive materials has enabled electro-

responsive films that are promising for biology-related applications.<sup>14</sup> For instance, electrical stimulation of LbL films comprising electroactive components has been reported to induce local changes in pH, ionic strength or even water electrolysis. These led to destabilization of the films and thus the release of the incorporated bio-active molecules such as DNA<sup>15</sup> or drugs.<sup>16,17</sup> Another work reported an LbL assembly of a redox active polymer and DNA that could electrochemically detect the oxidative damage of DNA.<sup>18</sup> Introduction of a redox enzyme such as lactate oxidase within an LbL assembly, at the gate of a field effect transistor resulted in sensitive detection of the corresponding metabolite, lactate, due to the preservation of the enzymatic activity.<sup>19</sup> Organic electrochemical transistors (OECTs) can efficiently transduce, as well as amplify, small ionic fluxes in biological systems into electrical outputs. The channel of the transistor, comprised typically of the CP PEDOT:PSS, is gated through an electrolyte (the biological medium), and any changes at this interface are expected to change the current outputs. OECTs differ from other electrolyte gated transistors in that the change in electronic charge density occurs over the entire volume of the channel, providing efficient ionic-to-electronic current transduction and leading to a high transconductance.<sup>20</sup> The transconductance (so far the highest reported among electrolyte-gated counterparts)<sup>21</sup> translates into high sensitivity in biosensing applications. OECTs have therefore been used for sensing of various biological species ranging from ions<sup>22</sup> to metabolites,<sup>23,24</sup> and processes such as cell proliferation and differentiation.<sup>25,26</sup>

In this work, we introduce for the first time, a LbL assembly of alternating polyelectrolytes, namely poly-L-lysine (PLL) and polystyrene sulfonate (PSS), on top of the channel of a PEDOT:PSS based OECT combining the advantages of well-established PEMs as a sensitive biofunctionalization approach with a highly performant electronic device. We demonstrate the formation of LbLs on the PEDOT:PSS channel and investigate how the device performance is affected upon the addition of the polyelectrolytes and further, how these changes can be translated into an efficient bio-sensing strategy. In particular, we show that the addition of a charged layer can modulate injection of ions into the channel, allowing for sensing applications in physiologically relevant electrolyte concentrations. A similar modulation effect was previously achieved by Magliulo *et al.*, via the use of a phospholipid bilayer on top of an organic semiconductor channel of an electrolyte gated field effect transistor.<sup>27</sup> As a proof of concept, we show the use of our LbL modified OECTs for the controlled immobilization as well as electrical detection of nucleic acids, en route to design more sophisticated biosensing systems. Since the technique allows for control over film formation, LbL modified transistors

sense nucleic acids with a higher sensitivity and broader dynamic range compared to unmodified devices.

## 2. Experimental Section

### *Fabrication of OECTs*

The devices are fabricated photolithographically using a parylene-C lift-off process.<sup>28</sup> Patterned gold lines serving as source, drain, and gate electrodes were patterned using Shipley 1813 photoresist, exposed to UV light with a SUSS MJB4 contact aligner, developed in MF-26 followed by thermal evaporation of chromium (10 nm) and gold (100 nm) and metal lift-off in acetone/isopropanol. Two 2  $\mu\text{m}$  thick parylene C layers (SCS Coating) separated by an anti-adhesive (industrial cleaner, Micro-90) were successively deposited using a SCS Labcoater 2. The first parylene layer, was attached to the substrate via an adhesion promoter, namely 3 (trimethoxysilyl)propyl methacrylate (A-174 Silane). For the patterning of the PEDOT:PSS channel (W/L, 100  $\mu\text{m}$ /10  $\mu\text{m}$ ), AZ9260 photoresist was spin cast, exposed, and developed in AZ developer (AZ Electronic Materials) followed by reactive ion etching by O<sub>2</sub> plasma (Oxford 80 Plasmalab plus) of the unprotected parts of parylene. The deposition parameters of the PEDOT:PSS films is as follows.

### *Preparation and biofunctionalization of PEDOT:PSS films with the LbL assemblies*

For the deposition of PEDOT:PSS films on transistor channels, a formulation of the commercial aqueous dispersion PH-1000 (Heraeus Clevis GmbH), consisting of 5%V/V ethylene glycol, 0.4%V/V dodecyl benzene sulphonic acid and 25wt% of polyvinyl alcohol was sonicated before spin-casting (2500rpm/ 35sec, for a thickness of 90 nm). The resulting films were subsequently baked at 110 °C for 1 h followed by 2 rinsing/soaking cycles in deionized water to remove any excess of low molecular weight compounds. For the polyelectrolyte assembly, PLL (MW: 70-150 kPa, Sigma Aldrich) and PSS (MW: 70kPa, Sigma Aldrich) at concentrations of 1 mg/ml in PBS were sequentially cast on the unmodified PEDOT:PSS films. During the PEM construction, each polyelectrolyte was left on top of the film for 20 min and all rinsing steps were performed with an aqueous solution of PBS at pH 7. In the particular case of the covalent attachment of the PLL initial layer, the PEDOT:PSS film was further modified as follows. O<sub>2</sub> plasma treatment (Oxford 80 Plasmalab plus) at mild conditions (25Watt/ 1min) was applied to modify the surfaces with hydroxyl groups for subsequent silanization via a



condensation reaction. 3-glycidoxo-propyltrimethoxysilane (GOPS) was deposited by vapor deposition at 90°C for 1h under vacuum. The films were then baked after washing with ethanol (15 sec) for the formation of the epoxy-modified surface. PLL solution at pH 9 was cast on top of these functionalized films and left for 2h. For the fluorescent-based evaluation of the PLL layer on top of PEDOT:PSS, a fluorescein isothiocyanate (FITC) labeled PLL of 1 mg/ml in PBS (MW: 15-30 kDa, Sigma-aldrich) was immobilized on a PEDOT:PSS patterned glass-slide and monitored with a fluorescence microscope (Axio Observer Z1, Carl Zeiss MicroImaging GmbH).

#### *Assessment of LbL assembly on top of PEDOT:PSS films via Quartz Crystal Microbalance with Dissipation module (QCM-D)*

The QCM-D measurements were carried out on a commercially available Q-Sense E4 instrument. (LOT-QuantumDesign, France). All measurements were carried out at 25 °C with a flow rate of 50  $\mu$ l/min controlled by a peristaltic pump. PEDOT:PSS films were cast on sensor crystals ( $\text{SiO}_2$ ) as described above. After stabilization in PBS, PLL and PSS were alternately injected into the system for a duration of 20 min for each polyelectrolyte. The sensors were rinsed with PBS after each layer formation. The assembly of PEMs was monitored through changes in resonance frequency ( $\Delta f$ ) and energy dissipation ( $\Delta D$ ) of crystals as a function of time using several overtones. All QCM-D data presented in this paper were measured at the fifth overtone.

#### *Assessment of the film morphology using Atomic Force Microscopy (AFM)*

The AFM investigation was carried out using a commercially available (Bruker) instrument. For better image acquisition, tapping mode was used at a scan rate of 1.0-1.2 Hz, with ultrasharp silicon cantilevers at a resolution of 512 points per line.

#### *Characterization of the LbL modified OECTs*

All measurements were performed using a Ag/AgCl wire (Warner Instruments) as the gate electrode and PBS or PBS diluted in DI water (pH 7.4), as electrolyte. The steady-state measurements of the OECT (output and transfer curves) were performed using a Keithley 2612A with customized LabVIEW software. For the transient characterization of the OECTs, an NI-PXI-4071 digital multimeter was employed to simultaneously measure drain and gate current ( $I_D$  and  $I_G$ ). For the transient response, a square pulse was applied to the gate and the

drain current was measured. The response time of the devices was determined using an exponential fit on the  $I_D$  profile. For the frequency dependent measurements, a sinusoidal voltage signal was applied at the gate, with varying frequency and amplitude ( $\Delta V_G=10$  mV peak-to-peak,  $1 \text{ Hz} < f < 20 \text{ kHz}$ ), while measuring  $I_D$  (at a constant drain voltage,  $V_D$ , of 0.6 V), and therefore transconductance ( $g_m$ ) as a function of frequency. The recorded signals were saved using customized LabVIEW and analyzed with Matlab.

#### *RNA immobilization on OECTs and its characterization*

For the nucleic acid immobilization on the transistor channel, increasing concentrations of single stranded mRNA (0.01 – 50 ng/ml) were deposited on the device and left for 30 min in humid conditions to avoid evaporation. Subsequently, the devices were rinsed in PBS and characterized. The  $I_D$  was extracted at a specific operation conditions ( $V_G=0\text{V}$  and  $V_D=-0.6\text{V}$ ) and for the different RNA concentrations and a calibration curve of the mRNA immobilization/detection was generated.

### **3. Results and Discussion**

#### **3.1 LbL on top of PEDOT:PSS : Optimizing the immobilization of the supporting layer by QCM-D**

PLL and PSS were chosen in this work as the positively and the negatively charged polyelectrolytes respectively, for alternated deposition on top of PEDOT:PSS. PLL is a polypeptide with pKa values ranging between 9 to 11 due to its amino side groups,<sup>29</sup> while the sulfonic acid groups of PSS result in pKa values ranging from 0.5 to 1.5.<sup>30</sup> **Figure 1a** shows the chemical structures of all the polymers, along with a schematic representation of the LbL assembly on top of PEDOT:PSS.

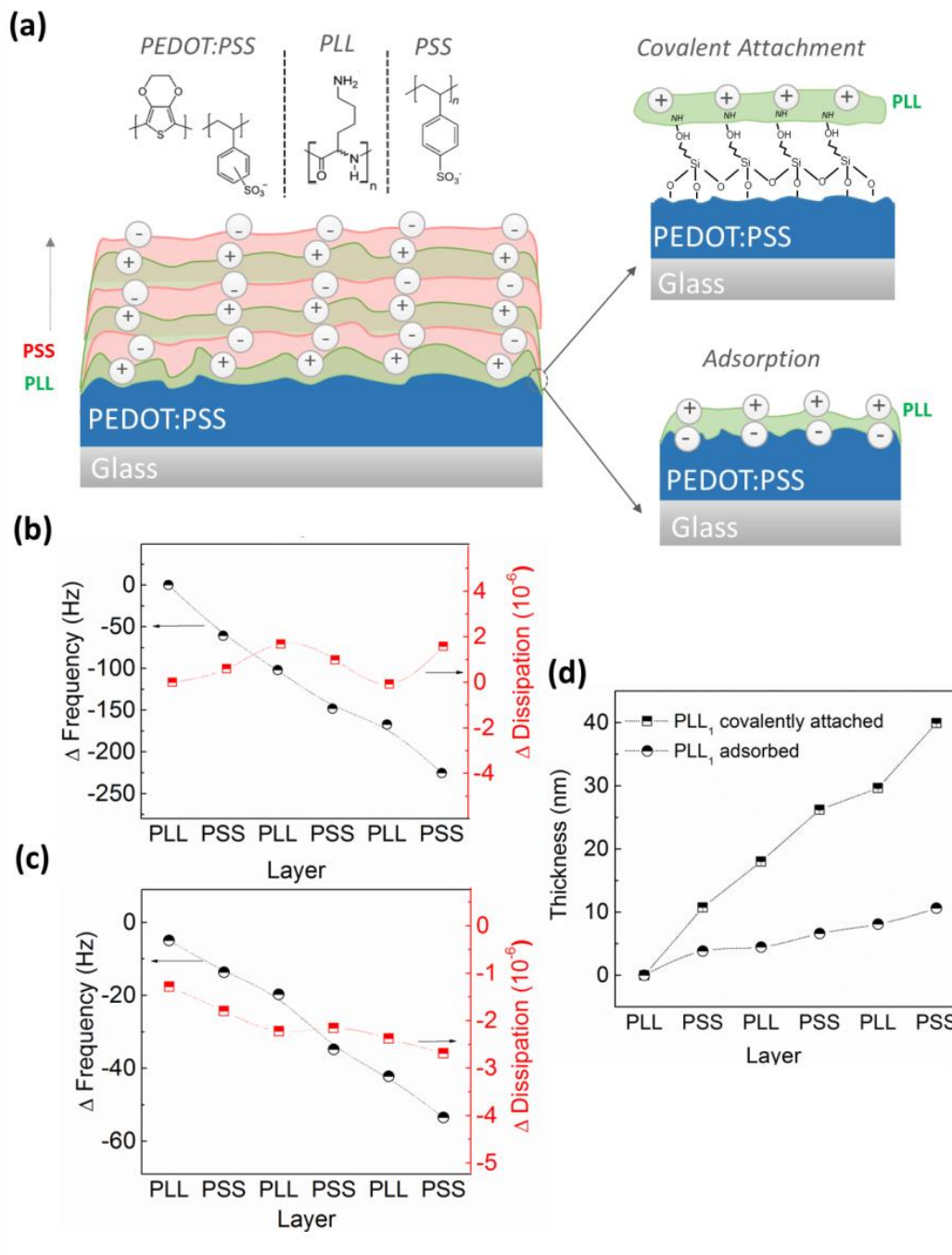


**Figure 1.** Building a LbL assembly on top of a PEDOT:PSS film. **(a)** Chemical structures of PEDOT:PSS and of the two polyelectrolytes employed, PLL and PSS and schematic of the PEM built up on top of PEDOT:PSS where the initial PLL layer is either covalently attached to the epoxy-modified PEDOT:PSS or electrostatically adsorbed to PEDOT:PSS film. **(b,c)** Changes in QCM-D frequency (black circles) and dissipation (red squares) properties of the PEDOT:PSS film as consecutive layers are formed for the case of covalent attachment of the supporting PLL layer as well as for the case its electrostatic adsorption, respectively. **(d)** The calculated film thickness using the Sauerbrey model, upon each layer addition for the two distinct cases, adsorption (black circles) and covalent attachment (black squares).

Bearing in mind the importance of the direct interface of the CP with the first polyelectrolyte layer, our first goal was to optimize the deposition of this initial layer. In our study, we used two approaches to deposit the first PLL layer: either covalently or via electrostatic adsorption. We utilized an epoxy-terminated silane on top of the plasma activated PEDOT:PSS surface as a means for subsequent polypeptide covalent attachment.<sup>31,32</sup> In order to monitor the *in-situ* LbL assembly formation on PEDOT:PSS film involving these two distinct functionalization approaches, we performed QCM-D measurements. QCM-D is a surface-sensitive technique used typically for the mass and viscoelasticity estimation of materials adsorbed on a quartz crystal. **Figure 1b** presents the shifts in the frequency and dissipation of the PEDOT:PSS coated SiO<sub>2</sub> crystals as each layer is built up, in the case where the supporting layer PLL, is covalently attached. The presence of this layer on top of the PEDOT:PSS film was as well evidenced by fluorescence microscopy using a fluorescent dye-conjugated analog of PLL (PLL-FITC) (**Figure S1**). During the assembly of the layers, we observe a gradual decrease in frequency and attribute it to the accumulation of polymers on the CP film. Simultaneously, the small change in dissipation ( $\Delta D < 1.7 \times 10^{-6}$ ) reveals the rigidity of the assembled film. The second approach relied on electrostatic adsorption of the initial PLL layer and the associated QCM-D signals summarized in **Figure 1c** indicate that the LbL formed herein is significantly thinner than for the case of the covalently attached PLL. Moreover, a gradual decrease in the dissipation values with each successive layer indicates that the structure gets softer. The properties of this assembly in terms of thickness and softness are similar to an identical one formed on a bare SiO<sub>2</sub> crystal (**Figure S2**). Overall, it is likely that the properties of the initial layer, governed by how it is deposited - either electrostatically or via covalent attachment, affect not only the thickness but also the softness of the final assembly – for at least three consecutive bilayers shown in this study. AFM studies demonstrate no significant morphological differences between these different foundation layers, as well as between the PEMs built on top them (**Figure S3**). The uppermost PSS film was, however, thicker for the case of covalently attached PLL layer. These results are in agreement with several studies reporting on the versatility of the LbL technique. Depending on the targeted application, process parameters can be fine-tuned modulating LbL film properties in return.<sup>33,34</sup> The specific needs of an application would therefore determine the optimum biofunctionalization approach.<sup>32</sup>

### 3.2 Characterization of LbL on top of an OECT

The LbL assembled film was subsequently implemented in a device configuration, and built-up on top of the channel of an OECT, as shown in **Figure 2a**. We chose to use the approach based on the covalently attached supporting layer, since the resulting film was found to be more rigid through the QCM-D studies and we anticipated that the low potentials applied for the OECT characterization would not affect the assembly. The typical steady-state characteristics of the OECT prior to any surface modification on the channel are shown in **Figure S4a**. Upon each layer addition, we observe a decrease in the current passing through the channel between the source and drain electrodes ( $I_D$ ) (**Figure 2b**). It is plausible that upon contact with the transistor channel, the positively charged PLL de-dopes PEDOT:PSS due to electrostatic interactions with the negatively charged sulfonate groups on the PSS that normally compensate for the mobile holes in PEDOT. This would lower the charge carrier density in the channel and consequently its electrical conductivity. Additional layers on the other hand could contribute to further de-doping. To elucidate this potential mechanism, we investigated the effect of the layers on the electrical conductance of the channel. For these measurements, the gate electrode was taken out of the electrolyte solution and the I-V characteristics of three identical PEDOT:PSS channels between gold contacts were recorded, upon each layer formation. While the first PLL layer increases the resistance of the channel slightly, the conductance seems to recover as the PSS layer is added (**Figure 2c**). Nevertheless, we do not observe a clear trend dependent on the polyelectrolyte on top.

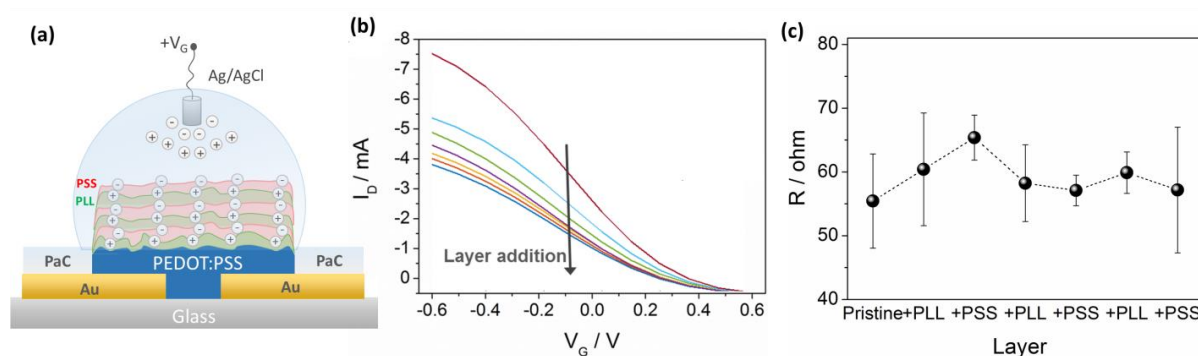


**Figure 2.** Steady state characteristics of the LbL modified OECT. **(a)** Schematic representation of an LbL modified channel of an OECT. Upon application of a positive gate bias ( $+V_G$ ), cations of the electrolyte are injected into the channel, modulating its conductivity; thereby changing the current between the source and drain contacts ( $I_D$ ). The gate electrode is Ag/AgCl, parylene (PaC) is the insulator and gold (Au) is used as the contacts of the electrodes. **(b)** Transfer curves recorded at  $V_D = -0.6$  V after formation of each polyelectrolyte layer. **(c)** The resistance of the channel as a function of consecutive layers deposited. The electrolyte is 0.1 X PBS.

One possible explanation for the decrease in  $I_D$  with successive layers is that each polyelectrolyte layer adds an additional capacitance to the ionic circuit between the gate and the channel.<sup>35</sup> OECTs are typically described by an electronic (within the channel) and an ionic circuit (along the gate and the channel) which may be thought of as a capacitor in series with a resistor.<sup>35</sup> The capacitance term here includes the two electrode/electrolyte interfaces. Since we use a nonpolarizable Ag/AgCl electrode as the gate, the application of  $V_G$  induces a steady-state current in the electrolyte endorsed by oxidation/reduction reactions at the gate. The device performance is thus affected by the channel/electrolyte interface where almost all the potential drop takes place.<sup>36</sup> We anticipate that as a new charged layer is formed on top of PEDOT:PSS, the potential profile in the electrolyte is modulated, irrespective of the polarity of pendant groups. In fact, as the polyelectrolytes accumulate on top of PEDOT:PSS, not only does the  $I_D$  decrease, but also the gating of the channel becomes less effective, as shown by the gradual decrease in transconductance ( $g_m = \Delta I_D / \Delta V_G$ ) (**Figure S4b**). This shows that the trend observed in the I-V characteristics that are related to changes in the ionic circuit, is visible due to the inherent amplification of the OECT.

The decrease in the  $g_m$  led us to investigate whether the films act as blocking layers and prevent free charges in the electrolyte from entering the channel. This would be best reflected in the temporal response of the device and, in a similar fashion, has been used to evaluate the integrity of barrier forming tissues.<sup>25,26,37</sup> We therefore recorded the transient characteristics of the devices before and after addition of the polyelectrolytes using two techniques which differ by the type of pulses applied at the gate; either sinusoidal or square. In the case of a sinusoidal voltage signal applied with varying frequency and amplitude, the resulting drain current is measured and extracted as the  $g_m$  of the OECT as a function of frequency.<sup>39</sup> Typically, below the device cut-off, the ions from the electrolyte can readily enter the channel and the OECT exhibits stable and high  $g_m$ . Above the device cut-off, however, the  $g_m$  drops since the ions do not have enough time to move into the channel, and this defines the speed of the transistor (see **Figure S5a**). Square voltage pulses at the gate similarly modify the drain current and the switching speed of the transistor is then extracted from the obtained current-time profiles.

**Figure 3a** shows the change in the cut-off frequency upon addition of each polyelectrolyte layer. Rather than a continuous barrier for ions, which would result in a gradual increase in switching speed, we observe a “ping-pong” effect with the alternating polyelectrolyte layers. For instance, the OECTs switch faster with the initial PLL layer (lower

cut-off), but slow down (higher cut-off) with the addition of a PSS layer; a trend that is consistent for the consecutive layers. We observe the same trend upon application of a square pulse at the gate electrode (**Figure 3b**). Moreover, with an increase in the bias magnitude at the gate ( $V_G=500\text{mV}$ ), devices that contain PSS as the uppermost layer recover to the initial switching speed more efficiently.

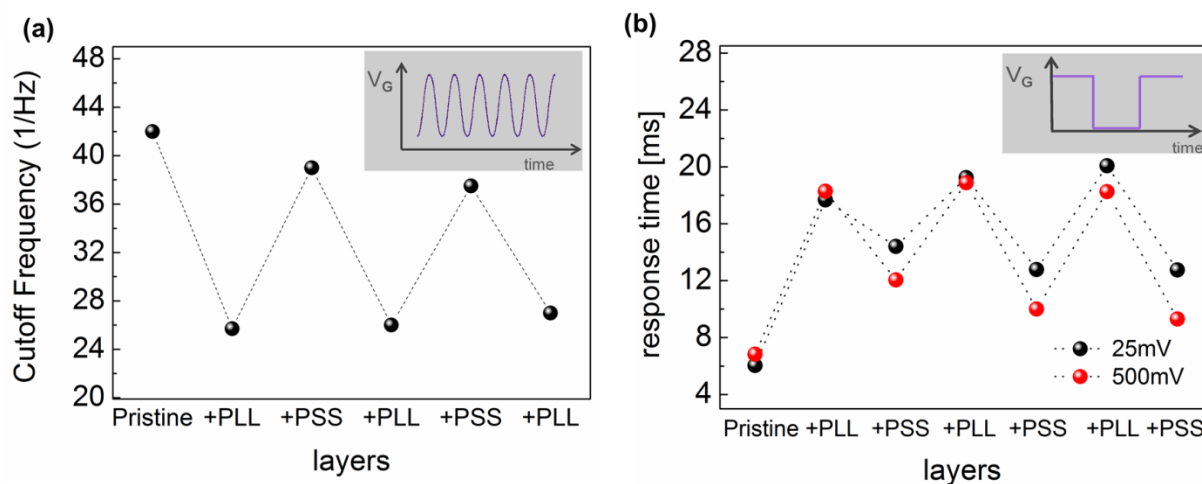


**Figure 3.** Transient characteristics of the LbL modified OECT. **a)** The change in the cut-off frequency of the devices upon addition of polyelectrolyte layers. The cut-off frequency was estimated from transconductance vs frequency plots acquired for each device configuration. **b)** The change in the response time of the devices determined from the drain current response to a square pulse at the gate which is 25mV (black) and 500 mV (red). All experiments were performed at PBS (diluted 100X).

In a multilayer assembly based on sequential adsorption of oppositely charged polyelectrolytes such as the one used here, once the polyelectrolyte is in excess, the “fixed charges” render the multilayer semi-permeable to ions. The electric potential difference between the PEM surface and the electrolyte is known as the Donnan potential and typically results in the repulsion of mobile ions of the same polarity with the fixed ions at the uppermost polyelectrolyte layer.<sup>40</sup> In our case, based on the transient behavior of the OECT, we observe that the Donnan exclusion effect is taking place when the PLL is the uppermost layer, since it requires more time for the cations to enter and dedope the channel. This leads us to hypothesize that the PSS intrinsically compensates for the PLL beneath and that there is a small excess of charges uncompensated on the PSS surface acting as the driving force for subsequent polyelectrolyte deposition. Due to the reduced repulsion/attraction, when PSS is the outermost layer, ions have less difficulty in entering the film. Furthermore, the increase in the injection bias (gate voltage) helps the ions to interact with PEDOT:PSS. Notably, in contrast to steady-state characteristics, the LbL-induced changes in the transient profile were more pronounced

when the measurements were performed at dilute electrolyte concentrations (diluted 100X) as shown in **Figure S5b**.

### 3.3 LbL for the controlled immobilization and monitoring of nucleic acid

Similar to alternate adsorption of polyelectrolyte systems, LbL can be used to deposit almost any type of charged species, e.g., oligonucleotides: RNA, DNA.<sup>15</sup> In particular, nucleic acid detection using organic electronic devices has received interest in the recent years as a label-free, faster more cost-effective method for diagnostic applications.<sup>41,42</sup> Non-specific RNA sensing has applications for example in viral diagnostics, when probing the RNA release from a purified virus.<sup>43</sup> As a proof-of-concept for biosensing, we used our LbL functionalized OECTs for electrical monitoring of a nucleic acid. The platform is based on the electrostatic adsorption of a single stranded negatively charged polymer (mRNA; messenger ribonucleic acid), onto the positively charged PLL layer of the LbL immobilized on top of the transistor channel. At physiologically relevant buffer concentration (1 X PBS), mRNA attachment does not lead to any notable change in the transient characteristics of the LbL modified OECT (**Figure S5c**). On the other hand, we observe a continuous decrease in the steady-state drain current values upon increasing mRNA concentration in the solution (**Figure 4a**). Note that without the PLL functionalization, PEDOT:PSS devices are insensitive to mRNA, even at a relatively high concentration, indicating that the polymer does not have non-specific interactions with the channel (**Figure 4b and S6**).

**Figure 4b** shows the calibration curves of the mRNA loading with respect to the normalized current response of the OECT for a selected gate voltage ( $V_G=0$  V) Here, we compare the detection sensitivity of two devices, one comprising an LbL modified channel, and a second which contains only one layer of PLL. We note that the response observed upon binding of mRNA is predominantly linear, although at lower concentrations, there may be some cooperativity type effects.<sup>44</sup> The mechanism of detection is based on the compensation of charges on the backbone of the mRNA, by positive charges on the upper layer of PLL. However, there may be more complex interactions occurring between the polypeptide and the nucleotide such as hydrogen bonding and hydrophobic interactions,<sup>45</sup> which will merit further investigation. There appears to be a difference in sensing capability of one versus the other: we posit that in the case of an LbL modified surface there is likely a more even surface charge distribution on the uppermost layer of the LbL which may enable sensing with a broader



dynamic range and higher sensitivity. In other words, the effect observed upon binding of mRNA to the LbL modified OECT appears not to saturate as early as that seen on a PLL modified device. Notably, the measurement error is larger for the OECT comprising a single PLL layer as the sensing-active component compared to the device modified with the LbL assembly.

The drawback of most electrolyte gated transistors used for sensing of such electrically charged species is the necessity to use low salt concentrations due to the Debye length limitations.<sup>46,47</sup> Current-voltage characteristics of LbL modified OECTs are, on the other hand, sensitive to RNA at ionic concentrations similar to those found in biological media such as the blood. Similar to the effect of the charged layers on top of the OECT, acting as an additional capacitor to our circuit, RNA layer changes the potential profile at the electrolyte shown at the steady state measurements.

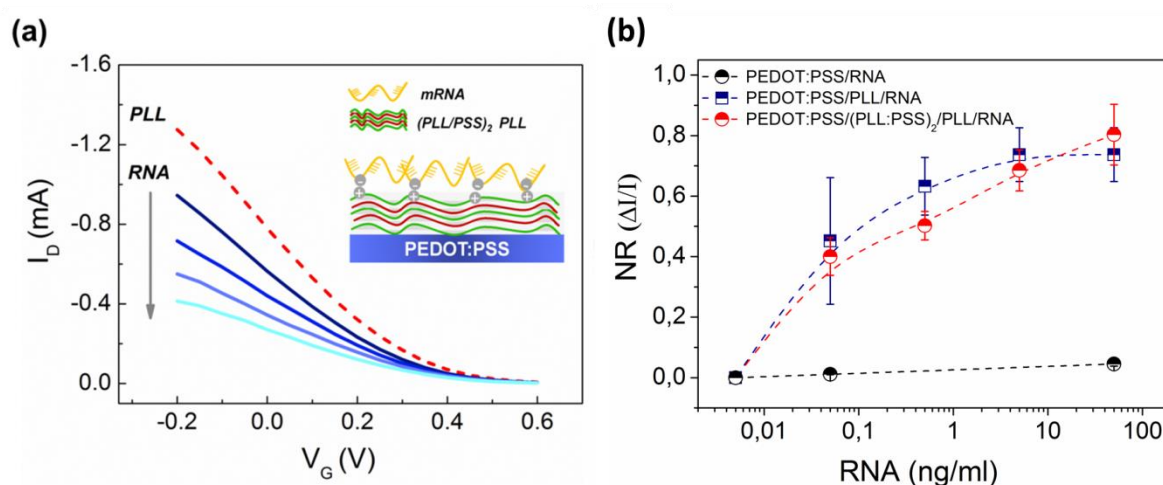


**Figure 4.** RNA sensing using LbL modified OECT. **a)** The change in transfer characteristics of the LbL modified OECT upon additions of increasing concentrations of the mRNA **b)** Comparative mRNA titration curves at  $V_G = 0$  V for an LbL modified device, a single layer PLL modified device and for a typical device (i.e. bare PEDOT:PSS in the channel serving as the control), showing an increased sensitivity with a broader linear range for the LbL assembly. All experiments were performed at physiologically relevant concentrations. The error bars were deduced from four measurements on two identical channels ( $100 \times 10 \mu\text{m}$  in length\*width)

## 4. Conclusions

In conclusion, we functionalized the conducting polymer channel of OECTs with an LbL assembly of polyelectrolytes, aiming to confer new functionalities on the device. This highly versatile technique enables fine tuning of crucial film parameters such as thickness and rigidity. We find that the PEMs modulate the electrical potential in the electrolyte and affect the injection of ions into the channel, which we utilize as a strategy to sense charged biological species such as mRNA. The LbL modified OECTs are able to sense nucleic acid in the electrolyte with a high sensitivity and broad linear range at low operating voltages. Notably, the devices signal the presence of mRNA at physiologically relevant electrolyte concentrations, visible in the steady state current profile. Future experiments will address specific nucleic acid detection using a complementary probe based on our LbL functionalization method.

## Acknowledgments

A-M. P and S. I. contributed equally to the present work. This work was supported by the Marie Curie ITN project OrgBio No. 607896 and the Agence Nationale de la Recherche 3Bs project. The authors are grateful to Alberto Salleo for fruitful discussions, and to NeuroSys for the kind gift of mRNA.

## AUTHOR INFORMATION

Corresponding Authors: [owens@emse.fr](mailto:owens@emse.fr); [sahika.inal@kaust.edu.sa](mailto:sahika.inal@kaust.edu.sa). Anna-Maria Pappa and Sahika Inal contributed equally to this work

## References

- (1) Chiang, C. K.; Fincher, C. R.; Park, Y. W.; Heeger, A. J.; Shirakawa, H.; Louis, E. J.; Gau, S. C.; MacDiarmid, A. G. Electrical Conductivity in Doped Polyacetylene. *Phys. Rev. Lett.* **1978**, *40* (22), 1472–1472.
- (2) Simon, D. T.; Gabrielsson, E. O.; Tybrandt, K.; Berggren, M. Organic Bioelectronics: Bridging the Signaling Gap between Biology and Technology. *Chem. Rev.* **2016**, *116* (21), 13009–13041.
- (3) Guimard, N. K.; Gomez, N.; Schmidt, C. E. Conducting Polymers in Biomedical Engineering. *Prog. Polym. Sci.* **2007**, *32*, 876–921.
- (4) Owens, R. M.; Malliaras, G. G. Organic Electronics at the Interface with Biology. *MRS Bull.* **2011**, *35* (06), 449–456.
- (5) Molino, P. J.; Yue, Z.; Zhang, B.; Tibbens, A.; Liu, X.; Kapsa, R. M. I.; Higgins, M. J.; Wallace, G. G. Influence of Biodopants on PEDOT Biomaterial Polymers: Using QCM-D to Characterize Polymer Interactions with Proteins and Living Cells. *Adv. Mater. Interfaces* **2014**, *1* (3), 1300122.
- (6) Goddard, J. M.; Hotchkiss, J. H. Polymer Surface Modification for the Attachment of Bioactive Compounds. *Prog. Polym. Sci.* **2007**, *32* (7), 698–725.
- (7) Inal, S.; Rivnay, J.; Hofmann, A. I.; Uguz, I.; Mumtaz, M.; Katsigiannopoulos, D.; Brochon, C.; Cloutet, E.; Hadziioannou, G.; Malliaras, G. G. Organic Electrochemical Transistors Based on PEDOT with Different Anionic Polyelectrolyte Dopants. *J. Polym. Sci. Part B Polym. Phys.* **2016**, *54* (2), 147–151
- (8) *Iontronics: Ionic Carriers in Organic Electronic Materials and Devices*; Leger, J., Berggren, M., Carter, S., Eds.; CRC Press, 2010.
- (9) Decher, G.; Hong, J. D.; Schmitt, J. Buildup of Ultrathin Multilayer Films by a Self-Assembly Process: III. Consecutively Alternating Adsorption of Anionic and Cationic Polyelectrolytes on Charged Surfaces. *Thin Solid Films* **1992**, *210–211*, 831–835.

- (10) Ariga, K.; Hill, J. P.; Ji, Q. Layer-by-Layer Assembly as a Versatile Bottom-up Nanofabrication Technique for Exploratory Research and Realistic Application. *Phys. Chem. Chem. Phys.* **2007**, *9* (19), 2319–2340.
- (11) Rydzek, G.; Ji, Q.; Li, M.; Schaaf, P.; Hill, J. P.; Boulmedais, F.; Ariga, K. Electrochemical Nanoarchitectonics and Layer-by-Layer Assembly: From Basics to Future. *Nano Today* **2015**, *10* (2), 138–167.
- (12) Vendra, V. K.; Wu, L.; Krishnan, S. *Polymer Thin Films for Biomedical Applications; Nanomaterials for the Life Sciences 5*; Wiley-VCH:Weinheim, Germany, 2010, pp 1–54.
- (13) Pérez, R. A.; Won, J. E.; Knowles, J. C.; Kim, H. W. Naturally and Synthetic Smart Composite Biomaterials for Tissue Regeneration. *Adv. Drug Deliv. Rev.* **2013**, *65* (4), 471–496.
- (14) Boudou, T.; Crouzier, T.; Ren, K.; Blin, G.; Picart, C. Multiple Functionalities of Polyelectrolyte Multilayer Films: New Biomedical Applications. *Adv. Mater.* **2009**, *22* (4), 441–467.
- (15) Diéguez, L.; Darwish, N.; Graf, N.; Vörös, J.; Zambelli, T. Electrochemical Tuning of the Stability of PLL/DNA Multilayers. *Soft Matter* **2009**, *5* (12), 2415–2421.
- (16) Wohl, B. M.; Engbersen, J. F. J. Responsive Layer-by-Layer Materials for Drug Delivery. *J. Control. Release* **2012**, *158* (1), 2–14.
- (17) Wood, K. C.; Zacharia, N. S.; Schmidt, D. J.; Wrightman, S. N.; Andaya, B. J.; Hammond, P. T. Electroactive Controlled Release Thin Films. *Proc. Natl. Acad. Sci. U. S. A.* **2008**, *105* (7), 2280–2285.
- (18) Wang, B.; Rusling, J. F. Voltammetric Sensor for Chemical Toxicity Using [Ru(bpy)<sub>2</sub>poly(4-vinylpyridine)<sub>10</sub>Cl]<sup>+</sup> as Catalyst in Ultrathin Films. DNA Damage from Methylating Agents and an Enzyme-Generated Epoxide. *Anal. Chem.* **2003**, *75* (16), 4229–4235.
- (19) Xu, J.-J.; Zhao, W.; Luo, X.-L.; Chen, H.-Y. A Sensitive Biosensor for Lactate Based on Layer-by-Layer Assembling MnO<sub>2</sub> Nanoparticles and Lactate Oxidase on Ion-Sensitive Field-Effect Transistors. *Chem. Commun.* **2005**, (6), 792–794.

- (20) Inal, S.; Rivnay, J.; Leleux, P.; Ferro, M.; Ramuz, M.; Brendel, J. C.; Schmidt, M. M.; Thelakkat, M.; Malliaras, G. G. A High Transconductance Accumulation Mode Electrochemical Transistor. *Adv. Mater.* **2014**, *26* (44), 7450–7455.
- (21) Khodagholy, D.; Rivnay, J.; Sessolo, M.; Gurfinkel, M.; Leleux, P.; Jimison, L. H.; Stavrinidou, E.; Herve, T.; Sanaur, S.; Owens, R. M.; Malliaras, G. G. High Transconductance Organic Electrochemical Transistors. *Nat. Commun.* **2013**, *4*, 2133.
- (22) Sessolo, M.; Rivnay, J.; Bandiello, E.; Malliaras, G. G.; Bolink, H. J. Ion-Selective Organic Electrochemical Transistors. *Adv. Mater.* **2014**, *26* (28), 4803–4807.
- (23) Tang, H.; Yan, F.; Lin, P.; Xu, J.; Chan, H. L. W. Highly Sensitive Glucose Biosensors Based on Organic Electrochemical Transistors Using Platinum Gate Electrodes Modified with Enzyme and Nanomaterials. *Adv. Funct. Mater.* **2011**, *21* (12), 2264–2272.
- (24) Pappa, A.-M.; Curto, V. F.; Braendlein, M.; Strakosas, X.; Donahue, M. J.; Fiocchi, M.; Malliaras, G. G.; Owens, R. M. Organic Transistor Arrays Integrated with Finger-Powered Microfluidics for Multianalyte Saliva Testing. *Adv. Healthc. Mater.* **2016**, *5* (17), 2295–2302.
- (25) Ramuz, M.; Hama, A.; Rivnay, J.; Leleux, P.; Owens, R. Monitoring of Cell Layer Coverage and Differentiation with the Organic Electrochemical Transistor. *J. Mater. Chem. B* **2015**, *3* (29), 5971–5977.
- (26) Tria, S. A.; Ramuz, M.; Jimison, L. H.; Hama, A.; Owens, R. M. Sensing of Barrier Tissue Disruption with an Organic Electrochemical Transistor. *J. Vis. Exp.* **2014**, No. 84, e51102.
- (27) Magliulo, M.; Mallardi, A.; Mulla, M. Y.; Cotrone, S.; Pistillo, B. R.; Favia, P.; Vikholm-Lundin, I.; Palazzo, G.; Torsi, L. Electrolyte-Gated Organic Field-Effect Transistor Sensors Based on Supported Biotinylated Phospholipid Bilayer. *Adv. Mater.* **2013**, *25* (14), 2090–2094.
- (28) Sessolo, M.; Khodagholy, D.; Rivnay, J.; Maddalena, F.; Gleyzes, M.; Steidl, E.; Buisson, B.; Malliaras, G. G. Easy-to-Fabricate Conducting Polymer Microelectrode Arrays. *Adv. Mater.* **2013**, *25* (15), 2135–2139.
- (29) Choi, J.-H.; Kim, S.-O.; Linardy, E.; Dreaden, E. C.; Zhdanov, V. P.; Hammond, P. T.; Cho, N.-J. Influence of pH and Surface Chemistry on Poly(L-Lysine) Adsorption onto Solid

Supports Investigated by Quartz Crystal Microbalance with Dissipation Monitoring. *J. Phys. Chem. B* **2015**, *119* (33), 10554–10565.

(30) Lewis, S. R.; Datta, S.; Gui, M.; Coker, E. L.; Huggins, F. E.; Daunert, S.; Bachas, L.; Bhattacharyya, D. Reactive Nanostructured Membranes for Water Purification. *Proc. Natl. Acad. Sci. U. S. A.* **2011**, *108* (21), 8577–8582.

(31) Strakosas, X.; Sessolo, M.; Hama, A.; Rivnay, J.; Stavrinidou, E.; Malliaras, G. G.; Owens, R. M. A Facile Biofunctionalisation Route for Solution Processable Conducting Polymer Devices. *J. Mater. Chem. B* **2014**, *2* (17), 2537–2545.

(32) Strakosas, X.; Wei, B.; Martin, D. C.; Owens, R. M. Biofunctionalization of Polydioxythiophene Derivatives for Biomedical Applications. *J. Mater. Chem. B* **2016**, *4* (29), 4952–4968.

(33) El Haitami, A. E.; Martel, D.; Ball, V.; Nguyen, H. C.; Gonthier, E.; Labbé, P.; Voegel, J.-C.; Schaaf, P.; Senger, B.; Boulmedais, F. Effect of the Supporting Electrolyte Anion on the Thickness of PSS/PAH Multilayer Films and on Their Permeability to an Electroactive Probe. *Langmuir* **2009**, *25* (4), 2282–2289.

(34) Kolasińska, M.; Krastev, R.; Warszyński, P. Characteristics of Polyelectrolyte Multilayers: Effect of PEI Anchoring Layer and Posttreatment after Deposition. *J. Colloid Interface Sci.* **2007**, *305* (1), 46–56.

(35) Bernardis, D. A.; Malliaras, G. G. Steady-State and Transient Behavior of Organic Electrochemical Transistors. *Adv. Funct. Mater.* **2007**, *17* (17), 3538–3544.

(36) Demelas, M.; Scavetta, E.; Basiricò, L.; Rogani, R.; Bonfiglio, A. A Deeper Insight into the Operation Regime of All-Polymeric Electrochemical Transistors. *Appl. Phys. Lett.* **2013**, *102* (19), 193301.

(37) Tria, S. A.; Jimison, L. H.; Hama, A.; Bongo, M.; Owens, R. M. Validation of the Organic Electrochemical Transistor for in Vitro Toxicology. *Biochim. Biophys. Acta* **2013**, *1830* (9), 4381–4390.

(38) Ramuz, M.; Hama, A.; Rivnay, J.; Leleux, P.; Owens, R. M. Monitoring of Cell Layer Coverage and Differentiation with the Organic Electrochemical Transistor. *J Mater Chem B* **2015**, *3* (29), 5971–5977.

- (39) Rivnay, J.; Ramuz, M.; Leleux, P.; Hama, A.; Huerta, M.; Owens, R. M. Organic Electrochemical Transistors for Cell-Based Impedance Sensing. *Appl. Phys. Lett.* **2015**, *106* (4), 043301.
- (40) Calvo, E. J.; Wolosiuk, A. Donnan Permselectivity in Layer-by-Layer Self-Assembled Redox Polyelectrolyte Thin Films. *J. Am. Chem. Soc.* **2002**, *124* (28), 8490–8497.
- (41) Lai, S.; Demelas, M.; Casula, G.; Cosseddu, P.; Barbaro, M.; Bonfiglio, A. Ultralow Voltage, OTFT-Based Sensor for Label-Free DNA Detection. *Adv. Mater.* **2013**, *25* (1), 103–107.
- (42) Demelas, M.; Lai, S.; Casula, G.; Scavetta, E.; Barbaro, M.; Bonfiglio, A. An Organic, Charge-Modulated Field Effect Transistor for DNA Detection. *Sens. Actuators, B* **2012**, *171*, 198–203.
- (43) Hsu, H.-L.; Millet, J. K.; Costello, D. A.; Whittaker, G. R.; Daniel, S. Viral Fusion Efficacy of Specific H3N2 Influenza Virus Reassortant Combinations at Single-Particle Level. *Sci. Rep.* **2016**, *6*, 35537.
- (44) Liu, G.; Molas, M.; Grossmann, G. A.; Pasumathy, M.; Perales, J. C.; Cooper, M. J.; Hanson, R. W. Biological Properties of Poly-L-Lysine-DNA Complexes Generated by Cooperative Binding of the Polycation. *J. Biol. Chem.* **2001**, *276* (37), 34379–34387.
- (45) Jones, S.; van Heyningen, P.; Berman, H. M.; Thornton, J. M. Protein-DNA Interactions: A Structural Analysis. *J. Mol. Biol.* **1999**, *287* (5), 877–896.
- (46) Kergoat, L.; Piro, B.; Berggren, M.; Pham, M.-C.; Yassar, A.; Horowitz, G. DNA Detection with a Water-Gated Organic Field-Effect Transistor. *Org. Electron.* **2012**, *13* (1), 1–6.
- (47) Wang, D.; Noël, V.; Piro, B. Electrolytic Gated Organic Field-Effect Transistors for Application in Biosensors - A Review. *Electronics* **2016**, *5* (1), 9.

## Supporting information

*Supporting information:* Transfer characteristics of a pristine OECT and after addition of mRNA; The transconductance ( $g_m$ ) vs. frequency plots of an OECT channel upon each

consecutive polyelectrolyte formation; Typical output characteristics of the OECT prior to any surface modification on top of the channel; Changes in QCM-D frequency and dissipation of a SiO<sub>2</sub> crystal upon formation of an LbL assembly of PEMs; Fluorescence microscopy image of the fluorescein isothiocyanate (FITC) labeled PLL covalently attached on the surface of epoxy-modified PEDOT:PSS and AFM images of LbL modified PEDOT:PSS films.

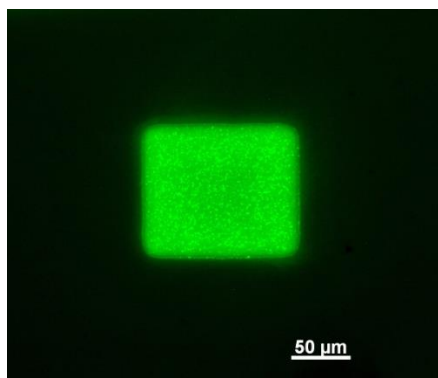


**Figure S1.** Fluorescence microscopy image of the fluorescein isothiocyanate (FITC) labeled PLL covalently attached on the surface of epoxy-modified PEDOT:PSS.

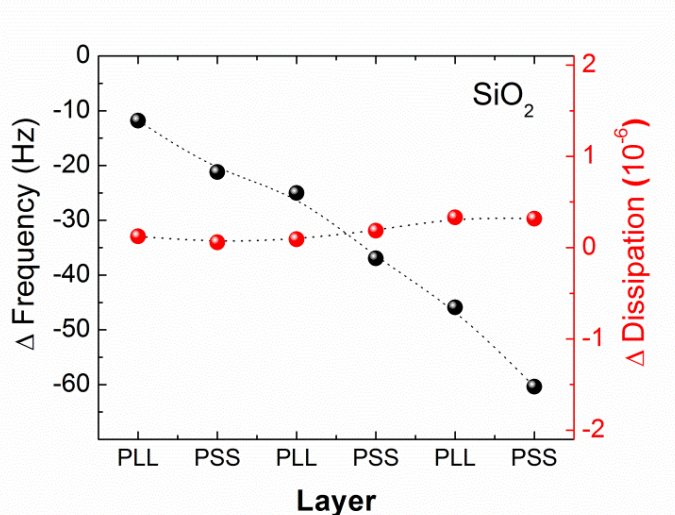


**Figure S2.** Changes in QCM-D frequency (black) and dissipation (red) of a SiO<sub>2</sub> crystal upon formation of an LbL assembly of PEMs.



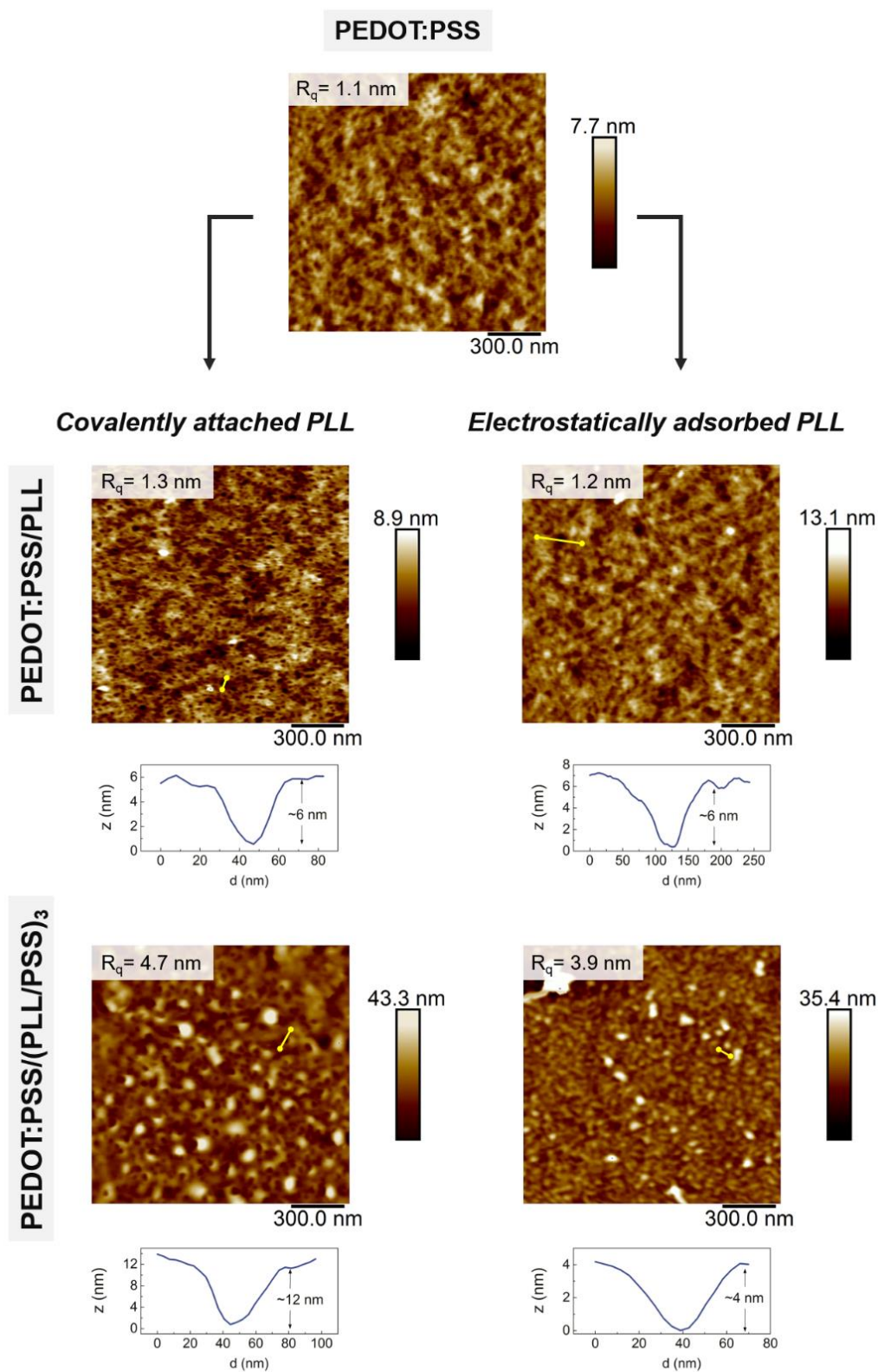


**Figure S3.** Morphological evaluation of a PEDOT:PSS film upon formation of the foundation PLL layer and of the consecutive polyelectrolyte layers (PLL/PSS)<sub>3</sub> via the LbL deposition. The foundation layer PLL was either covalently attached or electrostatically adsorbed.

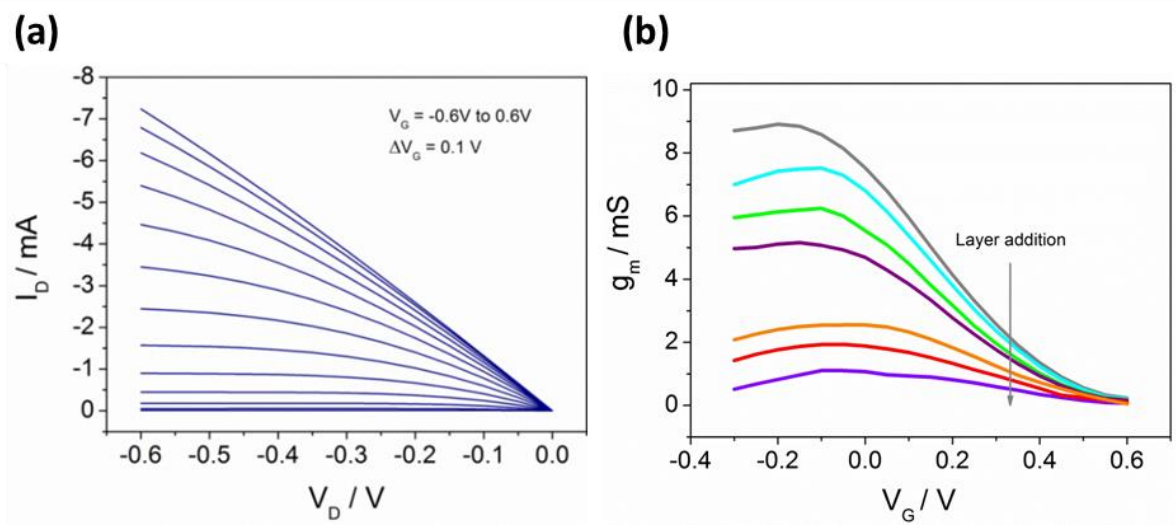


**Figure S4.** **a)** Typical output characteristics of the OEET prior to any surface modification on top of the channel **b)** The transconductance ( $g_m$ ) as a function of the gate bias ( $V_G$ ) of the pristine OEET (black) and upon each consecutive polyelectrolyte formation (color map)

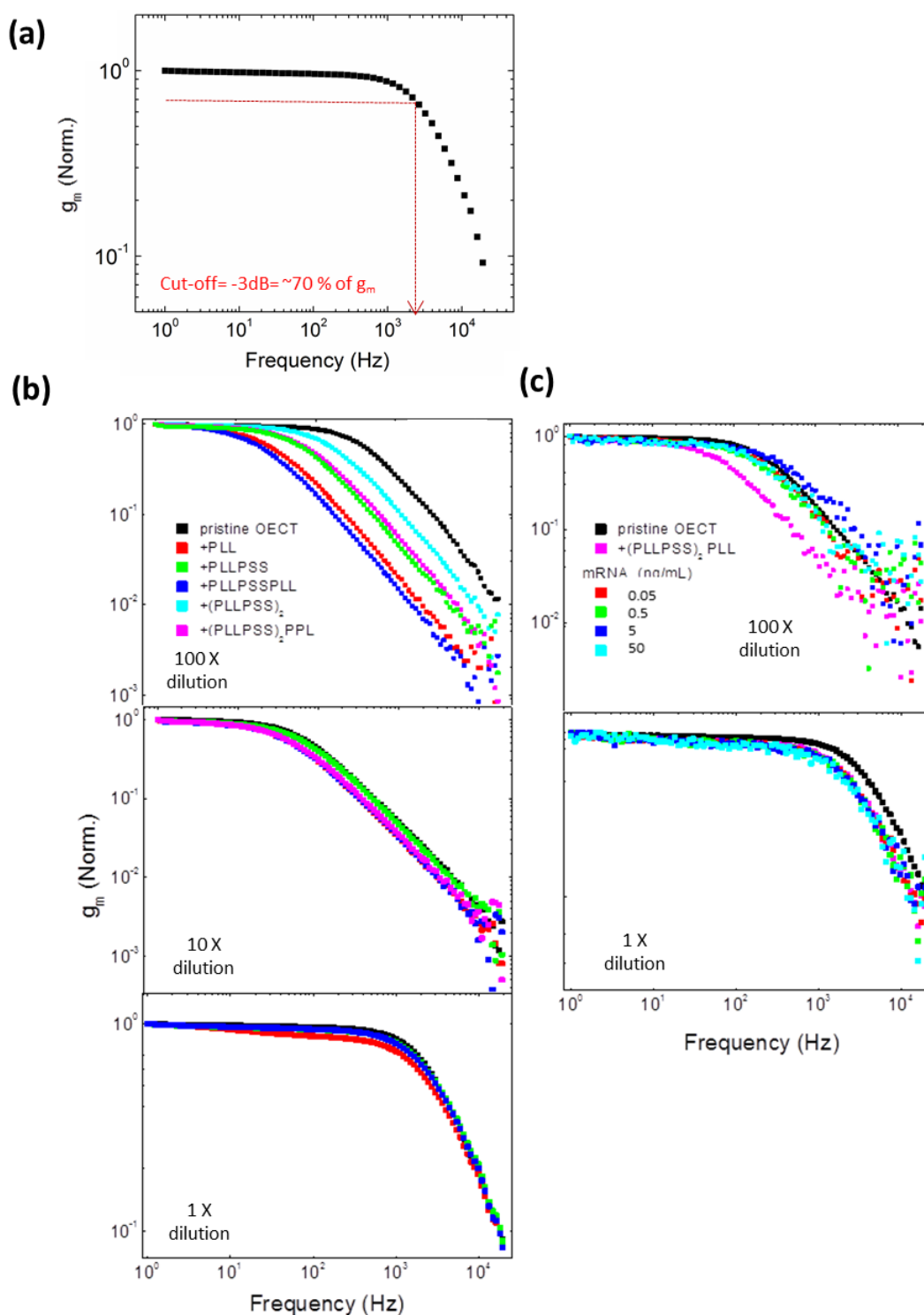


**Figure S5.** a) The transconductance ( $g_m$ ) vs. frequency plot of a typical OECT, showing the device cut-off calculation. b) The transconductance ( $g_m$ ) vs. frequency plots of an OECT channel upon each consecutive polyelectrolyte formation. The measurements were performed on the same channel using different electrolyte concentrations (upper to lower panel, the PBS concentration increases). c) Effect of electrolyte concentration on the sensitivity of RNA detection based on the transient OECT response as measured in PBS diluted 100X (upper panel) and PBS not diluted (lower panel).

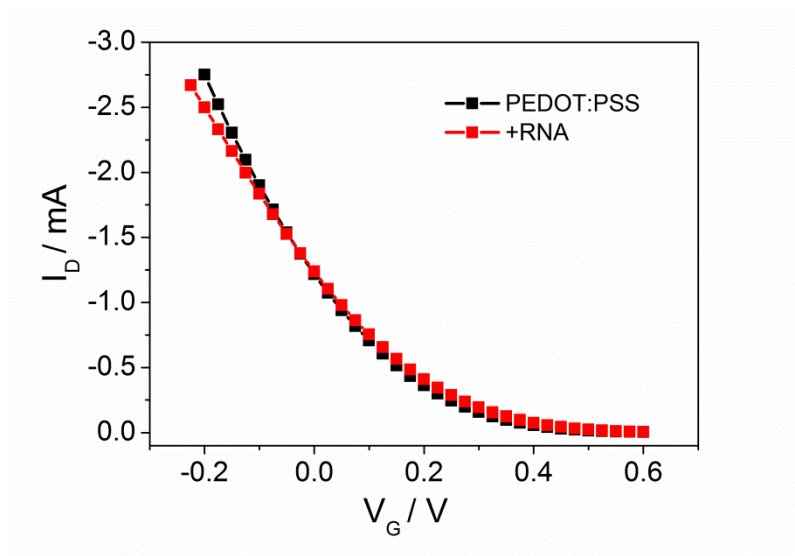


**Figure S6.** Transfer characteristics of a pristine OEET and after addition of mRNA (50ng/ml) at  $V_D=-0.6V$

# Conclusions and Outlook

---

Having already demonstrated technological maturity and successful commercialization in applications such as light emitting diodes or photovoltaics, organic electronics have made a mark in the biomedical field with a plethora of research prototypes already showing potential for commercialization. The present work aims to show how organic electronic materials can improve existing healthcare technologies or even provide new solutions to unmet clinical needs due to their unique material properties and their versatility. With a particular emphasis in enzymatic detection of human metabolites, the present thesis aims to solve critical issues in real world applications related to complex sensing environment and the need for multiplexing and system integration. We address this, i) by showcasing the implementation of innovative device configurations based on organic electronics and ii) by exploring the structural tunability as well as versatility in surface chemistry of organic electronic materials toward an optimized interface with the biological milieu.

In **Chapter 1**, the state-of-the-art in organic electronic materials for enzymatic sensing of metabolites is initially summarized and discussed. By highlighting specific examples from literature, organic electronic materials' adaptability to challenging performance requirements (related to complex biological milieu) and their ability to serve simultaneously as immobilization matrices for the biorecognition elements (i.e., enzymes) and as biotransducers, are showcased. For example, their polymeric structure allows for an intimate electrochemical contact with the biorecognition element and/or their facile implementation into innovative device configurations facilitating system integration are only some of the factors that are credited for their success in biological applications.

Indeed, the major challenges when it comes to real world applications in biosensing are two-fold; the sensitivity and specificity of the biosensor in the highly interferent environment of the biological samples and the system integration toward automated, standalone and user-friendly platforms. Electrochemical detection combined with microelectronics technology can provide a fast, label-free and versatile alternative to the existing detection methods that rely on heavy instrumentation and highly trained personnel. One great example of such electrochemical transducer is the organic electrochemical transistor (OECT). OECTs, operate in aqueous

electrolytes and transduce as well as amplify signals of biological origin (ionic) to electronic ones without requiring freestanding conventional reference electrodes used in common electrochemical setups. Taking advantage of the design freedom and ease of integration of such technology, in **Chapter 2**, OECT arrays were fabricated on glass substrates using a straightforward monolithic lithographic approach, serving as a highly integrated platform for the simultaneous detection of clinically relevant metabolites (i.e., glucose, lactate and cholesterol) in untreated saliva samples of human volunteers. The OECTs, comprised of Poly(3,4-ethylenedioxythiophene) polystyrene sulfonate (PEDOT:PSS), an intrinsically p-type doped organic semiconductor, were individually functionalized with the corresponding enzymes and an electron transfer mediator to ensure an intimate electrochemical contact with the sensing electrode avoiding free diffusing species and limiting electrochemical interference. The biosensor prototype exhibited excellent analytical performance with detection ranges that covered the physiological ranges in saliva for all the detected metabolites. The multiplexing biosensing platform was also combined with a portable microfluidic (pumpless) to enable sample distribution and automation.

Saliva, does not however represent a highly interfering biological matrix when compared to blood or live cell supernatants. Undeniably, in such cases it is far more challenging to ensure reliability and specificity ruling out the matrix effects. Bearing in mind the high complexity of cell culture media, in **Chapter 3**, a sensor circuit was developed that provided inherent background subtraction, comprising of two PEDOT:PSS based OECTs in a Wheatstone bridge sensor circuit where one transistor served as the sensing element and the other as the reference. The reference-based biosensing platform, functionalized with lactate oxidase provided highly sensitive lactate detection produced from as low as few tens of cells due to its high amplification in combination with the inherent background subtraction, thus ensuring elimination of any interference arising from other factors (i.e., electro-oxidizable compounds, electrolyte evaporation etc). As a proof-of-concept, the lactate produced from cultures of healthy peripheral blood mononuclear cells and malignant non-Hodgkin's lymphomas was compared and elevated lactate production was indeed monitored in the tumor cell cultures, confirming their intrinsic enhanced glycolytic metabolic activity. The proposed sensor can be used for the detection of lactate produced from circulating tumor cells in blood, paving the way to an in vitro prognostic model of the degree of malignancy in primary tumors as well as of the probability of metastasis opening a new direction in clinically relevant testing protocols that are important to follow tumor evolution or treatment efficiency in cancer patients.

Given that PEDOT:PSS is an intrinsically doped semiconductor the resulting OECTs, operate in the depletion regime meaning that they switch off upon application of a gate voltage (dedoping the organic semiconductor). This can pose specific disadvantages when it comes to biosensing as compared to devices that switch on upon detection/transduction of a biological event (accumulation mode). In principal, the accumulation mode transistors are identified with a large operation window, a high signal on/off response and a low-power operation. In **Chapter 4**, we sought to harness the structural versatility of organic electronics and design materials that will meet our dual requirements; *i*) being compatible with OECT operation and *ii*) exhibit N-type transport to serve as an electron acceptor material. Accumulation mode OECTs comprised of an electron acceptor organic semiconducting material were thus developed and optimized for the enzymatic detection of lactate, for the first time. Without the need for an artificial electron-transfer mediator, the N-type channel was directly doped from the electron(s) produced during the enzymatic reactions, leading to a sensor with superior sensitivity and detection range compared to PEDOT:PSS analogues. This novel concept of using accumulation mode OECT devices with active materials that act simultaneously as electron acceptors opens up a wide range of possibilities both in biosensing but also in other fields such as biofuel cells.

Last but not least, the repertoire of biosensing capabilities and surface functionalization strategies of OECTs was extended beyond enzymatic based detection. A biofunctionalization method comprised of oppositely charged polyelectrolyte multilayers (PEMs) built up in a layer-by-layer (LbL) assembly on top of the conducting polymer channel of an OECT was developed in **Chapter 5**. The multilayered film served as a model system to investigate the impact of biofunctionalization on the operation of OECTs comprising a PEDOT:PSS film. It was found that the PEMs modulate the electrical potential in the electrolyte affecting the ion injection into the channel, which was utilized as a strategy to sense charged biological species such as mRNA. The LbL modified OECTs were able to sense nucleic acid at physiologically relevant electrolyte concentrations with high sensitivity and broad linear range at low operating voltages visible in the steady state current profile. Future experiments will address specific nucleic acid detection using a complementary probe based on our LbL functionalization method.

Despite the substantial progress in biosensor research and development there are only few examples that have successfully entered the market, with glucose sensors as an exception. The stringent requirements of high analytical performance along with cheap, easy-to-use, long-lasting devices restrict clinical implementation. Organic electronic materials are anticipated to shift the current trend providing novel concepts and devices at low cost, without compromising

the sensor performance. We showed, in this work, proof-of-concept studies where organic electronic devices based on PEDOT:PSS, can be engineered and optimized to meet current challenges in biosensing such as multiplexing, system integration and sensing in the harsh biological milieu. We tested our devices in real world applications, detecting clinically relevant biomarkers from human saliva as well as the lactate produced from tumor cells showing the direct applicability of our prototypes for cancer and other disease (i.e., diabetes) diagnostics. We also showed that novel organic electronic materials can be synthesized and customized to meet both the device and the application of interest requirements. For example an electron acceptor conjugated polymer, compatible with the OECT operation was used as electrode for the direct electrochemistry of lactate and lactate oxidase exhibiting excellent analytical characteristics owing to the material properties and the device operation. Finally, we showed that the OECT capabilities can be extended from the bioelectrocatalytic detection scheme that involves electrochemical reactions, to other types of molecular sensing (i.e., electrostatic).

In short term, future directions include the investigation of other materials beyond PEDOT:PSS (such as the N-type polymer presented in Chapter 4) and their implementation into the developed device circuits in order to improve the sensor analytical characteristics (stability, sensitivity, integration, etc.). One drawback for example of the Wheatstone bridge sensor presented in Chapter 3 is the need to use two separate reservoirs for the electrolyte in the two branches of the sensor circuit, hindering to some extent its use in some practical applications such as in *in vivo*. This is because PEDOT:PSS is a p-type depletion mode semiconductor (the transistor is on “on state” and the application of a positive gate voltage results in dedoping of the organic semiconductor and hence an attenuation of the source-drain current). Therefore, the enzymatic oxidation reaction takes place at the positively biased gate electrode of the transistor, (vs the negatively biased channel) requiring also the biofunctionalization to take place at that electrode. With an accumulation mode material however, such as the one reported in Chapter 4 (N-type accumulation material: a positive gate voltage results in doping of the organic semiconductor and hence an increase of the source-drain current), by fine tuning the applied voltages (gate and source-drain), the enzymatic oxidation reaction can be “forced” to take place at the channel electrode. In such case, the OECTs could be controlled through the same gate, meaning that in a Wheatstone bridge sensor circuit layout, a single electrolyte reservoir could be potentially used along with a single gate. This is expected to improve both the practical applicability of the sensor but also its analytical performance.



In a broader view, future directions include the implementation of the developed concepts and platforms toward more targeted and clinically relevant diagnostic and prognostic models. I envision for example, the use of the reference-based Wheatstone Bridge sensor as a tool to predict metastatic events in cancer patients by measuring their blood lactate concentration. Circulating tumor cells (CTCs), the cells that come from the vasculature or lymphatics from a primary tumor and circulate through the body via blood, are responsible for the metastasis in cancer. Since CTCs, represent only the  $1/10^5$  of the total cell amount in blood, it is somewhat challenging to detect their presence. Nonetheless, their excessive production of lactate (due to their high metabolic activity) in combination with a very sensitive sensor (sensitive over a high background of lactate concentration) could potentially provide a viable solution for the prognosis of cancer metastasis. Indeed, based on preliminary results of our ongoing work, we were able to observe elevated lactate concentration in serum samples containing CTCs vs control samples in human blood which encourages us to continue toward this direction. Furthermore, we are currently setting a collaborative project, that includes a multi-parametric platform for breast cancer where our sensor circuit could be combined with single-cell microfluidics and other (optical-based) sensing modalities to investigate the effect of several drugs on breast cancer cells (in a single-cell level), aiming to develop effective therapeutic strategies.

# Scientific contributions

---

## Publications in peer reviewed journals

1. Metabolite detection with an N-type accumulation mode organic electrochemical transistor  
**A.-M. Pappa**, A. Giovannitti, D. Ohayon, I. Uguz, I. McCulloch, R. M. Owens\*, S. Inal\*  
*In preparation*
2. Organic Electronics for Point-of-Care Metabolite Monitoring  
**A.M. Pappa**, O. Parlak, G. Scheiblin, P. Mailley, A. Salleo and R. M. Owens  
*Submitted in*, Trends in Biotechnology, (*invited Review*)
3. Laser Patterning of Self Assembled Monolayers on PEDOT:PSS Films for Controlled Cell Adhesion  
D. Ohayon, C. Pitsalidis, **A.M. Pappa**, A. Hama, Y. Zhang, L. Gallais, R. M. Owens  
Advanced Materials Interfaces, (2017) (DOI:10.1002/admi.201700191)
4. A Multi-parametric Organic Transistor Toolbox with Integrated Microfluidics for in line in vitro Cell Monitoring  
V.F. Curto, B. Marchiori, A. Hama, **A.M. Pappa**, M. Ferro, M. Braendlein, J. Rivnay, M. Fiocchi, M. Ramuz, R.M. Owens  
Microsystems and Nanoengineering, *in press*
5. Conducting Polymer Scaffolds for Monitoring 3D Cell Culture  
S. Inal, A. Hama, M.Ferro, C. Pitsalidis, J. Oziat, D. Iandolo, **A.M. Pappa**, M. Hadida, M. Huerta, D. Marchat, P. Mailley, R.M. Owens  
Advanced Biosystems, 1 (6), (2017)
6. A Microfluidic Ion-Pump for in vivo Drug Delivery  
I. Uguz, C. M. Proctor, V. F. Curto, **A.M. Pappa**, M. J. Donahue, M. Ferro, R. M. Owens, D. Khodagholy, S. Inal and G. G. Malliaras  
Advanced Materials, *in press* (DOI: 10.1002/adma.201701217)
7. Polyelectrolyte Layer by Layer Assembly on Organic Electrochemical Transistors  
**A.M. Pappa**, S. Inal, K. Roy, Y. Zhang, C. Pitsalidis, A. Hama, J. Pas, G.G. Malliaras, R.M. Owens  
ACS, Applied Materials & Interfaces, 9 (12), (2017)

8. Lactate Detection in Tumor Cell Cultures Using Organic Transistor Circuits  
M. Braendlein\*, **A.M. Pappa\***, A. Lopresti, C. Acquaviva, E. Mamessier, G.G. Malliaras, R.M. Owens  
*Advanced Materials*, 13 (29), (2017) *\*equal contribution*
9. Catalytically Enhanced Organic Transistors for in vitro Toxicology Monitoring through Hydrogel Entrapment of Enzymes  
X. Strakosas, M. Huerta, M.J. Donahue, A.Hama, **A.M. Pappa**, M. Ferro, M. Ramuz, J. Rivnay, R.M. Owens  
*Journal of Applied Polymer Science*, 134 (7), (2016)
10. Organic Transistor Arrays Integrated with Finger-Powered Microfluidics for Multianalyte Saliva Testing  
**A.M. Pappa**, V. F Curto, M. Braendlein, X. Strakosas, M.J. Donahue, M. Fiocchi, G.G. Malliaras, R.M Owens  
*Advanced Healthcare Materials*, 5 (17), (2016)
11. High Mobility Transistors based on Electro spray-Printed Small-Molecule/Polymer Semiconducting Blends  
C. Pitsalidis, **A.M. Pappa**, S. Hunter, A. Laskarakis, T. Kaimakamis, M.M. Payne, J.E. Anthony, T.D Anthopoulos, S. Logothetidis  
*Journal of Materials Chemistry C*, 4 (16), (2016)
12. Electro spray-Processed Soluble Acenes towards the Realization of High Performance Field-Effect Transistors  
C. Pitsalidis, **A.M. Pappa**, S Hunter, M.M. Payne, T. Anthopoulos, J.E. Anthony, S. Logothetidis  
*ACS Applied Materials & Interfaces*, 7 (12), (2015)
13. Oxygen Plasma Modified Biomimetic Nanofibrous Scaffolds for Enhanced Compatibility of Cardiovascular Implants  
**A.M. Pappa**, V. Karagkiozaki, S. Krol, S. Kassavetis, D. Konstantinou, C. Pitsalidis, L. Tzounis, N. Pliatsikas, S. Logothetidis  
*Beilstein Journal of Nanotechnology* 6, 254, (2015)
14. Nanomedicine for Atherosclerosis: Molecular Imaging and Treatment  
V. Karagkiozaki, S. Logothetidis, **A.M. Pappa**  
*Journal of Biomedical Nanotechnology* 11 (2), 191 (2015)

## Selected presentations in international conferences

- Polyelectrolyte layer-by-layer assemblies on top of organic electrochemical transistors,  
*Oral Presentation*, MRS Fall Meeting, November 27- December 2, **2016**, Boston, USA
- Real-time multianalyte screening of blood using organic electrochemical transistor arrays  
*Oral Presentation*, BioEl2017, 12-19 March, **2016**, Kirchberg in Tirol, Austria
- Highly sensitive enzymatic biosensors for the determination of key metabolites in biological media  
*Oral Presentation*, MRS Fall Meeting, November 29-December 4, **2015**

# Acknowledgements

---

This is by far the most difficult part of the Thesis. It is truly impossible to express my feelings and my gratitude for everyone who was beside me throughout this journey. During those three years in BEL I met wonderful people, great scientists, but above all I made true friends. It has been a period of extensive learning not only in the scientific field but also and more importantly on a personal level.

There are not enough words to thank you Roisin for your continuous support, your patience, motivation, enthusiasm, and foremost for your ability to calm me down whenever I got stressed with deadlines. You gave me intellectual freedom and you always supported my ideas being there silently and discretely whenever I needed guidance and help, making this experience a beautiful journey rather than a stressing period. George, thank you for your immense generosity and for the inspiring conversations we had. Apart from a great scientist you are also a great person. Nothing would have been accomplished without the great support of my lab-mates, collaborators and friends. Sahika (or Professor Sahika??) thank you so much for being there this whole time. You have been a great role model for me and gave me unprecedented support. Apart from the scientific guidance and advice you offered me your friendship and I am so grateful for that. I will always remember our philosophical conversations, our shopping delirium and of course our “fights”! Eloise, apart from a great scientist, you have a “gold heart”, as we would say in Greece! I am so lucky to have you as a friend! Ilke, thank you for letting me become your friend and for the endless pastis in le novo. You will do great in Columbia! Marcelinho, you’ve been a huge amount of help - without you none of this would have been accomplished- and more importantly a good friend. I am very happy that I met you and worked with you! Jolien, you rock never lose your spontaneity and enthusiasm! Vincenzo, I have greatly benefited from your keen scientific insight and knack for solving practical difficulties, thanks! David, you are incredible and you will be the best PhD student ever! Thanks for your help. Adel, Thomas you also helped a great deal and I am so grateful for that! Xenofon, you were there in my beginning to advise and train me, thanks! Shahab, Mahmoudy, Chris, Loig, Mary, Magali, Donata, Alex, Yi, Xenofon, Manue, Marc F., Marc R., Carol, Miriam, Gerwin, Adel, Esma, Rod, Pascal, Kirsty, Jon, Jonathan, Alex G, Lisa, Paschalis, Viviana, Aimie. Bastien, Veronique, Michelle, Michel, Ana, Usein, Isabel, Severine, Jake, Onur, Gaetan, Julie, Dimitris,

Jessica, Gaelle, Thierry, Melodie, Gracien, I want to express my gratitude for all the help and good moments! A huge thank you also to all of my Orgbio mates, it's been a great time traveling and spending great moments with you! You are ALL great!

I would like to thank also the coolest American Professors, Susan and Alberto who not only guided me to a fascinating project but also worked with us in the lab!

Last but not least, I want to thank my family and friends for always being there to support me and my crazy ideas, and of course Babis who is being tolerating me in both personal and professional life, making everything easier and more fun! I am sure the future will be even more fascinating!

Again a huge thank you to all of you!

de Saint-Étienne

NNT : *Communiqué le jour de la soutenance*

Anna-Maria PAPPA

## METABOLITE DETECTION USING ORGANIC ELECTRONIC DEVICES FOR POINT-OF-CARE DIAGNOSTICS

Speciality : Microelectronics

Keywords : Organic electrochemical transistors, metabolite sensing, biosensors. biofunctionalization. PEDOT:PSS

Abstract :

Rapid and early diagnosis of disease plays a major role in preventative healthcare. Undoubtedly, technological evolutions, particularly in microelectronics and materials science, have made the hitherto utopian scenario of portable, point-of-care personalized diagnostics a reality. Organic electronic materials, having already demonstrated a significant technological maturity with the development of high tech products such as displays for smartphones or portable solar cells, have emerged as especially promising candidates for biomedical applications. Their soft and fuzzy nature allows for an almost seamless interface with the biological milieu rendering these materials ideally capable of bridging the gap between electronics and biology. The aim of this thesis is to explore and validate the capabilities of organic electronic materials and devices in real-world biological sensing applications focusing on metabolite sensing, by combining both the right materials and device engineering. We show proof-of-concept studies including microfluidic integrated organic electronic platforms for multiple metabolite detection in bodily fluids, as well as more complex organic transistor circuits for detection in tumor cell cultures. We finally show the versatility of organic electronic materials and devices by demonstrating other sensing strategies such as nucleic acid detection using a simple biofunctionalization approach. Although the focus is on *in vitro* metabolite monitoring, the findings generated throughout this work can be extended to a variety of other sensing strategies as well as to applications including on body (wearable) or even *in vivo* sensing.

NNT : *Communiqué le jour de la soutenance*

Anna-Maria PAPPA

## REALISATION DE DISPOSITIFS ELECTRONIQUES ORGANIQUES POUR LA DETECTION DES METABOLITES.

Spécialité: Microélectronique

Mots clefs : bioélectronique, électrodes, biodétection, OEET, PEDOT :PSS,

Résumé :

De nos jours, efficacité et précision des diagnostics médicaux sont des éléments essentiels pour la prévention en termes de santé et permettre une prise en charge rapide des maladies des patients. Les récentes innovations technologiques, particulièrement dans les domaines de la microélectronique et des sciences des matériaux ont permis le développement de nouvelles plateformes personnalisées de diagnostics portatifs. Les matériaux électroniques organiques qui ont déjà par le passé démontré leur potentiel en étant intégrés dans des produits de grande consommation tels que les écrans de smartphones ou encore les cellules solaires montrent un fort potentiel pour une intégration dans des dispositifs biomédicaux. En effet, de par leurs natures et leurs propriétés physiques et chimiques, ils peuvent être à la fois en contact avec les milieux biologiques et constituer l'interface entre les éléments biologiques à l'étude, et les dispositifs électroniques. L'objectif de mes travaux de thèse est d'étudier et d'évaluer les performances des matériaux organiques électroniques intégrés dans des dispositifs biomédicaux en étudiant leurs interactions avec des milieux biologiques et par l'utilisation et l'optimisation de ces dispositifs permettre la détection de métabolites tel que le glucose ou lactate par exemple. Pendant ma thèse, j'ai notamment créé une plateforme de diagnostics combinant à la fois microfluidique et électronique organique permettant la multi détection de métabolites présents dans des fluides corporels humains, j'ai également conçu des capteurs intégrant des transistors organiques au sein des circuits électroniques classiques afin de détecter la présence des cellules tumorales. D'autres applications biologiques ont également été envisagées telles que la détection d'acides nucléiques par l'utilisation d'une approche simple de biofonctionnalisation. Bien que l'objectif ma thèse était de de créer des capteurs biomédicaux en utilisant une approche *in vitro*, il pourrait être également possible d'intégrer ces dispositifs « *in vivo* » ou encore dans des e-textiles.